



Universiteit  
Leiden  
The Netherlands

## Enhancing reovirus for use in oncolytic virotherapy

Kemp, V.

### Citation

Kemp, V. (2019, February 7). *Enhancing reovirus for use in oncolytic virotherapy*. Retrieved from <https://hdl.handle.net/1887/68327>

Version: Not Applicable (or Unknown)

License: [Licence agreement concerning inclusion of doctoral thesis in the Institutional Repository of the University of Leiden](#)

Downloaded from: <https://hdl.handle.net/1887/68327>

**Note:** To cite this publication please use the final published version (if applicable).

Cover Page



Universiteit Leiden



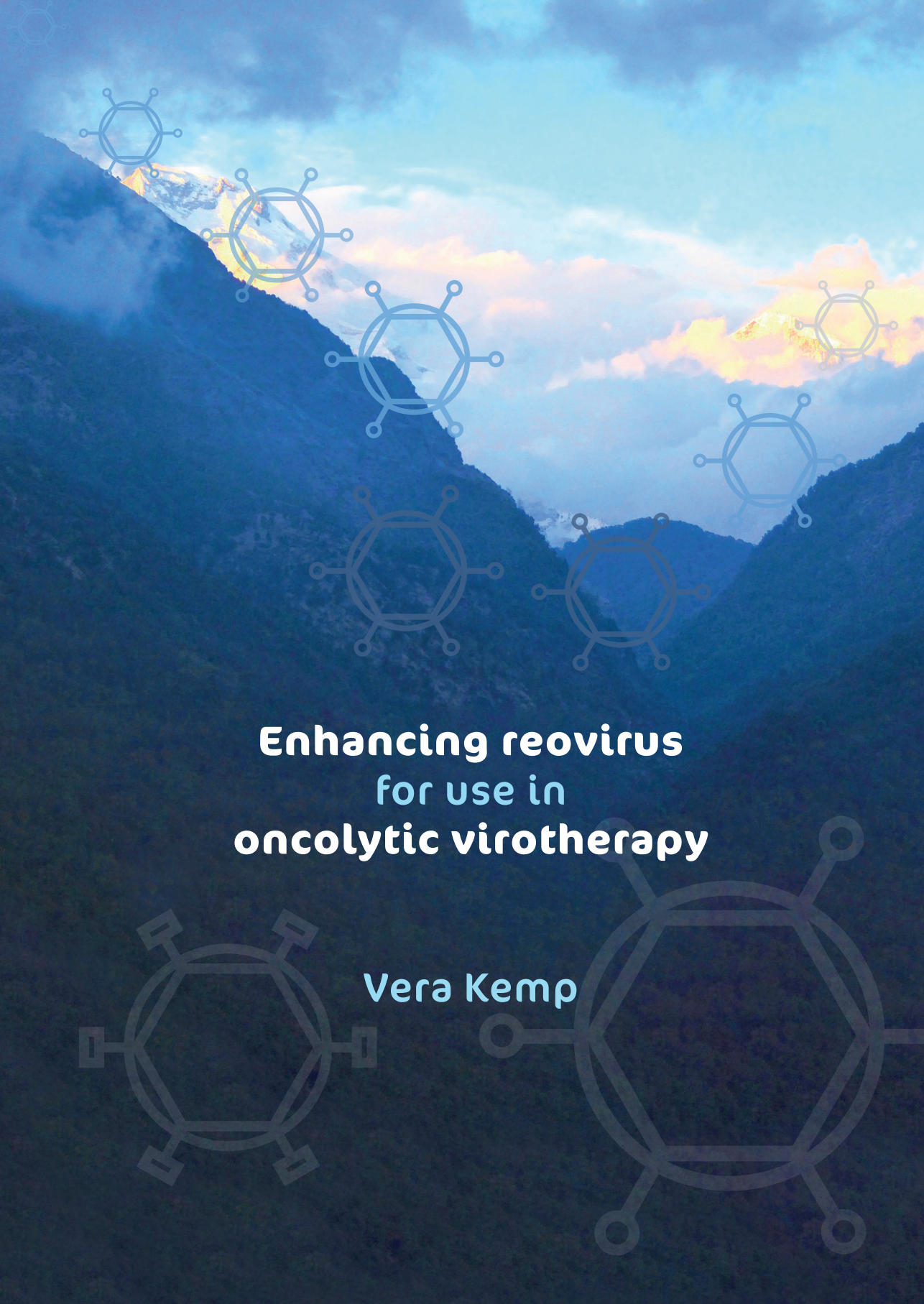
The following handle holds various files of this Leiden University dissertation:

<http://hdl.handle.net/1887/68327>

**Author:** Kemp, V.

**Title:** Enhancing reovirus for use in oncolytic virotherapy

**Issue Date:** 2019-02-07



**Enhancing reovirus  
for use in  
oncolytic virotherapy**

**Vera Kemp**



# Enhancing reovirus for use in oncolytic virotherapy

Vera Kemp

*Enhancing reovirus for use in oncolytic virotherapy*

Vera Kemp

Copyright © 2018 V. Kemp, Leiden, the Netherlands. All rights reserved. No part of this publication may be reproduced or transmitted in any form without permission of the copyright owner.

ISBN: 978-94-6332-440-3

Cover design: Chris Beresford, Grey For Colour, Leiden, the Netherlands

Layout and printing: GVO Drukkers & Vormgevers, Ede, the Netherlands

Printing of this thesis was financially supported by Boehringer Ingelheim.

# Enhancing reovirus for use in oncolytic virotherapy

PROEFSCHRIFT

ter verkrijging van  
de graad van Doctor aan de Universiteit Leiden,  
op gezag van Rector Magnificus  
prof. mr. C.J.J.M. Stolker,  
volgens besluit van het College voor Promoties  
te verdedigen op donderdag 7 februari 2019  
klokke 13:45 uur

door

**Vera Kemp**

geboren te Hazerswoude  
in 1990

**Promotor**

Prof. Dr. R.C. Hoeben

**Co-promotor**

Dr. Ing. D.J.M. van den Wollenberg

**Leden promotiecommissie**

Prof. Dr. J.H. Meijer

Dr. T. van Hall

Prof. Dr. F.M. Reggiori (Universitair Medisch Centrum Groningen)

Prof. Dr. C.H. J. van Eijck (Erasmus Medisch Centrum Rotterdam)

Try to be a person of value, not of success  
*(Albert Einstein, 14 March 1879 – 18 April 1955)*



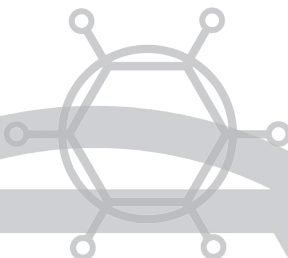
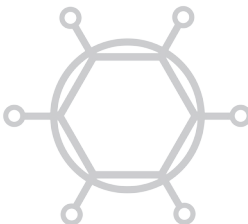
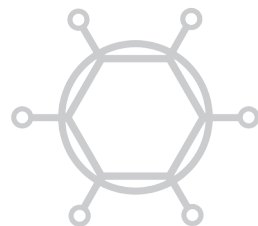
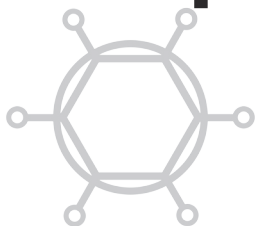
## CONTENTS

<b>Chapter 1</b>	General introduction	9
<b>Chapter 2</b>	Exploring reovirus plasticity for improving its use as oncolytic virus	15
<b>Chapter 3</b>	Oncolytic reovirus infection is facilitated by the autophagic machinery	41
<b>Chapter 4</b>	Characterization of a replicating expanded-tropism oncolytic reovirus carrying the adenovirus E4orf4 gene	67
<b>Chapter 5</b>	Arming oncolytic reovirus with GM-CSF gene to enhance immunity	97
<b>Chapter 6</b>	Yields and genetic stability of replicating recombinant reoviruses	125
<b>Chapter 7</b>	General discussion	153
<b>Addendum</b>	Nederlandse samenvatting	161
	Curriculum Vitae	165
	List of publications	167
	Acknowledgements (Dankwoord)	169



General introduction

**1**



## **CANCER**

Despite a tremendous amount of (pre)clinical research into therapeutic approaches, millions of new cancer cases occur each year worldwide, causing many deaths [1]. The heterogeneity between different tumors and within the tumors, as well as the frequent occurrence of metastases, makes it difficult to design treatments that efficiently combat all cancer cells in all patients. Most of the current new approaches comprise some form of cancer immunotherapy, including checkpoint inhibition, cytokines, and cell-based therapies. Still only a minority of patients respond well to treatment. Therefore, novel strategies are needed to improve the clinical perspective of more cancer patients.

## **ONCOLYTIC VIRUSES**

One of the anti-cancer approaches that has recently gained more attention uses oncolytic viruses. These are viruses that are engineered or have the natural preference to kill transformed cells while sparing normal cells. Therefore, they have been studied as anti-cancer moieties in several clinical trials for various cancer types [2, 3]. Whereas in the past oncolytic viruses were simply regarded as tools to kill off (part of) the tumor, it has now become clear that they can also be exploited to induce anti-tumor immune responses. The virus can trigger both innate and adaptive immune responses in the tumor (microenvironment), potentially breaking the immune tolerance that is often induced by cancer cells. As a result, long-lasting and systemic anti-cancer immunity can be established. Indeed, (pre)clinical studies have shown that local oncolytic virus treatment can trigger immune effects and tumor reduction at distant locations. Moreover, pre-existing anti-viral immunity may enhance treatment efficacy rather than hamper it [4, 5]. In 2015, the FDA approved the first oncolytic virus for treatment of melanoma patients [6]. The approval of this herpes simplex virus expressing GM-CSF, T-VEC, may pave the way for other viruses to be approved for clinical application.

## **REOVIRUS**

Mammalian orthoreovirus, hereafter referred to as reovirus, is a non-enveloped virus harboring a genome consisting of 10 dsRNA segments. Already in 1977, reovirus was found to have the natural preference to replicate in and kill transformed cells and leave normal cells unharmed [7]. It is believed to be not associated with serious disease in humans and therefore represents a promising candidate anti-cancer agent. Later, the underlying mechanism was found to be associated with an active Ras signaling pathway, which hampers a PKR-mediated anti-viral immune response. At least 30% of all cancers show aberrant Ras signaling. Reovirus has been shown to be safe for use in clinical trials, demonstrating clinical benefit rates in some but not

all of these. It seems that the clinical efficacy of reovirus is insufficient to be used as a stand-alone therapy, and remains to be improved. Therefore we seek ways to enhance the therapeutic potency of reovirus.

## THESIS OUTLINE

In this thesis, we discuss several aspects that are important for the design of a potent anti-cancer therapeutic strategy using reovirus. In **chapter 2**, we review the different factors and approaches to consider when exploring reovirus for use as an oncolytic virus. In **chapter 3**, we sought to explore which cellular factors and pathways are important for an efficient reovirus replication cycle. We describe a role of autophagy-related proteins Atg3 and Atg5 in viral replication. Interestingly, Atg13 expression does not affect reovirus replication. From these data we conclude that there is non-canonical use of the autophagy machinery, and propose possible alternative functions of Atg3 and Atg5 that could influence reovirus replication. In **chapter 4 and 5**, we genetically modified the reovirus genome to encode potentially therapeutic transgenes. Genetic modification of dsRNA genomes is less straightforward than for viruses with DNA genomes. Nevertheless, a reverse genetics system has been developed that allows researchers to generate reoviruses with modified genome segments. We generated reoviruses encoding E4orf4 (**chapter 4**), an adenovirus-derived pro-apoptotic protein, and GM-CSF (**chapter 5**), an immunomodulatory cytokine that stimulates dendritic cell generation and maturation. We tested the potency of these recombinant reoviruses, and describe what we believe is the most promising strategy to move forward. **Chapter 4** describes that expression of E4orf4 does not further augment the cytolytic capacity of our recombinant reoviruses. We postulated that our recombinant reoviruses are potent inducers of cell death by themselves, and therefore a further amplification of oncolysis may be obsolete. **Chapter 5** describes the successful generation of recombinant reoviruses expressing GM-CSF. The viruses triggered the secretion of functional GM-CSF, and we showed that they can systemically modulate the immune composition in mice bearing pancreatic tumors. In **chapter 6**, we discuss the physical and genetic stability issues that we encountered during the generation of recombinant reoviruses. The relatively low infectivity, and the appearance of deletion mutants are described and possible underlying causes are proposed. **Chapter 7** summarizes all findings, and discusses the various challenges and opportunities in how to proceed.

## REFERENCES

1. Cancer Research UK. Worldwide cancer statistics. Available online: <https://www.cancerresearchuk.org/health-professional/cancer-statistics/worldwide-cancer> (Accessed July 2018).
2. Ungerechts, G.; Bossow, S.; Leuchs, B.; Holm, P.S.; Rommelaere, J.; Coffey, M.; Coffin, R.; Bell, J.; Nettelbeck, D.M. Moving oncolytic viruses into the clinic: clinical-grade production, purification, and characterization of diverse oncolytic viruses. *Mol Ther Methods Clin Dev* **2016**, *3*, 16018.
3. Maroun, J.; Munoz-Alia, M.; Ammayappan, A.; Schulze, A.; Peng, K.W.; Russell, S. Designing and building oncolytic viruses. *Future Virol* **2017**, *12*, 193-213.
4. Ilett, E.; Kottke, T.; Donnelly, O.; Thompson, J.; Willmon, C.; Diaz, R.; Zaidi, S.; Coffey, M.; Selby, P.; Harrington, K.; Pandha, H.; Melcher, A.; Vile, R. Cytokine conditioning enhances systemic delivery and therapy of an oncolytic virus. *Mol Ther* **2014**, *22*, 1851-63.
5. Ilett, E.J.; Barcena, M.; Errington-Mais, F.; Griffin, S.; Harrington, K.J.; Pandha, H.S.; Coffey, M.; Selby, P.J.; Limpens, R.W.; Mommaas, M.; Hoeben, R.C.; Vile, R.G.; Melcher, A.A. Internalization of oncolytic reovirus by human dendritic cell carriers protects the virus from neutralization. *Clin Cancer Res* **2011**, *17*, 2767-76.
6. Pol, J.; Kroemer, G.; Galluzzi, L. First oncolytic virus approved for melanoma immunotherapy. *Oncoimmunology* **2016**, *5*, e1115641.
7. Zhao, X.; Chester, C.; Rajasekaran, N.; He, Z.; Kohrt, H.E. Strategic Combinations: The Future of Oncolytic Virotherapy with Reovirus. *Mol Cancer Ther* **2016**, *15*, 767-73.





2

Exploring reovirus plasticity for  
improving its use as oncolytic virus

Vera Kemp, Rob C. Hoeben and Diana J.M.  
van den Wollenberg

Department of Molecular Cell Biology, Leiden  
University Medical Center, P.O. Box 9600,  
2300 RC Leiden, the Netherlands

Viruses 2016, 8(1), 4

## **ABSTRACT**

Reoviruses are non-enveloped viruses with a segmented double stranded RNA genome. In humans, they are not associated with serious disease. Human reoviruses exhibit an inherent preference to replicate in tumor cells, which makes them ideally suited for use in oncolytic virotherapies. Their use as anti-cancer agent has been evaluated in several clinical trials, which revealed that intra-tumoral and systemic delivery of reoviruses are well tolerated. Despite evidence of anti-tumor effects, the efficacy of reovirus in anti-cancer monotherapy needs to be further enhanced. The opportunity to treat both the primary tumor as well as metastases makes systemic delivery a preferred administration route. Several preclinical studies have been conducted to address the various hurdles connected to systemic delivery of reoviruses. The majority of those studies have been done in tumor-bearing immune-deficient murine models. This thwarts studies on the impact of the contribution of the immune system to the tumor cell eradication. This review focuses on key aspects of the reovirus/host-cell interactions and the methods that are available to modify the virus to alter these interactions. These aspects are discussed with a focus on improving the reovirus' anti-tumor efficacy.

## INTRODUCTION

The field of oncolytic virus therapy has evolved rapidly since the late 1990s as can be appreciated from the increase in publications on this topic. An overview of viruses currently used in clinical trials for different malignancies is given by Eisenstein *et al.* [1] and Bell *et al.* [2]. The different viruses that are tested can be roughly divided in two groups: (1) wild-type viruses or their attenuated derivatives; and (2) genetically modified viruses containing heterologous transgenes that encode efficacy-enhancing proteins such as cytokines or prodrug-activating enzymes. This review focuses on the use of mammalian orthoreoviruses (reoviruses for short) in oncolytic therapies, and on the various strategies that can be used to enhance their oncolytic potency.

Reoviruses are segmented dsRNA viruses that have not been firmly associated with serious disease in humans. Although reoviruses have been found in children with respiratory and gastrointestinal illnesses, their role remains unclear and there are no convincing data for a causal relation [3]. Early on, researchers recognized their capacity to induce cell death in tumor cells, while normal, diploid cells are largely resisting reovirus infection. This observation was first noted in the late 1970s when human cell lines and cell lines from rat, mouse, and monkey origins were exposed to reovirus Type 2 [4]. Most of the more recent clinical studies are carried out with the reovirus Type 3 Dearing (T3D) strain [5, 6]. A third reovirus serotype (Type 1 Lang; T1L) is frequently used in comparative studies with reovirus T3D, especially those concerning the mechanisms of infection and replication in cell lines, and the pathogenesis in mouse models [7–9]. The classification is based on the difference by the three strains in neutralization and hemagglutinin-inhibition assays [10, 11].

Exactly how and why reoviruses prefer to induce cell death in cancer cells has not yet been fully elucidated, despite many studies. A complicating factor here is that many studies reveal only pieces of the puzzle. The variation in responses in different cell lines makes it difficult to combine the results from the various studies. It has been demonstrated that the tumor cell preference of reoviruses can be explained in part by the higher sensitivity of cancer cells with an activated Ras pathway to reovirus-induced apoptosis [12–16]. However, Ras-transformed fibrosarcoma cells (HT1080) can acquire resistance to reovirus-induced cell death. When HT1080 cells are exposed to reovirus T3D, few cells survive. The reovirus-resistant cells (HTR1) still contain the Ras mutation and are persistently infected by the reovirus. They are resistant to reovirus-induced cell death even after re-infection with a high titer of reoviruses. The parental cells stayed sensitive to reovirus-induced cell death even if they were exposed at a low multiplicity of infection (MOI). In the HTR1 cells, the cathepsin B activity is reduced and this may contribute to the capacity

of the reovirus to establish a persistent infection in the cells [17]. For a productive replication cycle leading to lysis of cells, the following aspects are important: (i) attachment and entry into cells; (ii) uncoating by proteases to facilitate escape of the virus from the endosomes; (iii) transcription and replication of viral genomes leading to production of progeny viruses; and (iv) the induction of cell death to release the nascent viruses [18–22]. It has been demonstrated that cathepsin B plays an important role in cell death induction for several viruses [23–25]. It remains to be established how the cathepsin B downregulation facilitates the persistent reovirus infection.

One therapeutic approach may not be sufficient to completely eliminate a tumor: this may also be true with oncolytic virotherapies [2]. The heterogeneity of the tumor cells, the presence of therapy-resistant cancer stem cells, and the micro-compartmentalization of the tumor all impede the efficiency of virus entry, replication, and spread, and could lead to the expansion of virus-resistant cell populations. In addition to the heterogeneity within the tumor, there may be heterogeneity between tumors at different locations in the patient, and between tumors in different patients. An example of the latter was provided in cultures of human glioblastoma stem-like cells (GSCs). Seven independent serum-free GSC cultures derived from glioblastoma resections were exposed to two different reovirus variants (*i.e.* wild-type reovirus T3D and the JAM-A independent *jin-1* mutant, described in [26]). Five parameters were assessed to define the sensitivity of the GSCs to reovirus infection. One of the parameters is the distribution of  $\sigma 3$  protein within spheroids cultures of the GSCs as an indicator of the capacity of the reoviruses to penetrate and spread in the 3D-cell structure. There were large differences in distribution of the reovirus-infected cells between the different GSC spheroids cultures. Also in the monolayer cultures there was a large variation in the infection efficiency, the amount of virus produced per culture and per reovirus-infected cell, as well as in the susceptibility to reovirus-induced cytolysis. These data illustrate the difficulties in establishing proper parameters for predicting the susceptibility of the cells to reovirus-induced oncolysis *in vivo* [27]. These tests only involved *in vitro* cultures and such cultures are obviously not fully representing the clinical tumor *in situ*. In the clinical situation the activity of an active immune system and the tumor microenvironment further add to the heterogeneity of the anti-tumor efficacy of the oncolytic viruses.

## **REOVIRUS' ENGAGEMENT TO CELL SURFACE MOLECULES**

Initiation of an infection starts with attachment of the virus to host cells, mostly to cell surface molecules that are used as receptors. All three reovirus prototype strains can bind with the spike protein  $\sigma 1$  to the canonical reovirus receptor junction

adhesion molecule-A (JAM-A). Nevertheless, the three reovirus types differ in their neural tropism in mice [28–30]. JAM-A is a cell adhesion molecule that belongs to the tight junction Ig superfamily. It is involved in cell–cell interactions of epithelial and endothelial cells as well as to leucocytes and platelets. Many of these cell adhesion molecules are exploited by viruses to gain entry into cells. Reovirus strains T1L and T3D are extensively studied with regard to  $\sigma 1$  binding in cell culture systems and the crystal structure of the  $\sigma 1$  complexed to JAM-A has been determined.

Recently, a different protein on cells in the central nervous system (CNS) was identified as a receptor for reovirus, the Nogo receptor NgR1. This is a leucine-rich repeat protein expressed on the cell surface of neurons [31]. Reovirus T3D, but not T1L, can infect cultured mouse primary cortical neurons that express NgR1. However, when NgR1 is constitutively expressed in Chinese Hamster Ovary (CHO) cells, not only T3D but also T1L can infect these cells. The precise mechanism for this unexpected observation remains to be established. The difference in glycan binding may route the viruses to different regions in the brain. This may allow T3D to bind to the NgR1 receptor on neurons and T1L to ependymal cells, although more research is required to elucidate the NgR1 pathway in neurons [32].

Most of the receptor studies are done in cells cultured in monolayers [33–35]. Monolayer cultures, however, are not representative for tumors when it comes to cell–cell interactions, since the cells are forced to grow on a plastic substrate leaving the apical side exposed to the culture medium and only small areas contact the neighboring cells. In more complex systems, such as in 3D spheroid cell cultures, reoviruses seem to be less dependent on JAM-A for infection. When JAM-A negative U118-MG cells are grown in spheroids, they become susceptible to wild-type T3D reovirus, whereas the same cells grown in monolayer cultures are fully resistant to reovirus infection. The increased sensitivity to reovirus infection of the cells in spheroid cultures may be related to the high levels of active cathepsin B within the spheroids [36]. The activated cathepsin B promotes the proteolytic uncoating of reovirus particles into intermediate subviral particles (ISVPs). These ISVPs mimic the partially uncoated particles that are formed in endosomes and that penetrate the endosomal membrane to escape into the cell's cytoplasm. In a similar manner, the ISVPs formed by the action of extracellular cathepsins in spheroids may penetrate the cell membrane independent of a high affinity receptor. This also has implications for the situation *in vivo*, since many cancer types contain increased levels of proteases in their tumor environment (including increased levels of cathepsin B) and this correlates with tumor progression and metastasis [37, 38]. Therefore, it remains to be established whether JAM-A expression on cancer cells is an important determinant for reovirus infectivity.

Before reoviruses attach to JAM-A with a high affinity, the viruses engage sialic acids (SA) on the surface of the cells [39]. The SA binding domain resides in the shaft of the  $\sigma 1$  spike protein. The JAM-A binding domain in the head region of  $\sigma 1$  is more conserved between the different reovirus serotypes [29] than the region binding to sialylated glycans [8, 40]. For T3D, the SA binding region is located in the tail part of  $\sigma 1$ . In contrast, the domain of T1L binding to ganglioside M2 (GM2) has been mapped to the head domain of the spike protein (Figure 1). The difference in carbohydrate binding accounts for the serotype-specific variances in viral spread in murine immune-compromised hosts. In newborn mice, T1L infects ependymal cells and spreads hematogenously causing non-lethal hydrocephalus [40, 41]. T3D, however, also infects neurons and uses the neural as well as the hematogenous route for its distribution, leading to lethal encephalitis [42–44]. An explanation for the difference in age-dependent neural pathogenicity can be explained by the preference for reovirus T3D to infect the unmyelinated CNS of newborn mice in which the NgR1 receptor is not fully associated to myelin and therefore available for reovirus binding, while in adult animals, the NgR1 receptor is myelin-associated, preventing binding to reovirus T3D [32]. This phenomenon had already been reported in 2002 [45]. Taken together, these data demonstrate that the viral spike protein  $\sigma 1$  is a key determinant of viral tropism and spread within the host.

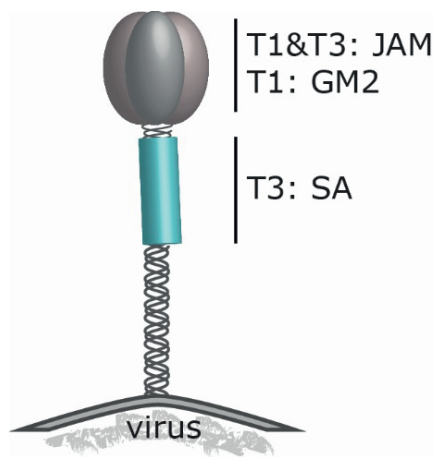


**Figure 1.** Schematic model of the  $\sigma 1$  trimer at the reovirus capsid. Depicted are the receptor-binding regions of T3D (T3) and T1L (T1). JAM: JAM-A (junction adhesion molecule-A), GM2: ganglioside M2, SA:  $\alpha 2,3$ ;  $\alpha 2,6$  and  $\alpha 2,8$ -linked sialic acid.

## REOVIRUS AND THE GREAT ESCAPE: WHAT PATHWAYS ARE INVOLVED IN REOVIRUS INDUCED CELL DEATH

Cell death induction by reovirus is strain-dependent, with T3D strains inducing more efficient cell death than the other strains [7]. T3D reovirus infects neurons and can cause lethal encephalitis, which has been shown to depend on the pro-apoptotic factor Bid [47]. After endosomal escape, but prior to cytoplasmic RNA production, reovirus stimulates essential steps for the induction of apoptosis, which is thought to be the primary mechanism of cell death induced by reovirus infection [48]. The apoptotic pathway is highly complex, and numerous apoptotic factors have been linked to reovirus-induced oncolysis [49–53], making it difficult to identify the trigger that activates the apoptotic cascade induced upon reovirus infection. It has been shown that reovirus-infected cells release soluble TRAIL that induces apoptosis, mainly via death-receptor signaling [54]. In H-RasV12-transformed fibroblasts, reovirus infection inhibits the palmitoylation of Ras, shifting the Ras localization from the plasma membrane to the Golgi system, which eventually stimulates apoptosis. Reovirus replication is favored during Ras localization at the plasma membrane, whereas Ras accumulation in the Golgi enhances apoptosis through increased MEKK1/MKK4/JNK signaling [55]. It seems that the viral  $\sigma 1$  and  $\mu 1$  proteins are key determinants in the induction of apoptosis, with  $\sigma 1$  binding to surface receptors and  $\mu 1$  facilitating viral disassembly steps [7, 56–58]. Moreover, the  $\sigma 1s$  protein may play a role in cell cycle arrest and the induction of apoptosis [59].

Interestingly, blocking essential components of the apoptotic pathway does not fully diminish reovirus-mediated cell death [60–62], prompting the question what other cell death routes are involved in oncolysis by reovirus. Berger and Danthi described that reovirus T3D, and to a lesser extent T1L, induce RIP1-dependent signaling resulting in necroptosis, a caspase-independent programmed cell death route resembling necrosis. This route is purportedly activated by either binding to death receptors, pattern recognition receptors, or via the loss of inhibitors of apoptosis [60]. As for apoptosis, the binding of  $\sigma 1$  to sialic acids affects the induction of necroptosis. However, necroptosis induction relies upon the increased viral gene expression induced by sialic acid binding rather than the binding itself [63].

Cells undergoing necroptosis often show features of autophagy (*i.e.* formation of autophagic vesicles) as well, and it remains to be determined whether autophagy is the main mechanism of cell death in necroptotic cells [64]. Autophagy is induced upon infection with various microbial pathogens [65]. It is a highly conserved process involving the degradation of cellular cytoplasmic contents within double-membraned vesicles and recycling of the components in the cytosol, which allows the cell to survive stressful conditions such as a nutrient-poor environment. Many viruses have evolved mechanisms to either suppress or induce autophagy to

enhance their replication and/or survival [66]. For avian reovirus, it has been found that the viral p17 protein acts as a nucleoporin Tpr suppressor leading to the activation of p53, p21, and PTEN as well as the repression of the PI3K/Akt/mTOR and ERK pathways stimulating autophagy, and that autophagy induction facilitates virus replication [67–69]. Mammalian reovirus induces autophagy in multiple myeloma cells [61, 62], but the function of autophagy in these cells remains largely unknown. Endoplasmic Reticulum (ER) stress can lead to the negative regulation of the mTOR signaling pathway, which in turn initiates autophagy [70]. Interestingly, apoptosis of reovirus-infected multiple myeloma cells has been shown to coincide with ER stress, and ER stress has been implicated to enhance the anti-tumor effects of reovirus, suggesting that autophagy is a potential mechanism of oncolysis by reovirus [71–73].

### **REOVIRUS AND ITS RELATION WITH NEUTRALIZING ANTIBODIES**

Many preclinical studies have been done in immune-deficient animals, *e.g.* to investigate the oncolytic effect in human tumor xenografts in mice [74–76]. An attractive route of administration of the oncolytic viruses is intravenous (iv) infusion since this would allow the infection of tumor (metastases) at multiple sites. In such applications, the presence of pre-existing circulating neutralizing antibodies (NABs) directed against the therapeutic virus is considered a major obstacle for an effective delivery [77–79]. In the human population most individuals are in their childhood exposed to reoviruses and hence carry NABs [80, 81].

However, in a recent study in patients with colorectal cancer metastases in the liver who received one single iv injection with reovirus, replicating reoviruses were detected in certain blood cell compartments (peripheral blood mononuclear cells (PBMCs), granulocytes and platelets) in the circulation, despite the presence of NABs in the blood. Furthermore, after resection of the tumor and surrounding liver tissue, in nine out of the ten patients, reovirus proteins were detected by immunohistochemistry intra-tumorally and some faint staining in the surrounding tumor stroma or healthy liver tissue. From four patients, freshly resected material was used to make a liver cell suspension and a tumor cell suspension to address the question if viable, replicating reoviruses could be detected by a hand-off assay on L929 indicator cells. Plaques were detected in L929 cells exposed to the tumor cell suspension, but not in the L929 cells subjected to the liver cell suspension. These data suggest that systemically administered reoviruses can reach tumors in patients and preferentially replicate in tumor cells, despite the presence of NABs. The mechanism that is proposed by the investigators is that reoviruses are associated with PMBCs, granulocytes and/or platelets and in that way are protected against the circulating NABs [82].

An earlier study in B16tk melanoma-bearing reovirus-immune mice already showed that *ex vivo* loading of dendritic cells (DCs) or T-cells with reovirus could deliver the virus to the melanoma cells *in vivo* after one single iv injection. In this experiment, iv administered reovirus alone, in contrast to the human study, was completely ineffective in killing the B16tk melanoma cells. This corroborates that reovirus hitchhikes on DCs or T-cells in a manner that protects them from the pre-existing antibodies [83]. In a follow-up experiment, the researchers investigated if cytokine conditioning prior to reovirus injection could enhance the oncolytic effectivity in the mouse model. Their experiments showed that in the presence of pre-existing NABs, the addition of granulocyte macrophage colony-stimulating factor (GM-CSF) prior to iv administration of reovirus in B16 melanoma-bearing reovirus-immune mice resulted in significantly reduced tumors and prolonged survival. The proposed mechanism is that reoviruses are transported on GM-CSF-activated monocytes/macrophages into the tumors where the viruses are delivered, start to replicate and destroy the tumor. The associated tumor-cell lysis in turn may activate an anti-tumor immune response [84].

The current dogma dictates that NABs frustrate effective oncolytic virotherapy, but this may not be fully correct. In fact, as the presence of NABs may even enhance the efficacy of virus delivery to the tumor site, the reverse could be true.

## REOVIRUS AND IMMUNE STIMULATION

Immunotherapy is an emerging field in the oncology with promising results for cancer patients [85–87]. The mission is to achieve lifelong immunity against the cancer in the patient, in order to eradicate the primary tumor as well as distant metastases. Tumors have evolved immune evasion strategies that allow their continued expansion despite active immune surveillance. The strategies include attraction of immune-suppressive regulatory T-cells (Treg) and myeloid-derived suppressor cells (MDSCs), the secretion of growth-promoting growth factors and cytokines, as well as secretion of soluble ligands to block tumor-specific effector T-cell recognition and function [88, 89]. In recent years, more knowledge has been acquired on the immune cells present in the tumor microenvironment. This results in the development of more therapeutic intervention strategies directed against tumor-associated immunosuppression [90].

The dual action of an oncolytic virus, *i.e.* preferentially target cancer cells and the strong induction of an anti-viral immune response, may help to inhibit the tumor-associated immune escape. The disruption of immune tolerance may even be more important than the direct oncolytic effect of the virus. In 2009, Prestwich *et al.* [91] showed that reovirus-loaded T-cells did not induce direct oncolysis or virus

replication. However, the T-cells could eliminate metastases in lymph nodes and spleen by stimulating anti-tumor immunity. This strategy can be further expanded in combination therapies [92, 93]. As mentioned above, the addition of GM-CSF activates and recruits the monocytes/macrophages, which can carry reovirus to the tumor in a mouse model [84]. The addition of GM-CSF in combination with oncolytic viruses is an attractive option. One such approach involves an oncolytic herpes simplex virus that carries a GM-CSF gene as a transgene. This virus is known as Talimogene laherparepvec (T-VEC), previously entitled OncoVex<sup>GM-CSF</sup> [94]. Promising results of a phase III clinical trial with T-VEC against melanoma have recently been published. In this randomized study, patients with stage IIIB to IV melanoma were treated with subcutaneously administered GM-CSF or intra-lesional injections with T-VEC. In the T-VEC treated group, the durable response rate was improved and the median overall survival was longer compared with the patients receiving GM-CSF alone. The best results were observed in patients with unresected stage IIIB, IIIC or IVM1a melanoma and the treatment was well tolerated with no fatal treatment-related adverse effects [95].

Based on these and other results, T-VEC has been approved by the Food and Drug Administration (FDA) for clinical use in a subset of melanoma patients [96]. Currently, new melanoma patients are enrolling in a clinical trial combining T-VEC and ipilimumab [97]. Ipilimumab is an antibody directed against cytotoxic T-lymphocyte-associated antigen 4 (CTLA4). The normal biological role of CTLA4, and other molecules involved in immune-checkpoint pathways, is the prevention of autoimmunity by inhibiting T-cell activation directed against “self-ligands” [98, 99]. In tumors, this mechanism is hijacked to prevent a tumor-directed T-cell response.

Thus far, no data are published on the combination of reovirus and ipilimumab, but preliminary results of studies with another immune-checkpoint receptor, programmed cell death 1 (PD1) seem promising [6]. In a subcutaneous B16 melanoma C57BL/6 mouse model, the combination of anti-PD1 and intra-tumoral administered reovirus enhanced the survival compared to intra-tumoral reovirus alone and the combination achieved a durable anti-tumor response in the surviving animals [100].

Patients with tumors expressing a ligand for PD1 (PDL-1) are the best responders to PD1- and PDL-1-targeted therapies. In some breast, kidney, and lung cancer cell lines, reovirus appears to upregulate PDL-1 expression on the cell surface in the presence of sunitinib. Sunitinib is used as a tumor angiogenesis inhibitor, blocking actions of vascular endothelial growth factor (VEGF). This suggests that a combination of reovirus, anti-PDL-1, and sunitinib would constitute a powerful strategy for some cancers [6, 101].

The availability in the clinic of the approved immune-checkpoint inhibitors makes them excellent candidates for the above mentioned combination therapies. However, care must be taken since the underlying mechanisms are not yet fully elucidated. For example, the optimal timing of the regimen still has to be established as suggested by Clements *et al.* [102]. Their study revealed that in the early days after reovirus injection in a murine model for peritoneal carcinomatosis the virus promotes the recruitment of special MDSCs (CD11b<sup>+</sup>, Gr-1<sup>+</sup>, Ly6C<sup>high</sup>) to the tumor microenvironment and thereby transiently (~7 days) induces tumor-associated immunosuppression. In that respect it is interesting to note that in a breast tumor mouse model, colon carcinoma cell and mammary carcinoma bearing mouse models, GM-CSF induces the suppressive MDSCs (CD11b<sup>+</sup>, Gr-1<sup>+</sup>, Ly6C<sup>high</sup>) [103, 104]. These data could support the findings by Ilett *et al.* [84] that upon stimulation with GM-CSF in the B16tk melanoma-bearing reovirus-immune mice, CD11b<sup>+</sup> cells transported the reoviruses to the tumors. The therapy was only effective when GM-CSF preceded the reovirus injections. Their experimental output was obtained after more than seven days, thereby possibly missing the initial induction of tumor-associated immunosuppression.

Another study with vaccinia virus (VV) and CTLA4 inhibition in a syngeneic subcutaneous mouse renal adenocarcinoma model showed that if the combination of virus with anti-CTLA4 was administered on the same day (day-0) the therapeutic effect of the addition of anti-CTLA4 was diminished. The tumor size decreased when VV was administered at day-0 and anti-CTLA4 therapy started after four days [105]. In the same report the authors showed that also the used VV strain was of importance. If a VV strain was used in which the gene encoding secreted type I IFN-binding protein (B18R) was deleted, the synergistic effect with anti-CTLA4 was more potent compared to a VV strain that retained the B18R gene. These data suggest that in designing combination therapies the viral strain and timing should be considered especially for viral vectors with immune-stimulating transgenes. This strategy of viro-immunotherapy is an extremely powerful one worth of exploring with oncolytic reoviruses as well.

## GENETIC MODIFICATION OF REOVIRUS

The RNA genome of the reovirus acquires mutations relatively fast. This provides a plasticity that can be exploited to select reovirus variants that have stronger oncolytic potency. It is also possible to genetically modify the reovirus genome, which offers further options for enhancing the oncolytic activity, for instance by inserting small therapeutic transgenes [46, 106]. The recent development of a plasmid-based reverse genetics system [106] for reoviruses provided new options for reovirologists to unveil more aspects of reovirus biology as well as for improving

the efficacy in oncolytic reovirus therapy. The powerful reovirus reverse genetics system has primarily been used to resolve issues where reovirus segments are involved in apoptosis, assembly or disassembly, cell tropism and pathogenesis in mice [59, 107–111].

Of the studies with the reverse genetics system only a few reports describe its use for generating recombinant reoviruses that harbor heterologous polypeptides in reovirus proteins. The addition of a 6x His-tag to the C-terminus of  $\sigma 1$  to modify the tropism was described in 2008, using a system relying on the expression of one modified segment and infection with a wild-type helper reovirus for providing the other nine gene segments [112]. In 2011 Brochu-Lafontaine *et al.* [113] used the plasmid-based reverse genetics system for adding heterologous polypeptides to  $\sigma 1$ . They showed that the addition of a sequence of 750 nucleotides at the C-terminus of  $\sigma 1$  was not tolerated and managed to add a sequence of about 40 nucleotides to  $\sigma 1$ . Demidenko *et al.* [114] added longer tandem repeats and inserted a tetra virus 2A element for exogenous polypeptide expression in three other segments (S3, M1 and L1). The maximum length of heterologous sequences added in the reovirus genome was 1500 nucleotides divided over two segments (L1 and M2). This technique could be useful in the vaccine development and has the possibility to simultaneously express peptides on different segments. The modified reoviruses created were genetically stable for at least three passages in L929 cells. It remains to be seen what will happen if the viruses are propagated for additional rounds on L929 cells.

Another approach to express exogenous proteins in reovirus segments is by replacing an open reading frame (ORF) of a segment for the ORF of the foreign protein. This requires that the viruses are propagated on cell lines that complement for the missing reovirus protein normally expressed from the selected segment [106,115]. Insight was obtained on the various signals in the genomic RNA that are important for replication of the reovirus segments. This allowed for the identification of locations that possibly could harbor transgenes. One such example is the insertion of the small fluorescent protein iLOV (improved Licht, Oxygen or Voltage sensing domain from *Arabidopsis thaliana*) replacing the JAM-A binding region in  $\sigma 1$  of a JAM-A independent *jin* mutant [46]. This confirmed the feasibility of creating autonomously replicating, genetically modified reoviruses carrying heterologous transgenes. In Figure 2 the schematic representation visualizes the region in S1 for inserting the transgene and the elements that are provided for entry and separation of the transgene-encoded protein from the  $\sigma 1$  tail in the virus capsid. More research is required to test these recombinant reoviruses in animal models. This platform allows for exploiting the genomic plasticity of reovirus by inserting small genes in the S1 segment to enhance its oncolytic properties.

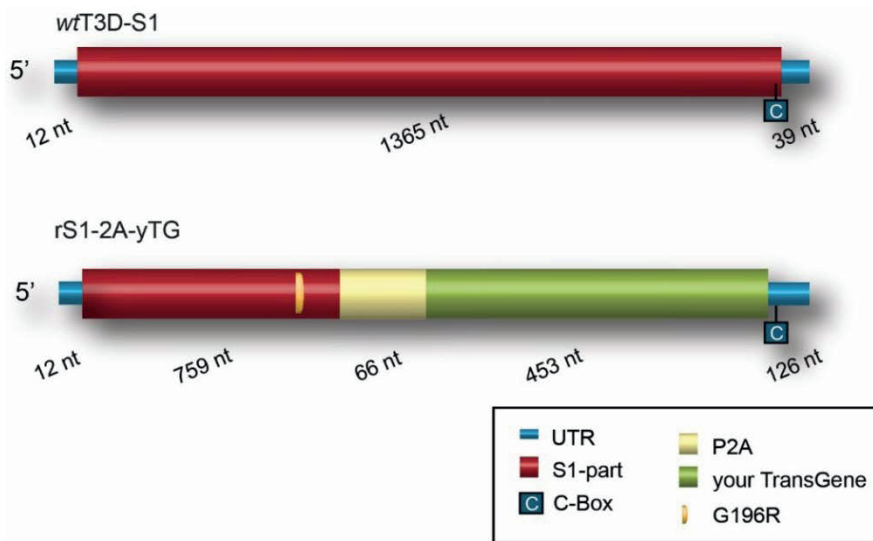


**Figure 2.** Scheme of recombinant S1 gene segment compared to wild-type T3D S1 (wtT3D-S1). rS1-2A-yTG is the recombinant S1 segment containing your transgene (yTG) downstream of a porcine teschovirus-1 2A element (P2A) to separate the encoded protein from the  $\sigma 1$  part. Entry of the recombinant reovirus by sialic acid binding is facilitated by a mutation in the S1 part that results in a G to R amino acid change at position 196 (G196R) in the truncated  $\sigma 1$  protein. In the 3'-untranslated region (UTR) of the recombinant gene the C-box is important for incorporation of the segment in the viral particles [46]. To not exceed the wild-type size of S1, the inserted transgene might be ~453 nt long. The size of each element is depicted in nucleotides (nt) below each segment.

## REOVIRUS AND ANIMAL MODELS

The orthoreoviruses are ubiquitous in their geographical distribution and infect many mammalian species including mice, chimpanzees, dogs, cats, cattle, sheep, swine, horses, and monkeys [116]. This indicates that reovirus is able to replicate in different hosts. As in humans, reovirus rarely causes clinical disease in non-human hosts. Upper respiratory or gastrointestinal symptoms are among the possible manifestations of reovirus infection in young and adult animals. It should be noted that in new-born mice, which are immune-compromised, reovirus can cause lethal encephalitis, bile-duct atresia, and vasculitis [20]. The pathogenicity of reovirus infection in mice has been reviewed by Montufar-Solis and Klein in 2005 [117].

The incidence of reovirus seropositivity in healthy humans rises from approximately 35% in early childhood, to approximately 60% in teenage years, and more than 85% in late adulthood.

Until now, reovirus has been mainly tested in murine models. Interestingly, the symptoms caused by reovirus infection differ in immune-deficient mice compared to immune-competent mice. Immune-competent mice usually show no severe pathology, whereas in immune-deficient mice the reovirus infection may cause diabetes, or problems with the gastrointestinal, hepatic and central nervous systems [118–120]. The fact that mice are permissive to reovirus infection allows studying the contribution of the immune system to the eradication of the tumor, as well as the contribution of the immune responses to control the reovirus infections. Kranenburg and collaborators demonstrated that immune suppression promoted anti-tumor efficacy of reovirus in the murine C26 colorectal cancer model [121].

The wide host range of reoviruses offers attractive options for preclinical research. Various animals such as dogs with spontaneous tumors have been recognized as important models to improve the efficacy of anti-cancer strategies. Since dogs suffer from cancers with a similar disease course as humans, the canine model may mimic the humans more faithfully than xenografted tumors. Several oncolytic viruses are currently being tested for their use in canine patients [111], mostly in preclinical-phase research. Canine adenoviruses, for example, have already been used in trials to treat dogs and few side effects were observed. Promising results were reported in a trial for the intra-tumoral treatment of canine melanoma. In this study a replication-deficient adenovirus type 5 (Ad5) vector expressing CD40 ligand was used (AdCD40L) to impair tumor angiogenesis by targeting cells expressing  $\alpha_v\beta_3$  integrin. Nineteen dogs with melanomas (14 oral, four cutaneous, and one conjunctival) were included in the trial and complete disease remission was reported in five of the dogs, eight showed partial remission and four with stable disease. In only two dogs the disease progressed [122]. Taken together, these data demonstrate the feasibility of using spontaneous tumors in companion animals for providing evidence of clinical efficacy before going to clinical trials in humans.

## **FUTURE DIRECTIONS**

When the first viruses were discovered, all the attention went to what disease is caused by the virus and what treatment is effective. During the mid-20th century it was discovered that some cancers were caused by viruses [123]. All of these are good reasons to not think of viruses as a solution to cure cancers. With the realization that viruses are very efficient in delivery of genetic material to cells, virologists started exploring viruses as tools.

Reoviruses have the advantage of not being connected to serious human disease and the number of clinical trials that involve the use of reovirotherapy for cancer is still growing. To date, the focus is shifting towards combination strategies, since the efficacy of reovirus as a monotherapy is moderate at best.

In addition to the genetic modification, classical bioselection is another tool that can be used for enhancing the oncolytic properties of reoviruses. It is good to realize that reoviruses have not been evolved as oncolytic agents. Hence the reovirus' ability to adapt to changing environments may facilitate the selection of more effective variants. One example of such mutants is the *jin* reoviruses. The prolonged propagation of wild-type reovirus on cells that lack JAM-A on the surface forced the virus to develop a strategy to bypass the JAM-A dependency [26]. This principle can be explored for tumor types that resist reovirus infection at other stages of the viral replicative cycle, such as endosomal escape or cell lysis. Some tumors have evolved strategies to evade cell death signaling pathways and resist cancer therapies that rely on triggering apoptosis [124]. For instance, one Ewing sarcoma cell line (STA-ET2.1) that resists most classical anti-cancer therapies, like chemotherapies and radiation treatments [125], also resists death by reovirus [126]. While the *jin-1*, but not wild-type T3D reovirus, can enter the STA-ET2.1 cells and replicate its genome, the replication is not lytic. By continued passaging of the *jin-1* virus on the STA-ET2.1 cells, a mutant was obtained that readily induces cell death in the infected cells [126]. Currently, the mutants are being characterized and evaluated. These mutants may be useful for obtaining more insight into the cell death pathways that are still functional in therapy-resistant cell lines. In this manner the reovirus demonstrates its plasticity and may have a dual use. On the one hand, reoviruses can be used as a potent anti-cancer agent, while, on the other hand, they may help us as probes to study cellular processes.

## REFERENCES

1. Eisenstein, S.; Chen, S.H.; Pan, P.Y. Immune cells: More than simple carriers for systemic delivery of oncolytic viruses. *Oncolytic Virother.* **2014**, *3*, 83–91.
2. Bell, J.; McFadden, G. Viruses for tumor therapy. *Cell Host Microbe* **2014**, *15*, 260–265.
3. Hammill, A.M.; Conner, J.; Cripe, T.P. Oncolytic virotherapy reaches adolescence. *Pediatric Blood Cancer* **2010**, *55*, 1253–1263.
4. Hashiro, G.; Loh, P.C.; Yau, J.T. The preferential cytotoxicity of reovirus for certain transformed cell lines. *Arch Virol* **1977**, *54*, 307–315.
5. Lee, P.; Clements, D.; Helson, E.; Gujar, S. Reovirus in cancer therapy: An evidence-based review. *Oncolytic Virother* **2014**, *3*, 69–82.
6. Chakrabarty, R.; Tran, H.; Selvaggi, G.; Hagerman, A.; Thompson, B.; Coffey, M. The oncolytic virus, pelareorep, as a novel anticancer agent: A review. *Invest New Drugs* **2015**, *33*, 761–774.
7. Tyler, K.L.; Squier, M.K.; Rodgers, S.E.; Schneider, B.E.; Oberhaus, S.M.; Grdina, T.A.; Cohen, J.J.; Dermody, T.S. Differences in the capacity of reovirus strains to induce apoptosis are determined by the viral attachment protein sigma 1. *J Virol* **1995**, *69*, 6972–6979.
8. Chappell, J.D.; Duong, J.L.; Wright, B.W.; Dermody, T.S. Identification of carbohydrate-binding domains in the attachment proteins of type 1 and type 3 reoviruses. *J Virol* **2000**, *74*, 8472–8479.
9. Sarkar, P.; Danthi, P. Determinants of strain-specific differences in efficiency of reovirus entry. *J Virol* **2010**, *84*, 12723–12732.
10. Weiner, H.L.; Fields, B.N. Neutralization of reovirus: The gene responsible for the neutralization antigen. *J Exp Med* **1977**, *146*, 1305–1310.
11. Weiner, H.L.; Ramig, R.F.; Mustoe, T.A.; Fields, B.N. Identification of the gene coding for the hemagglutinin of reovirus. *Virology* **1978**, *86*, 581–584.
12. Gong, J.; Mita, M.M. Activated ras signaling pathways and reovirus oncolysis: An update on the mechanism of preferential reovirus replication in cancer cells. *Front Oncol* **2014**, *4*, doi: 10.3389/fonc.2014.00167.
13. Marcato, P.; Shmulevitz, M.; Lee, P.W. Connecting reovirus oncolysis and ras signaling. *Cell Cycle* **2005**, *4*, 556–559.
14. Marcato, P.; Shmulevitz, M.; Pan, D.; Stoltz, D.; Lee, P.W.K. Ras transformation mediates reovirus oncolysis by enhancing virus uncoating, particle infectivity, and apoptosis-dependent release. *Mol Ther* **2007**, *15*, 1522–1530.
15. Norman, K.L.; Hirasawa, K.; Yang, A.D.; Shields, M.A.; Lee, P.W. Reovirus oncolysis: The Ras/RalGEF/p38 pathway dictates host cell permissiveness to reovirus infection. *Proc Natl Acad Sci USA* **2004**, *101*, 11099–11104.

16. Smakman, N.; Van Den Wollenberg, D.J.M.; Borel Rinkes, I.H.M.; Hoeben, R.C.; Kranenburg, O. Sensitization to apoptosis underlies KrasD12-dependent oncolysis of murine C26 colorectal carcinoma cells by reovirus T3D. *J Virol* **2005**, *79*, 14981–14985.
17. Kim, M.; Egan, C.; Alain, T.; Urbanski, S.J.; Lee, P.W.; Forsyth, P.A.; Johnston, R.N. Acquired resistance to reoviral oncolysis in ras-transformed fibrosarcoma cells. *Oncogene* **2007**, *26*, 4124–4134.
18. Alain, T.; Kim, T.S.; Lun, X.; Liacini, A.; Schiff, L.A.; Senger, D.L.; Forsyth, P.A. Proteolytic disassembly is a critical determinant for reovirus oncolysis. *Mol Ther* **2007**, *15*, 1512–1521.
19. Campbell, S.A.; Gromeier, M. Oncolytic viruses for cancer therapy I. Cell-external factors: Virus entry and receptor interaction. *Oncol Res Treat* **2005**, *28*, 144–149.
20. Danthi, P.; Holm, G.H.; Stehle, T.; Dermody, T.S. Reovirus receptors, cell entry, and proapoptotic signaling. *Adv Exp Med Biol* **2013**, *790*, 42–71.
21. Danthi, P.; Kobayashi, T.; Holm, G.H.; Hansberger, M.W.; Abel, T.W.; Dermody, T.S. Reovirus apoptosis and virulence are regulated by host cell membrane penetration efficiency. *J Virol* **2008**, *82*, 161–172.
22. Guglielmi, K.M.; Johnson, E.M.; Stehle, T.; Dermody, T.S. Attachment and cell entry of mammalian orthoreovirus. *Curr Top Microbiol Immunol.* **2006**, *309*, 1–38.
23. Morchang, A.; Panaampon, J.; Suttitheptumrong, A.; Yasamut, U.; Noisakran, S.; Yenchitsomanus, P.T.; Limjindaporn, T. Role of cathepsin B in dengue virus-mediated apoptosis. *Biochem Biophys Res Commun* **2013**, *438*, 20–25.
24. Di Piazza, M.; Mader, C.; Geletneky, K.; Herrero y Calle, M.; Weber, E.; Schlehofer, J.; Deleu, L.; Rommelaere, J. Cytosolic activation of cathepsins mediates parvovirus h-1-induced killing of cisplatin and trail-resistant glioma cells. *J Virol* **2007**, *81*, 4186–4198.
25. McGuire, K.A.; Barlan, A.U.; Griffin, T.M.; Wiethoff, C.M. Adenovirus type 5 rupture of lysosomes leads to cathepsin B-dependent mitochondrial stress and production of reactive oxygen species. *J Virol* **2011**, *85*, 10806–10813.
26. Van Den Wollenberg, D.J.M.; Dautzenberg, I.J.C.; Van Den Hengel, S.K.; Cramer, S.J.; De Groot, R.J.; Hoeben, R.C. Isolation of reovirus T3D mutants capable of infecting human tumor cells independent of junction adhesion molecule-A. *PLoS ONE* **2012**, *7*, e48064.
27. Van Den Hengel, S.K.; Balvers, R.K.; Dautzenberg, I.J.; Van Den Wollenberg, D.J.; Kloezeman, J.J.; Lamfers, M.L.; Sillivis-Smit, P.A.; Hoeben, R.C. Heterogeneous reovirus susceptibility in human glioblastoma stem-like cell cultures. *Cancer Gene Ther* **2013**, *20*, 507–513.

28. Campbell, J.A.; Schelling, P.; Wetzel, J.D.; Johnson, E.M.; Forrest, J.C.; Wilson, G.A.; Aurrand-Lions, M.; Imhof, B.A.; Stehle, T.; Dermody, T.S. Junctional adhesion molecule A serves as a receptor for prototype and field-isolate strains of mammalian reovirus. *J Virol* **2005**, *79*, 7967–7978.
29. Stettner, E.; Dietrich, M.H.; Reiss, K.; Dermody, T.S.; Stehle, T. Structure of serotype 1 reovirus attachment protein sigma1 in complex with junctional adhesion molecule a reveals a conserved serotype-independent binding epitope. *J Virol* **2015**, *89*, 6136–6140.
30. Kirchner, E.; Guglielmi, K.M.; Strauss, H.M.; Dermody, T.S.; Stehle, T. Structure of reovirus  $\sigma$ 1 in complex with its receptor junctional adhesion molecule-A. *PLoS Pathog* **2008**, *4*, e1000235.
31. Hunt, D.; Coffin, R.S.; Anderson, P.N. The Nogo receptor, its ligands and axonal regeneration in the spinal cord; a review. *J Neurocytol* **2002**, *31*, 93–120.
32. Konopka-Anstadt, J.L.; Mainou, B.A.; Sutherland, D.M.; Sekine, Y.; Strittmatter, S.M.; Dermody, T.S. The Nogo receptor NgR1 mediates infection by mammalian reovirus. *Cell Host Microbe* **2014**, *15*, 681–691.
33. Wang, C.Q.; Cheng, C.Y. A seamless trespass: Germ cell migration across the seminiferous epithelium during spermatogenesis. *J Cell Biol* **2007**, *178*, 549–556.
34. Pesavento, P.A.; Stokol, T.; Liu, H.; van der List, D.A.; Gaffney, P.M.; Parker, J.S. Distribution of the feline calicivirus receptor junctional adhesion molecule a in feline tissues. *Vet Pathol* **2011**, *48*, 361–368.
35. Bhella, D. The role of cellular adhesion molecules in virus attachment and entry. *Philos Trans R Soc Lond B Biol Sci* **2015**, *370*, 20140035.
36. Dautzenberg, I.J.; Van Den Wollenberg, D.J.; Van Den Hengel, S.K.; Limpens, R.W.; Barcena, M.; Koster, A.J.; Hoeben, R.C. Mammalian orthoreovirus T3D infects U-118 MG cell spheroids independent of junction adhesion molecule-a. *Gene Ther* **2014**, *21*, 609–617.
37. Mason, S.D.; Joyce, J.A. Proteolytic networks in cancer. *Trends Cell Biol* **2011**, *21*, 228–237.
38. Kallunki, T.; Olsen, O.D.; Jaattela, M. Cancer-associated lysosomal changes: Friends or foes? *Oncogene* **2013**, *32*, 1995–2004.
39. Barton, E.S.; Connolly, J.L.; Forrest, J.C.; Chappell, J.D.; Dermody, T.S. Utilization of sialic acid as a coreceptor enhances reovirus attachment by multistep adhesion strengthening. *J Biol Chem* **2001**, *276*, 2200–2211.
40. Reiss, K.; Stencel, J.E.; Liu, Y.; Blaum, B.S.; Reiter, D.M.; Feizi, T.; Dermody, T.S.; Stehle, T. The GM2 glycan serves as a functional coreceptor for serotype 1 reovirus. *PLoS Pathog* **2012**, *8*, e1003078.

41. Stencel-Baerenwald, J.; Reiss, K.; Blaum, B.S.; Colvin, D.; Li, X.N.; Abel, T.; Boyd, K.; Stehle, T.; Dermody, T.S. Glycan engagement dictates hydrocephalus induction by serotype 1 reovirus. *MBio* **2015**, *6*, e02356-14.
42. Reiter, D.M.; Frierson, J.M.; Halvorson, E.E.; Kobayashi, T.; Dermody, T.S.; Stehle, T. Crystal structure of reovirus attachment protein  $\sigma 1$  in complex with sialylated oligosaccharides. *PLoS Pathog* **2011**, *7*, e1002166.
43. Morrison, L.A.; Sidman, R.L.; Fields, B.N. Direct spread of reovirus from the intestinal lumen to the central nervous system through vagal autonomic nerve fibers. *Proc Natl Acad Sci USA* **1991**, *88*, 3852–3856.
44. Weiner, H.L.; Powers, M.L.; Fields, B.N. Absolute linkage of virulence and central nervous system cell tropism of reoviruses to viral hemagglutinin. *J. Infect Dis* **1980**, *141*, 609–616.
45. Mann, M.A.; Knipe, D.M.; Fischbach, G.D.; Fields, B.N. Type 3 reovirus neuroinvasion after intramuscular inoculation: Direct invasion of nerve terminals and age-dependent pathogenesis. *Virology* **2002**, *303*, 222–231.
46. Van den Wollenberg, D.J.; Dautzenberg, I.J.; Ros, W.; Lipinska, A.D.; van den Hengel, S.K.; Hoeben, R.C. Replicating reoviruses with a transgene replacing the codons for the head domain of the viral spike. *Gene Ther* **2015**, *22*, 51–63.
47. Danthi, P.; Pruijssers, A.J.; Berger, A.K.; Holm, G.H.; Zinkel, S.S.; Dermody, T.S. Bid regulates the pathogenesis of neurotropic reovirus. *PLoS Pathog* **2010**, *6*, e1000980.
48. Connolly, J.L.; Dermody, T.S. Virion disassembly is required for apoptosis induced by reovirus. *J Virol* **2002**, *76*, 1632–1641.
49. Knowlton, J.J.; Dermody, T.S.; Holm, G.H. Apoptosis induced by mammalian reovirus is  $\beta$  interferon (IFN) independent and enhanced by IFN regulatory factor 3- and NF- $\lambda$ B-dependent expression of Noxa. *J Virol* **2012**, *86*, 1650–1660.
50. Pan, D.; Pan, L.Z.; Hill, R.; Marcato, P.; Shmulevitz, M.; Vassilev, L.T.; Lee, P.W. Stabilisation of p53 enhances reovirus-induced apoptosis and virus spread through p53-dependent NF- $\lambda$ B activation. *Br J Cancer* **2011**, *105*, 1012–1022.
51. Kominsky, D.J.; Bickel, R.J.; Tyler, K.L. Reovirus-induced apoptosis requires mitochondrial release of Smac/DIABLO and involves reduction of cellular inhibitor of apoptosis protein levels. *J Virol* **2002**, *76*, 11414–11424.
52. Connolly, J.L.; Rodgers, S.E.; Clarke, P.; Ballard, D.W.; Kerr, L.D.; Tyler, K.L.; Dermody, T.S. Reovirus-induced apoptosis requires activation of transcription factor NF- $\kappa$ B. *J Virol* **2000**, *74*, 2981–2989.
53. Nuovo, G.J.; Garofalo, M.; Valeri, N.; Roulstone, V.; Volinia, S.; Cohn, D.E.; Phelps, M.; Harrington, K.J.; Vile, R.; Melcher, A.; *et al.* Reovirus-associated

- reduction of microRNA-let-7d is related to the increased apoptotic death of cancer cells in clinical samples. *Modern Pathol* **2012**, 25, 1333–1344.
54. Clarke, P.; Meintzer, S.M.; Gibson, S.; Widmann, C.; Garrington, T.P.; Johnson, G.L.; Tyler, K.L. Reovirus-induced apoptosis is mediated by trail. *J Virol* **2000**, 74, 8135–8139.
  55. Garant, K.A.; Shmulevitz, M.; Pan, L.; Daigle, R.M.; Ahn, D.G.; Gujar, S.A.; Lee, P.W. Oncolytic reovirus induces intracellular redistribution of Ras to promote apoptosis and progeny virus release. *Oncogene* **2015**, 35, 771–782.
  56. Connolly, J.L.; Barton, E.S.; Dermody, T.S. Reovirus binding to cell surface sialic acid potentiates virus-induced apoptosis. *J Virol* **2001**, 75, 4029–4039.
  57. Coffey, C.M.; Sheh, A.; Kim, I.S.; Chandran, K.; Nibert, M.L.; Parker, J.S. Reovirus outer capsid protein micro1 induces apoptosis and associates with lipid droplets, endoplasmic reticulum, and mitochondria. *J Virol* **2006**, 80, 8422–8438.
  58. Wisniewski, M.L.; Werner, B.G.; Hom, L.G.; Anguish, L.J.; Coffey, C.M.; Parker, J.S. Reovirus infection or ectopic expression of outer capsid protein micro1 induces apoptosis independently of the cellular proapoptotic proteins Bax and Bak. *J Virol* **2011**, 85, 296–304.
  59. Boehme, K.W.; Hammer, K.; Tollefson, W.C.; Konopka-Anstadt, J.L.; Kobayashi, T.; Dermody, T.S. Nonstructural protein sigma1s mediates reovirus-induced cell cycle arrest and apoptosis. *J Virol* **2013**, 87, 12967–12979.
  60. Berger, A.K.; Danthi, P. Reovirus activates a caspase-independent cell death pathway. *MBio* **2013**, 4, e00178–00113.
  61. Thirukkumaran, C.M.; Shi, Z.Q.; Luider, J.; Kopciuk, K.; Gao, H.; Bahlis, N.; Neri, P.; Pho, M.; Stewart, D.; Mansoor, A. *et al.* Reovirus modulates autophagy during oncolysis of multiple myeloma. *Autophagy* **2013**, 9, 413–414.
  62. Thirukkumaran, C.M.; Shi, Z.Q.; Luider, J.; Kopciuk, K.; Gao, H.; Bahlis, N.; Neri, P.; Pho, M.; Stewart, D.; Mansoor, A. *et al.* Reovirus as a viable therapeutic option for the treatment of multiple myeloma. *Clin Cancer Res* **2012**, 18, 4962–4972.
  63. Hiller, B.E.; Berger, A.K.; Danthi, P. Viral gene expression potentiates reovirus-induced necrosis. *Virology* **2015**, 484, 386–394.
  64. Christofferson, D.E.; Yuan, J.Y. Necroptosis as an alternative form of programmed cell death. *Curr. Opin. Cell Biol.* **2010**, 22, 263–268.
  65. Kudchodkar, S.B.; Levine, B. Viruses and autophagy. *Rev Med Virol* **2009**, 19, 359–378.
  66. Ma, Y.; Galluzzi, L.; Zitvogel, L.; Kroemer, G. Autophagy and cellular immune responses. *Immunity* **2013**, 39, 211–227.

67. Chi, P.I.; Huang, W.R.; Lai, I.H.; Cheng, C.Y.; Liu, H.J. The p17 nonstructural protein of avian reovirus triggers autophagy enhancing virus replication via activation of phosphatase and tensin deleted on chromosome 10 (PTEN) and AMP-activated protein kinase (AMPK), as well as dsRNA-dependent protein kinase (PKR)/EIF2 $\alpha$  signaling pathways. *J Biol Chem* **2013**, *288*, 3571–3584.
68. Huang, W.R.; Chiu, H.C.; Liao, T.L.; Chuang, K.P.; Shih, W.L.; Liu, H.J. Avian reovirus protein p17 functions as a nucleoporin tpr suppressor leading to activation of p53, p21 and PTEN and inactivation of P13K/AKT/mTOR and ERK signaling pathways. *PLoS ONE* **2015**, *10*, e0133699.
69. Meng, S.; Jiang, K.; Zhang, X.; Zhang, M.; Zhou, Z.; Hu, M.; Yang, R.; Sun, C.; Wu, Y. Avian reovirus triggers autophagy in primary chicken fibroblast cells and vero cells to promote virus production. *Arch Virol* **2012**, *157*, 661–668.
70. Qin, L.; Wang, Z.; Tao, L.; Wang, Y. Er stress negatively regulates AKT/TSC/mTOR pathway to enhance autophagy. *Autophagy* **2010**, *6*, 239–247.
71. Roulstone, V.; Pedersen, M.; Kyula, J.; Mansfield, D.; Khan, A.A.; McEntee, G.; Wilkinson, M.; Karapanagiotou, E.; Coffey, M.; Marais, R. *et al.* BRAF- and MEK-targeted small molecule inhibitors exert enhanced antimelanoma effects in combination with oncolytic reovirus through ER stress. *Mol Ther* **2015**, *23*, 931–942.
72. Carew, J.S.; Espitia, C.M.; Zhao, W.; Kelly, K.R.; Coffey, M.; Freeman, J.W.; Nawrocki, S.T. Reolysin is a novel reovirus-based agent that induces endoplasmic reticular stress-mediated apoptosis in pancreatic cancer. *Cell Death Dis* **2013**, *4*, e728.
73. Kelly, K.R.; Espitia, C.M.; Mahalingam, D.; Oyajobi, B.O.; Coffey, M.; Giles, F.J.; Carew, J.S.; Nawrocki, S.T. Reovirus therapy stimulates endoplasmic reticular stress, Noxa induction, and augments bortezomib-mediated apoptosis in multiple myeloma. *Oncogene* **2012**, *31*, 3023–3038.
74. Norman, K.L.; Coffey, M.C.; Hirasawa, K.; Demetrick, D.J.; Nishikawa, S.G.; DiFrancesco, L.M.; Strong, J.E.; Lee, P.W. Reovirus oncolysis of human breast cancer. *Hum. Gene Ther* **2002**, *13*, 641–652.
75. Hirasawa, K.; Nishikawa, S.G.; Norman, K.L.; Alain, T.; Kossakowska, A.; Lee, P.W.K. Oncolytic reovirus against ovarian and colon cancer. *Cancer Res* **2002**, *62*, 1696–1701.
76. Marcato, P.; Dean, C.A.; Giacomantonio, C.A.; Lee, P.W. Oncolytic reovirus effectively targets breast cancer stem cells. *Mol Ther* **2009**, *17*, 972–979.
77. Lech, P.J.; Pappoe, R.; Nakamura, T.; Tobin, G.J.; Nara, P.L.; Russell, S.J. Antibody neutralization of retargeted measles viruses. *Virology* **2014**, *454*, 237–246.

78. Calcedo, R.; Franco, J.; Qin, Q.; Richardson, D.W.; Mason, J.B.; Boyd, S.; Wilson, J.M. Preexisting neutralizing antibodies to adeno-associated virus capsids in large animals other than monkeys may confound *in vivo* gene therapy studies. *Hum Gene Ther Methods* **2015**, *26*, 103–105.
79. Bradley, R.R.; Lynch, D.M.; Iampietro, M.J.; Borducchi, E.N.; Barouch, D.H. Adenovirus serotype 5 neutralizing antibodies target both hexon and fiber following vaccination and natural infection. *J Virol* **2012**, *86*, 625–629.
80. Selb, B.; Weber, B. A study of human reovirus IgG and IgA antibodies by elisa and western blot. *J Virol Methods* **1994**, *47*, 15–25.
81. Minuk, G.Y.; Paul, R.W.; Lee, P.W. The prevalence of antibodies to reovirus type 3 in adults with idiopathic cholestatic liver disease. *J Med Virol* **1985**, *16*, 55–60.
82. Adair, R.A.; Roulstone, V.; Scott, K.J.; Morgan, R.; Nuovo, G.J.; Fuller, M.; Beirne, D.; West, E.J.; Jennings, V.A.; Rose, A. *et al.* Cell carriage, delivery, and selective replication of an oncolytic virus in tumor in patients. *Sci Transl Med* **2012**, *4*, 138ra77.
83. Ilett, E.J.; Prestwich, R.J.; Kottke, T.; Errington, F.; Thompson, J.M.; Harrington, K.J.; Pandha, H.S.; Coffey, M.; Selby, P.J.; Vile, R.G. *et al.* Dendritic cells and T cells deliver oncolytic reovirus for tumour killing despite pre-existing anti-viral immunity. *Gene Ther* **2009**, *16*, 689–699.
84. Ilett, E.; Kottke, T.; Donnelly, O.; Thompson, J.; Willmon, C.; Diaz, R.; Zaidi, S.; Coffey, M.; Selby, P.; Harrington, K. *et al.* Cytokine conditioning enhances systemic delivery and therapy of an oncolytic virus. *Mol Ther* **2014**, *22*, 1851–1863.
85. Khalil, D.N.; Budhu, S.; Gasmı, B.; Zappasodi, R.; Hirschhorn-Cymerman, D.; Plitt, T.; de Henau, O.; Zamarin, D.; Holmgaard, R.B.; Murphy, J.T. *et al.* The new era of cancer immunotherapy: Manipulating T-cell activity to overcome malignancy. *Adv Cancer Res* **2015**, *128*, 1–68.
86. Hodi, F.S.; O’Day, S.J.; McDermott, D.F.; Weber, R.W.; Sosman, J.A.; Haanen, J.B.; Gonzalez, R.; Robert, C.; Schadendorf, D.; Hassel, J.C. *et al.* Improved survival with ipilimumab in patients with metastatic melanoma. *N Engl J Med* **2010**, *363*, 711–723.
87. Rosenberg, S.A. IL-2: The first effective immunotherapy for human cancer. *J Immunol* **2014**, *192*, 5451–5458.
88. Devaud, C.; John, L.B.; Westwood, J.A.; Darcy, P.K.; Kershaw, M.H. Immune modulation of the tumor microenvironment for enhancing cancer immunotherapy. *Oncoimmunology* **2013**, *2*, e25961.
89. Nishikawa, H.; Sakaguchi, S. Regulatory T cells in cancer immunotherapy. *Curr Opin Immunol* **2014**, *27*, 1–7.

90. Kerkar, S.P.; Restifo, N.P. Cellular constituents of immune escape within the tumor microenvironment. *Cancer Res* **2012**, *72*, 3125–3130.
91. Prestwich, R.J.; Ilett, E.J.; Errington, F.; Diaz, R.M.; Steele, L.P.; Kottke, T.; Thompson, J.; Galivo, F.; Harrington, K.J.; Pandha, H.S. *et al.* Immune-mediated antitumor activity of reovirus is required for therapy and is independent of direct viral oncolysis and replication. *Clin Cancer Res* **2009**, *15*, 4374–4381.
92. Lichty, B.D.; Breitbach, C.J.; Stojdl, D.F.; Bell, J.C. Going viral with cancer immunotherapy. *Nat Rev Cancer* **2014**, *14*, 559–567.
93. Gujar, S.A.; Lee, P.W. Oncolytic virus-mediated reversal of impaired tumor antigen presentation. *Front Oncol* **2014**, *4*, 77.
94. Hu, J.C.; Coffin, R.S.; Davis, C.J.; Graham, N.J.; Groves, N.; Guest, P.J.; Harrington, K.J.; James, N.D.; Love, C.A.; McNeish, I. *et al.* A phase I study of oncovexgm-CSF, a second-generation oncolytic herpes simplex virus expressing granulocyte macrophage colony-stimulating factor. *Clin Cancer Res* **2006**, *12*, 6737–6747.
95. Andtbacka, R.H.; Kaufman, H.L.; Collichio, F.; Amatruda, T.; Senzer, N.; Chesney, J.; Delman, K.A.; Spitler, L.E.; Puzanov, I.; Agarwala, S.S. *et al.* Talimogene laherparepvec improves durable response rate in patients with advanced melanoma. *J Clin Oncol* **2015**, *33*, 2780–2788.
96. Sheridan, C. First oncolytic virus edges towards approval in surprise vote. *Nat Biotech* **2015**, *33*, 569–570.
97. The angeles clinic and research institute. Available online: <http://www.theangelesclinic.org> (Accessed December 2015).
98. Egen, J.G.; Kuhns, M.S.; Allison, J.P. CTLA-4: New insights into its biological function and use in tumor immunotherapy. *Nat Immunol* **2002**, *3*, 611–618.
99. Bauzon, M.; Hermiston, T. Armed therapeutic viruses—A disruptive therapy on the horizon of cancer immunotherapy. *Front Immunol* **2014**, *5*, 74.
100. Rajani, K.; Parrish, C.; Shim, K.; Ilett, L.; Thompson, J.; Kottke, T.; Pulido, J.; Errington-Mais, F.; Selby, P.; Pandha, H. *et al.* Combination therapy with reovirus and PD-1 blockade effectively establishes tumor control via innate and adaptive immune responses, In *Proceedings of AACR Tumor Immunology and Immunotherapy Conference*, Orlando, FL, USA, **2014**.
101. Chen, D.S.; Mellman, I. Oncology meets immunology: The cancer-immunity cycle. *Immunity* **2013**, *39*, 1–10.
102. Clements, D.R.; Sterea, A.M.; Kim, Y.; Helson, E.; Dean, C.A.; Nunokawa, A.; Coyle, K.M.; Sharif, T.; Marcato, P.; Gujar, S.A. *et al.* Newly recruited cd11b<sup>+</sup>, gr-1<sup>+</sup>, ly6c<sup>high</sup> myeloid cells augment tumor-associated immunosuppression

- immediately following the therapeutic administration of oncolytic reovirus. *J Immunol* **2015**, 194, 4397–4412.
103. Dolcetti, L.; Peranzoni, E.; Ugel, S.; Marigo, I.; Fernandez Gomez, A.; Mesa, C.; Geilich, M.; Winkels, G.; Traggiai, E.; Casati, A. Hierarchy of immunosuppressive strength among myeloid-derived suppressor cell subsets is determined by gm-csf. *Eur J Immunol* **2010**, 40, 22–35.
  104. Morales, J.K.; Kmiecik, M.; Knutson, K.L.; Bear, H.D.; Manjili, M.H. GM-CSF is one of the main breast tumor-derived soluble factors involved in the differentiation of CD11b-Gr1-bone marrow progenitor cells into myeloid-derived suppressor cells. *Breast Cancer Res Trans* **2010**, 123, 39–49.
  105. Rojas, J.; Sampath, P.; Hou, W.; Thorne, S.H. Defining effective combinations of immune checkpoint blockade and oncolytic virotherapy. *Clin Cancer Res* **2015**, 21, 5543–5551.
  106. Kobayashi, T.; Antar, A.A.R.; Boehme, K.W.; Danthi, P.; Eby, E.A.; Guglielmi, K.M.; Holm, G.H.; Johnson, E.M.; Maginnis, M.S.; Naik, S. *et al.* A plasmid-based reverse genetics system for animal double-stranded RNA viruses. *Cell Host Microbe* **2007**, 1, 147–157.
  107. Nygaard, R.M.; Lahti, L.; Boehme, K.W.; Ikizler, M.; Doyle, J.D.; Dermody, T.S.; Schiff, L.A. Genetic determinants of reovirus pathogenesis in a murine model of respiratory infection. *J Virol* **2013**, 87, 9279–9289.
  108. Pruijssers, A.J.; Hengel, H.; Abel, T.W.; Dermody, T.S. Apoptosis induction influences reovirus replication and virulence in newborn mice. *J Virol* **2013**, 87, 12980–12989.
  109. Sarkar, P.; Danthi, P. The  $\mu$ 1 72–96 loop controls conformational transitions during reovirus cell entry. *J Virol* **2013**, 87, 13532–13542.
  110. Mohamed, A.; Johnston, R.N.; Shmulevitz, M. Potential for improving potency and specificity of reovirus oncolysis with next-generation reovirus variants. *Viruses* **2015**, 7, 6251–6278.
  111. MacNeill, A. On the potential of oncolytic virotherapy for the treatment of canine cancers. *Oncolytic Virother* **2015**, 4, 95–107.
  112. Van Den Wollenberg, D.J.M.; Van Den Hengel, S.K.; Dautzenberg, I.J.C.; Cramer, S.J.; Kranenburg, O.; Hoeben, R.C. A strategy for genetic modification of the spike-encoding segment of human reovirus T3D for reovirus targeting. *Gene Ther* **2008**, 15, 1567–1578.
  113. Brochu-Lafontaine, V.; Lemay, G. Addition of exogenous polypeptides on the mammalian reovirus outer capsid using reverse genetics. *J Virol Methods* **2012**, 179, 342–350.
  114. Demidenko, A.A.; Blattman, J.N.; Blattman, N.N.; Greenberg, P.D.; Nibert, M.L. Engineering recombinant reoviruses with tandem repeats and a tetra virus 2A-

- like element for exogenous polypeptide expression. *Proc Natl Acad Sci USA* **2013**, 110, E1867–E1876.
115. Roner, M.R.; Joklik, W.K. Reovirus reverse genetics: Incorporation of the cat gene into the reovirus genome. *Proc Natl Acad Sci USA* **2001**, 98, 8036–8041.
  116. Kapikian, A.Z.; Shope, R.E. Rotaviruses, reoviruses, coltivirus, and orbiviruses. In *Medical microbiology*, 4th ed.; Baron, S., Ed. The University of Texas Medical Branch at Galveston: Galveston TX, Mexico, **1996**.
  117. Montufar-Solis, D.; Klein, J.R. Experimental intestinal reovirus infection of mice: What we know, what we need to know. *Immunol Res* **2005**, 33, 257–265.
  118. Major, A.S.; Rubin, D.H.; Cuff, C.F. Mucosal immunity to reovirus infection. In *Reoviruses II*, Tyler, K.; Oldstone, M.A., Eds. Springer-Verlag Berlin Heidelberg; Heidelberg, Germany, **1998**; 233/2, 163–177.
  119. Tyler, K.L. Pathogenesis of reovirus infections of the central nervous system. In *Reoviruses II*, Tyler, K.; Oldstone, M.A., Eds. Springer-Verlag Berlin Heidelberg; Heidelberg, Germany, **1998**; 233/2, 93–124.
  120. Organ, E.L.; Rubin, D.H. Pathogenesis of reovirus gastrointestinal and hepatobiliary disease. In *Reoviruses II*, Tyler, K.; Oldstone, M.A., Eds. Springer-Verlag Berlin Heidelberg; Heidelberg, Germany, **1998**; 233/2, 67–83.
  121. Smakman, N.; Van Der Bilt, J.D.W.; Van Den Wollenberg, D.J.M.; Hoeben, R.C.; Borel Rinkes, I.H.M.; Kranenburg, O. Immunosuppression promotes reovirus therapy of colorectal liver metastases. *Cancer Gene Ther* **2006**, 13, 815–818.
  122. Westberg, S.; Sadeghi, A.; Svensson, E.; Segall, T.; Dimopoulou, M.; Korsgren, O.; Hemminki, A.; Loskog, A.S.; Totterman, T.H.; von Euler, H. Treatment efficacy and immune stimulation by *adcd40l* gene therapy of spontaneous canine malignant melanoma. *J Immunother* **2013**, 36, 350–358.
  123. Moore, P.S.; Chang, Y. Why do viruses cause cancer? Highlights of the first century of human tumour virology. *Nat Rev Cancer* **2010**, 10, 878–889.
  124. Debatin, K.M.; Krammer, P.H. Death receptors in chemotherapy and cancer. *Oncogene* **2004**, 23, 2950–2966.
  125. Van Valen, F.; Fulda, S.; Truckenbrod, B.; Eckervogt, V.; Sonnemann, J.u.r.; Hillmann, A.; Rodl, R.; Hoffmann, C.; Winkelmann, W.; Schafer, L. *et al.* Apoptotic responsiveness of the Ewing's sarcoma family of tumours to tumour necrosis factor-related apoptosis-inducing ligand (trail). *Int J Cancer* **2000**, 88, 252–259.
  126. Van Den Wollenberg, D.J.M. Unpublished observations. *Manuscript in preparation*.



**3**

Oncolytic reovirus infection  
is facilitated by the autophagic  
machinery

Vera Kemp, Iris J.C. Dautzenberg, Ronald W.  
Limpens, Diana J.M. van den Wollenberg,  
and Rob C. Hoeben

Department of Molecular Cell Biology, Leiden  
University Medical Center, P.O. Box 9600,  
2300 RC Leiden, the Netherlands

Viruses 2017, 9(10), 266

## **ABSTRACT**

Mammalian reovirus is a double-stranded RNA virus that selectively infects and lyses transformed cells, making it an attractive oncolytic agent. Despite clinical evidence for anti-tumor activity, its efficacy as a stand-alone therapy remains to be improved. The success of future trials can be greatly influenced by the identification and the regulation of the cellular pathways that are important for reovirus replication and oncolysis. Here, we demonstrate that reovirus induces autophagy in several cell lines, evident from the formation of Atg5-Atg12 complexes, microtubule-associated protein 1 light chain 3 (LC3) lipidation, p62 degradation, the appearance of acidic vesicular organelles, and LC3 puncta. Furthermore, in electron microscopic images of reovirus-infected cells, autophagosomes were observed without evident association with viral factories. Using UV-inactivated reovirus, we demonstrate that a productive reovirus infection facilitates the induction of autophagy. Importantly, knock-out cell lines for specific autophagy-related genes revealed that the expression of Atg3 and Atg5 but not Atg13 facilitates reovirus replication. These findings highlight a central and Atg13-independent role for the autophagy machinery in facilitating reovirus infection and contribute to a better understanding of reovirus-host interactions.

## INTRODUCTION

Mammalian orthoreovirus, henceforth referred to as reovirus, is broadly studied as an anti-cancer agent both as a monotherapy and in combination with existing therapies [1]. It has the natural preference to replicate in and lyse tumor cells, while an antiviral response in normal cells hinders virus replication and cytolysis. The name reovirus is an acronym for respiratory and enteric orphan virus, as it infects the respiratory and enteric tract and has not been associated with serious disease in humans. Reovirus is one of the first viruses for which a molecular mechanism has been suggested to explain its tumor cell preference [2]. This mechanism contributed to its clinical evaluation as viral oncolytic agent. To date, a variety of clinical trials have been completed in several cancer types, but while the virus administration has been found safe, its efficacy in stand-alone treatments remains to be improved. A better understanding of what intracellular factors and pathways are important to reovirus replication and oncolysis would facilitate the improved design of clinical studies.

Various viruses have been shown to induce a host-cell adaptive response called macroautophagy, hereafter referred to as autophagy [3]. During autophagy, the cytoplasmic cellular contents are sequestered within double-membraned vesicles termed autophagosomes, which ultimately fuse to endosomes or lysosomes to form amphisomes or autolysosomes, respectively. This process facilitates the degradation of the cellular contents, even whole organelles, upon which the degradation products can be shuttled back into the cytosol for recycling. This highly conserved homeostatic process allows the cell to survive stressful conditions such as a nutrient-poor environment. Autophagy can also be exploited to combat viral infections. For instance, it can promote the intracytoplasmic degradation of viruses such as Sindbis virus and HIV-1 [4, 5].

Alternatively, it can activate an anti-viral immune response through the delivery of viral genomic components to endosomal Toll-like receptors (TLRs) or through the facilitation of viral antigen presentation on major histocompatibility complex (MHC) molecules [3, 6]. On the other hand, it has been demonstrated that viruses have evolved ways to either suppress or induce the autophagy machinery to facilitate their replication and/or survival [3]. For example, autophagy facilitates cancer cell death induction by human adenovirus type 5, presumably through the triggering of caspase activity [7]. Autophagy has also been shown to facilitate the infection of several dsRNA virus family members. Rotavirus induces microtubule-associated protein 1 light chain 3 (LC3) lipidation and inhibition of this process decreases virus replication [8].

Interestingly, rotavirus does not induce the formation of autophagosomes. Furthermore, the non-structural avian reovirus protein p17 triggers autophagy

which enhances virus replication [9]. For bluetongue virus, a similar correlation has been found, as inhibition of autophagy decreases viral protein production and virus titer, and the stimulation of autophagy conversely resulted in increased viral protein synthesis and virus yields [10]. It has been suggested that mammalian reovirus induces autophagy as well, though the precise function during reovirus infection remained unclear [11, 12].

In the present study, we show that reovirus induces the full autophagic flux in immortalized mouse embryonic fibroblasts. The presence of a distinct set but not all of the autophagy-related proteins seems to facilitate reovirus replication. Importantly, autophagic features could also be observed in human glioblastoma cell lines. Moreover, a productive reovirus infection facilitates the induction of autophagy.

## **MATERIALS AND METHODS**

### *Reagents and buffers*

Rapamycin (Rapa) and Bafilomycin A1 (BafA1) were purchased from Sigma-Aldrich (St. Louis, MO). Stock solutions were stored at -20°C. Rapa was reconstituted in pure ethanol at a concentration of 1 mM, and BafA1 in pure ethanol at a concentration of 50 µM. Acridine orange (Sigma-Aldrich) was reconstituted in milli-Q at a concentration of 2 mM.

RIPA lysis buffer contains 50 mM Tris-HCl pH 7.5, 150 mM sodium chloride, 0.1% sodium dodecyl sulphate (SDS), 0.5% sodium deoxycholate, and 1% NP40. Giordano lysis buffer contains 50 mM Tris-HCl pH 7.4, 250 mM sodium chloride, 0.1% Triton X-100, and 5 mM EDTA. Lysis buffers were supplemented with protease inhibitors (Complete mini tablets, Roche Diagnostics, Almere, the Netherlands). Western sample buffer has the following concentrations: 50 mM Tris-HCl pH 6.8, 10% glycerol, 2.5% β-mercaptoethanol, 2% SDS, and 0.025% bromophenol blue.

### *Cell lines*

Human embryonic kidney 293T [13], embryonic retinoblast-derived 911 [14], glioblastoma U87-MG (ATCC) and U251-MG (ATCC) cell lines were cultured at 37°C in high glucose Dulbecco's Modified Eagle Medium (DMEM) (Invitrogen, Breda, the Netherlands), supplemented with penicillin, streptomycin (pen-strep) and 8% fetal bovine serum (FBS) (Invitrogen, Breda, the Netherlands). Immortalized Atg3<sup>-/-</sup> and the control wild-type Atg3<sup>WT</sup> mouse embryonic fibroblasts (MEFs) were kindly provided by Masaaki Komatsu, the Tokyo Metropolitan Institute Medical Science [15]; Atg5<sup>-/-</sup>, and the wild-type Atg5<sup>WT</sup> MEFs by Noboru Mizushima, the University of Tokyo [16]; Atg13<sup>-/-</sup> with the control Atg13<sup>WT</sup> MEFs by Xiaodong Wang, Beijing National Institute of Biological Sciences [17]. Atg3 and Atg5 genes were reintroduced

in the immortalized knock-out MEFs by lentiviral or retroviral transductions. Lentivirus and retrovirus was produced by standard production protocols. MEFs with a reintroduced Atg13 gene were kindly provided by Fulvio Reggiori (University Medical Center Groningen, the Netherlands), and were previously described in literature [18]. All MEFs were cultured in DMEM plus pen-strep and 10% FBS. The Atg3<sup>WT</sup>, Atg3<sup>-/-</sup>, and Atg3<sup>+/+</sup> MEFs were cultured at 32°C, and all other MEFs at 37°C. All cell lines were maintained in a 5% CO<sub>2</sub> atmosphere.

### *Viruses*

The wild-type (wt) Type 3 Dearing (T3D) strain R124 was isolated from a reovirus T3D stock obtained from ATCC and propagated as previously described [19]. The *jln* mutant reoviruses were isolated from U118-MG cells upon infection with wt T3D [19]. Infectious virus titers were determined by plaque assays on 911 cells. All experiments were performed with cesium chloride (CsCl) purified virus stocks.

For UV inactivation, R124 was reconstituted at a concentration of 5.95x10<sup>9</sup> pfu/ml in MEM supplemented with pen-strep and 2% FBS. UV inactivation was achieved by exposure to shortwave UV light for 15 minutes. The absence of infectious virus was confirmed by plaque assay on 911 cells (≤ 10 pfu/ml).

### *Yield quantification*

To determine the replication of R124 and *jln-3* in MEFs, cells were seeded in 24-well plates at a density of 1x10<sup>5</sup> cells/well. Infections with R124 or *jln-3* reoviruses were performed at the indicated multiplicity of infection (MOI), in DMEM containing 2% FBS and pen-strep. After the indicated time periods, when cytopathic effect (CPE) became clearly visible, reoviruses were harvested from the cells and medium by 3 freeze-thaw cycles. Virus yields were quantified by plaque assays on 911 cells.

### *Western blotting*

For western blot analysis, the total protein concentrations were determined by a BCA assay kit (Thermo Scientific Pierce, Rockford, IL). Equal amounts of protein (30 µg) were separated by gel electrophoresis on gels with the indicated percentage of polyacrylamide, and transferred onto Immobilon-P membranes (Millipore, Etten-Leur, the Netherlands). The proteins were visualized using standard protocols. Primary antibodies rabbit anti-Atg5 [ab108327], mouse anti-LC3B [ab129376], rabbit anti-Atg3 [EPR4801] (Abcam, Cambridge, UK), mouse anti-p62 [ab56416] (Abcam, Cambridge, UK) were purchased from Abcam, rabbit anti-LC3B [NB600-1384] from Novus Biologicals (Littleton, CO, USA), mouse anti-β-actin from MP Biomedicals (Santa Ana, CA, USA), and rabbit anti-Atg13 from Sigma-Aldrich (St. Louis, MO, USA). Primary 4F2 mouse anti-reovirus σ3 was obtained from the Developmental Studies

Hybridoma Bank developed under the auspices of the NICHD and maintained by the University of Iowa, Department of Biology (Iowa City, IA, USA) [20].

#### *eGFP-LC3 fluorescence microscopy*

The eGFP-LC3 fusion orf from plasmid Addgene #11546 was cloned downstream of the internal CMV promoter of plasmid pLV-CMV-IRES Puro expressing a puromycin-resistance cassette. Atg3<sup>WT</sup> MEFs were transduced with the lentivirus, and puromycin selection was performed. The resulting eGFP-LC3 expressing Atg3<sup>WT</sup> MEFs will be referred to as Atg3<sup>WT-G</sup> MEFs. To analyze the localization of LC3, Atg3<sup>WT-G</sup> MEFs were seeded on cover slips in 24-well plates at 100,000 cells/well, and infected with R124 or *jin-3* at an MOI of 10. As a positive control, cells were treated with Rapa at a concentration of 1  $\mu$ M, and 50 nM BafA1 was supplemented 16 hours before the end of the experiment. After 72 hours, the cells were fixed in 4% paraformaldehyde (PFA), permeabilized with 0.5% Triton, blocked with 3% BSA, and stained with primary and secondary antibodies. The primary antibody used is the 10F6 mouse anti- $\mu$ 1C antibody, obtained from the Developmental Studies Hybridoma Bank developed under the auspices of the NICHD and maintained by the University of Iowa, Department of Biology (Iowa City, IA, USA) [20]. A647-coupled anti-mouse antibody was used as a secondary antibody. After the antibody stainings, the coverslips were incubated in anti-fade reagent (ProLong Gold with DAPI, Cell Signaling Technology, Leiden, the Netherlands) on a glass microscopic slide, and imaged the next day using a Leica DM6B fluorescence microscope (Wetzlar, Germany) and home-made ColourProc software (Leiden University Medical Center, Leiden, the Netherlands).

#### *Acridine Orange staining*

To examine the presence of acidic vesicular organelles, U87-MG cells were grown on cover slips in 24-well plates at 100,000 cells/well, and exposed to R124 at an MOI of 10. Alternatively, cells were treated with 400 nM Rapa. After 48 hours, acridine orange was added (15 minutes, 37°C). The cover slips were transferred to glass microscopic slides and analyzed by fluorescence microscopy using a Leica DMRA fluorescence microscope and ColourProc software.

#### *Electron microscopy*

For electron microscopy analysis, U87-MG cells were seeded in 10cm dishes at  $3 \times 10^6$  cells/dish, and exposed to R124 at an MOI of 10 or 400 nM Rapa. After 48 hours, cells were fixed in 1.5% glutaraldehyde in 0.1 M Cacodylate buffer (1 hour, room temperature), post-fixed in 1% OsO<sub>4</sub> in 0.1 M Cacodylate buffer (1 hour, 4°C), dehydrated in a graded ethanol series, and embedded in epon. Ultrathin cell sections

(100nm) were post-stained with uranyl acetate and lead citrate. Analyses were performed using a Tecnai 12 electron microscope at 120 kV, equipped with a 4K Eagle CCD Camera (FEI Company, Eindhoven, the Netherlands).

## RESULTS

### *Reovirus induces LC3 puncta in MEFs*

During autophagy, microtubule-associated protein 1 light chain 3 (LC3) is recruited to autophagosomal membranes [21]. To determine whether reovirus induces autophagy, the localization of LC3 was examined. To this end, mouse embryonic fibroblasts (MEFs) were stably transduced with the GFP-LC3 lentivirus and infected with R124 or *jin-3* reovirus. R124 is our wild-type type 3 Dearing (T3D) strain, and *jin-3* was obtained through serial passaging of the T3D reovirus on glioblastoma cells that lack the expression of the reovirus receptor junction adhesion molecule-A (JAM-A) [19]. As a positive control, cells were treated with Rapamycin (Rapa) and Bafilomycin A1 (BafA1). Rapa is an mTOR inhibitor and a known autophagy inducer [21]. BafA1 blocks the acidification of lysosomes or the fusion between autophagosomes and lysosomes, and thereby arrests the autophagic flux through blocking the degradation of autophagosomes and their content. If autophagy is induced, the localization of the GFP-LC3 fusion protein shifts from a diffuse cytoplasmic appearance to a punctuate pattern. Immunofluorescent images revealed the induction of clear LC3 puncta upon reovirus infection and upon treatment with Rapa and BafA1 (Figure 1). Notably, LC3 puncta appeared to be present in cells that showed reovirus protein expression as well, as shown by a co-staining for reovirus protein  $\mu$ 1C. These findings suggest that reovirus induces autophagy.

### *Reovirus induces Atg5-Atg12 conjugation, p62 degradation, and LC3 lipidation in MEFs*

Autophagy is characterized by the conjugation of Atg5 to Atg12 [21], resulting in a loss of free Atg5. Moreover, LC3-I is lipidated to form LC3-II. To examine whether reovirus induces these autophagic features, MEFs were infected with R124 or *jin-3*, and analyzed for the expression of free Atg5, and LC3. Reovirus infection clearly decreased the levels of free Atg5 and increased the conversion of LC3-I to LC3-II (Figure 2), most evident from the reduction in LC3 levels. These findings support the hypothesis that reovirus induces autophagy in MEFs. The *jin* strain seems to be a more potent inducer of autophagy than R124, probably caused by its ability to enter cells through a JAM-A independent mechanism. MEFs express modest levels of JAM-A on their cell surface hampering infection by R124 [22].

During the later steps in the autophagic process, p62 will be degraded inside the autophagolysosomes [21]. To establish whether the complete autophagic flux is induced by reovirus, p62 expression was determined. Upon infection with R124 and *jin-3*, a clear decrease in p62 levels could be detected, indicating that the full flux of autophagy was induced.

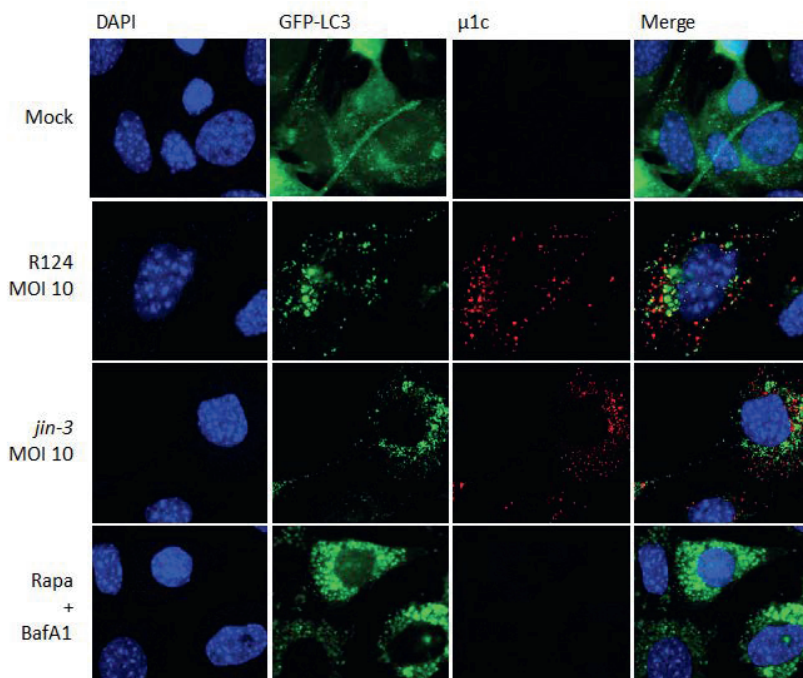


**Figure 1.** Reovirus infection triggers microtubule-associated protein 1 light chain 3 (LC3) puncta in MEFs. MEFs were infected with R124 or *jin-3* at a multiplicity of infection (MOI) of 10. Alternatively, cells were treated with 1  $\mu$ M Rapamycin (Rapa) and after 32 hours, 50 nM BafA1 was supplemented to the Rapa-treated cells. Cells were fixed after 48 hours treatment, and stained for reovirus  $\mu$ 1C protein in red. Cell nuclei are visible in blue (DAPI), and GFP-LC3 in green.

#### *Atg3 and Atg5 but not Atg13 expression facilitate reovirus replication*

To examine the importance of the autophagy machinery for reovirus infection, we used SV40-transformed MEF cell lines with a knock-out for a specific autophagy-related gene: Atg3, Atg5, or Atg13. Western blot results confirmed the absence of Atg3, Atg5, and Atg13 protein expression in the corresponding knock-out cell line (Figures 3-5). We infected the MEFs with R124 or *jin-3* and examined the cell

viability, reovirus  $\sigma 3$  protein expression and virus titer in the cells. For the different knock-outs, minor effects were seen on reovirus-induced cytolysis [23]. However,  $\sigma 3$  protein expression and virus titers were markedly decreased in MEFs lacking Atg3 or Atg5 compared to the corresponding wild-type and rescued cells (Figures 3 and 4). Interestingly, a knock-out for Atg13 did neither affect the reovirus  $\sigma 3$  expression nor the titer (Figure 5). Altogether, these results indicate that the expression of Atg3 and Atg5 but not Atg13 facilitates the replication of reovirus in SV40-transformed MEFs.

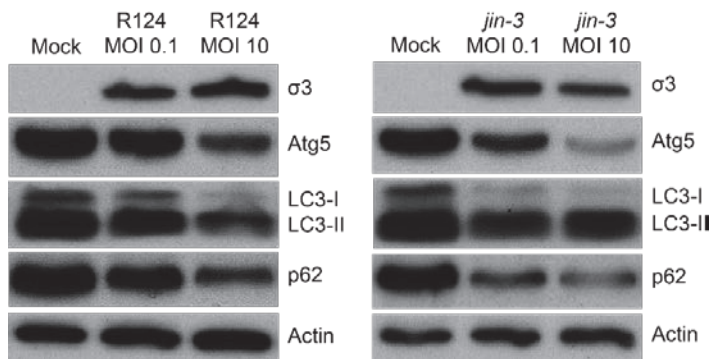


**Figure 2.** Reovirus infection induces Atg5-Atg12 conjugation, LC3-I to LC3-II conversion, and p62 degradation in MEFs. MEFs were infected with R124 or *jin-3* at an MOI of 0.1 or 10. Protein lysates were prepared in Giordano lysis buffer 48 hours post infection (hpi), and analyzed for the amounts of  $\sigma 3$ , Atg5, LC3, p62, and Actin by western analysis.

#### *Reovirus induces Atg5-Atg12 conjugation, LC3 lipidation, and acidic vesicular organelles in glioblastoma cell lines*

With the finding that reovirus induces several autophagic features in SV40-transformed MEFs, the question remains whether the same holds true for human cell lines. To study whether reovirus induces autophagy in human tumor cell lines, glioblastoma cell lines U251-MG and U87-MG were infected with R124 or *jin-1*, or stimulated with Rapa. *Jin-1* was the first mutant reovirus we isolated from reovirus-infected JAM-A deficient glioblastoma cells [19]. At the indicated time points after treatment, protein lysates were made and analyzed for the expression of unconjugated Atg5 and LC3-I/LC3-II. Upon infection or Rapa treatment, Atg5 expression was decreased and the LC3-II/LC3-I ratio increased in U87-MG cells (Figure 6). U251-MG cells can be infected and killed efficiently by the *jin* reoviruses but not R124 [24]. Corresponding to this, altered Atg5 and LC3-II expression levels were observed upon Rapa treatment and *jin-1* but not R124 infection. Altogether, these data suggest that reovirus induces autophagy in human glioblastoma cell lines.

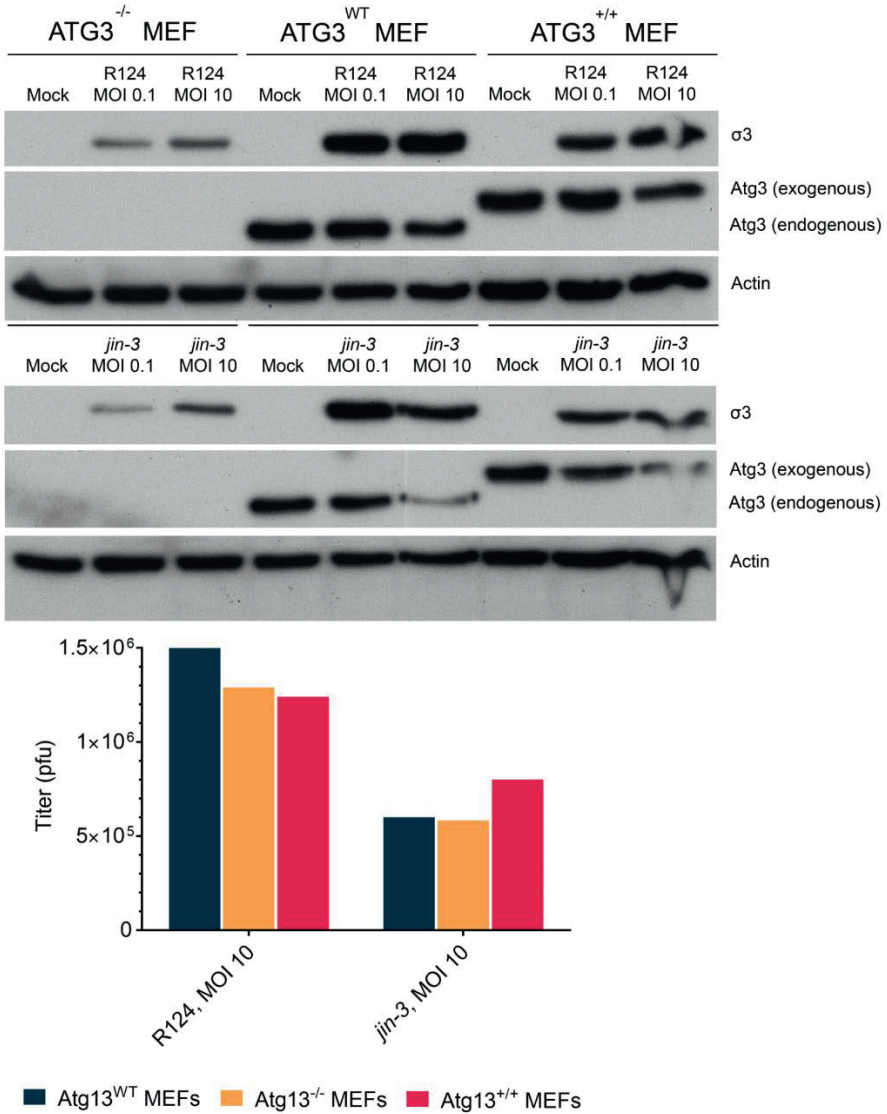


**Figure 3.** Reovirus replication in MEFs is facilitated by the expression of Atg3. Atg3<sup>WT</sup>, Atg3<sup>-/-</sup> and Atg3<sup>+/+</sup> MEFs were infected with R124 or *jin-3* at an MOI of 0.1 or 10. After 48 hours, protein lysates were prepared in Giordano lysis buffer and analyzed for the expression of  $\sigma 3$ , Atg3, and Actin. In parallel, cells were collected in the supernatant, lysed by 3 freeze-thaw cycles, and the total amount of infectious virus particles in the 24-well plate well was determined by plaque assays.

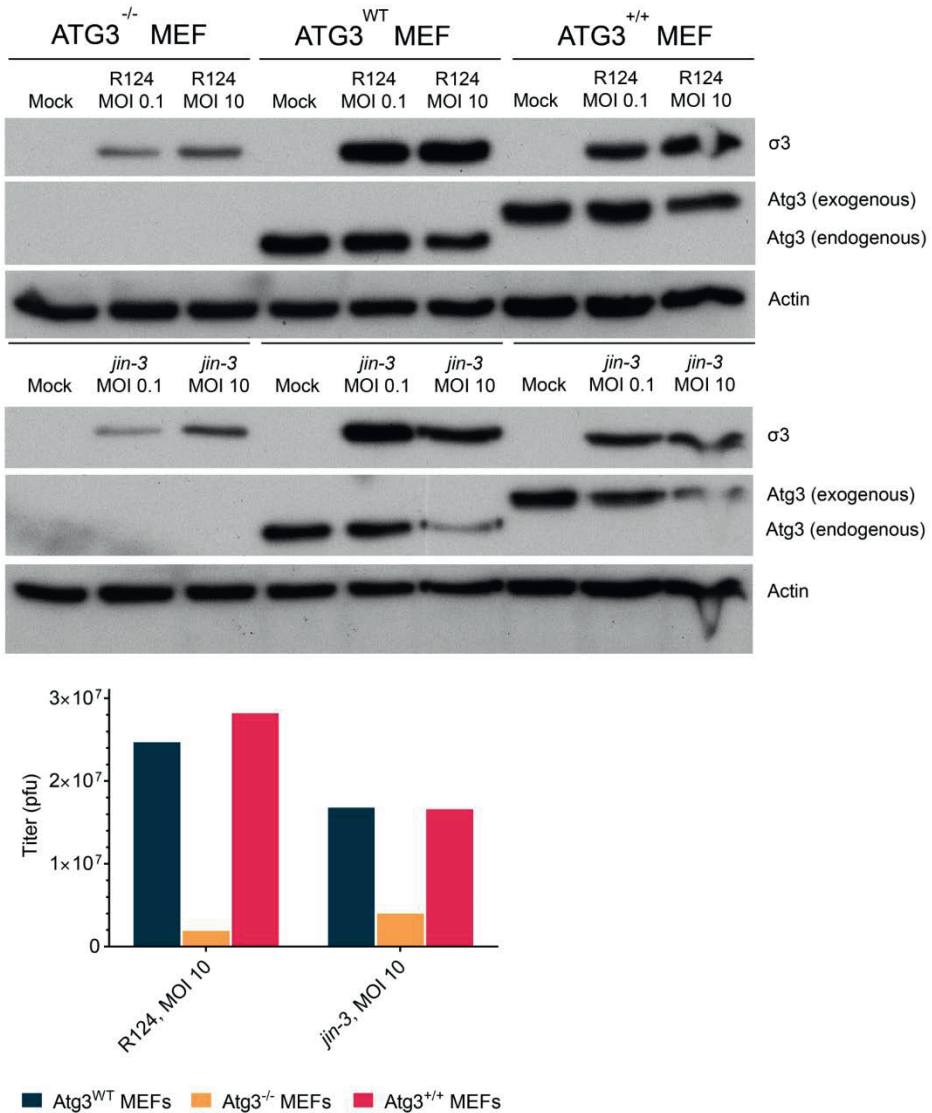


**Figure 4.** Reovirus replication is facilitated by the expression of Atg5. Atg5<sup>WT</sup>, Atg5<sup>-/-</sup>, and Atg5<sup>+/+</sup> MEFs were infected with R124 or *jin-3* at an MOI of 1. After 72 hours, protein lysates were prepared in Giordano lysis buffer and analyzed for the expression of σ3, Atg5, and Actin. Alternatively, cells were collected in the supernatant, lysed by 3 freeze-thaw cycles, and the total amount of infectious virus particles in the 24-well plate well was determined by plaque assays.

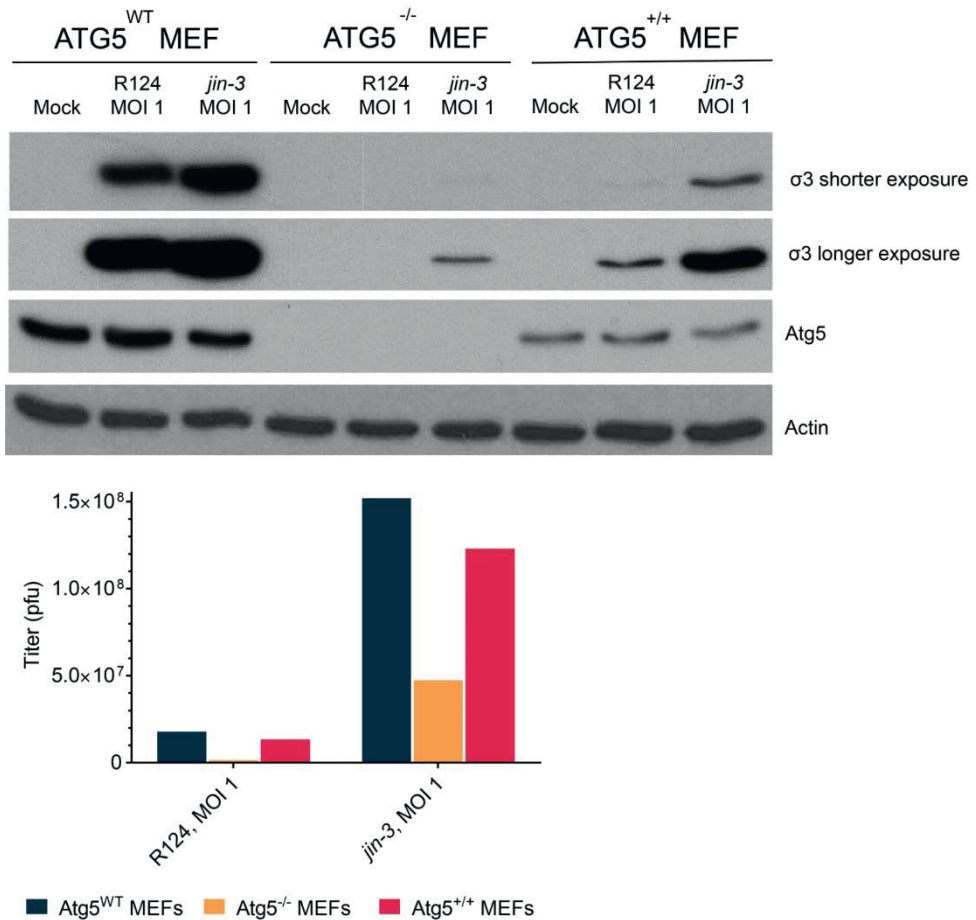


**Figure 5.** Reovirus replication is not influenced by Atg13 expression. Atg13<sup>WT</sup>, Atg13<sup>-/-</sup>, and Atg13<sup>+/+</sup> MEFs were infected with R124 or *jln-3* at an MOI of 0.1 or 10. After 48 hours, protein lysates were prepared in Giordano lysis buffer and analyzed for the expression of σ3, Atg13, and Actin. In parallel, cells were collected in the supernatant, lysed by 3 freeze-thaw cycles, and the total amount of infectious virus particles in the 24-well plate well was determined by plaque assays.

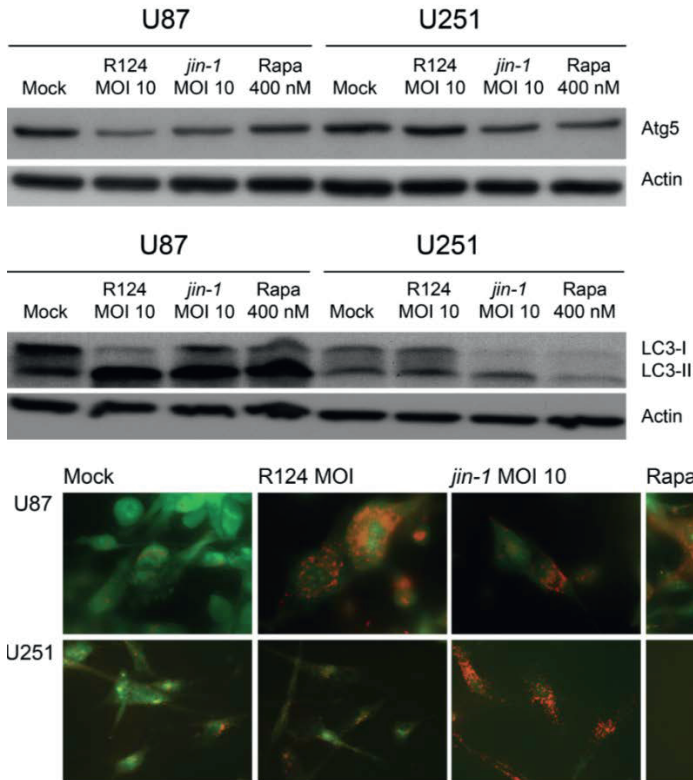


**Figure 6.** Reovirus infection induces Atg5-Atg12 conjugation, LC3-I to LC3-II conversion, and acidic vesicular organelles in U87-MG and U251-MG glioblastoma cells. U87-MG and U251-MG glioblastoma cells were infected with R124 or *jin-1* at an MOI of 10, or treated with 400 nM Rapa. After 48 hours (U87-MG) or 54 hours (U251-MG), protein lysates were prepared in RIPA lysis buffer and analyzed for the expression of Atg5, LC3, and Actin. Alternatively, cells were incubated with acridine orange after 48 hours (U87-MG) or 120 hours (U251-MG), and fluorescence microscopy pictures were taken.

Autophagic vacuoles ultimately fuse to lysosomes, resulting in the formation of enlarged acidic vesicles in cells undergoing autophagy. To study the degree to which acidic vesicles are present in U87-MG and U251-MG cells upon reovirus infection, acridine orange was used. When added to cells, this dye diffuses throughout the cell and once in an acidic environment it becomes protonated and trapped. Upon excitation with UV light, the dye fluoresces green in neutral environments, and orange-to-red in acidic compartments. To study whether reovirus

infection induces the formation of enlarged acidic vesicles, U87-MG and U251-MG cells were treated with R124, *jln-1*, or Rapa as before, incubated with acridine orange at the indicated time points and analyzed by fluorescence microscopy. Upon reovirus infection or Rapa treatment, enlarged orange-to-red vesicles were clearly visible in the U87-MG cells, indicating that reovirus induces the formation of autophagolysosomes. As for the Atg5 and LC3 expression, acidic vesicles were detected in U251-MG upon Rapa treatment and *jln-1* but not R124 infection, as expected. Taken together, our data indicate that both R124 and *jln-1* are able to induce autophagy in human glioblastoma cell lines.

*Autophagosomes can be observed in reovirus-infected U87-MG cells*

To further study the presence of double-membraned autophagosomes, we used electron microscopy. To this end, U87-MG cells were infected with R124 or treated with 400 nM Rapa as before, and analyzed by transmission electron microscopy. The results revealed the presence of viral replication factories upon R124 infection (Figure 7), indicative for a productive infection. Autophagosome-like structures could be observed in mock-treated U87-MG cells, and seemed to be enriched upon Rapa treatment. Importantly, such vesicles were present in reovirus-infected cells, without evident localization in close proximity of the viral factories. This suggests that the autophagosomes are not used to compartmentalize reovirus double-stranded RNA and reovirus assembly from the cytosol.

*Reovirus replication facilitates the induction of acidic vesicular organelles, Atg5-Atg12 conjugation, p62 degradation and LC3 lipidation in U87-MG cells*

Previous studies by Lv *et al.* and Arnoldi *et al.* on autophagy induction by bluetongue virus and rotavirus showed that the induction of autophagy is dependent on virus replication [8, 10]. To examine whether autophagy can be induced by replication-defective reovirus particles, U87-MG cells were exposed to UV-inactivated R124, or the corresponding replication-competent virus, at the indicated MOIs. The absence of infectious virus in the UV-inactivated R124 batch was confirmed by plaque assay on 911 cells ( $\leq 10$  pfu/ml). The MOI of UV-inactivated reovirus particles is based on the infectious titer prior to UV inactivation, and is referred to as MOI\*. Replication-competent R124 at an MOI of 10 clearly induced the appearance of enlarged acidic vesicles (Figure 8), indicative for autophagy. UV-inactivated virus particles gave a slight increase in the number of these autophagic vacuoles at an MOI\* of 200 and 1000. Consistently, Atg5-Atg12 conjugation and LC3 lipidation were visible after infection with replication-competent R124 at an MOI of 10 or UV-inactivated R124 at an MOI\* of 200 and 1000. This suggests that the reovirus genome is dispensable for the induction of autophagy. However, as high amounts of virus particles are

needed for autophagy induction, productive R124 infection is more efficient in autophagy induction. Interestingly, levels of p62 were decreased only upon infection with replication-competent R124. Therefore, it seems that replication-incompetent R124 particles do not induce the later steps of the autophagic flux. Altogether, the obtained results demonstrate that a productive R124 infection is not strictly necessary, but R124 replication strongly stimulates the induction of autophagy.

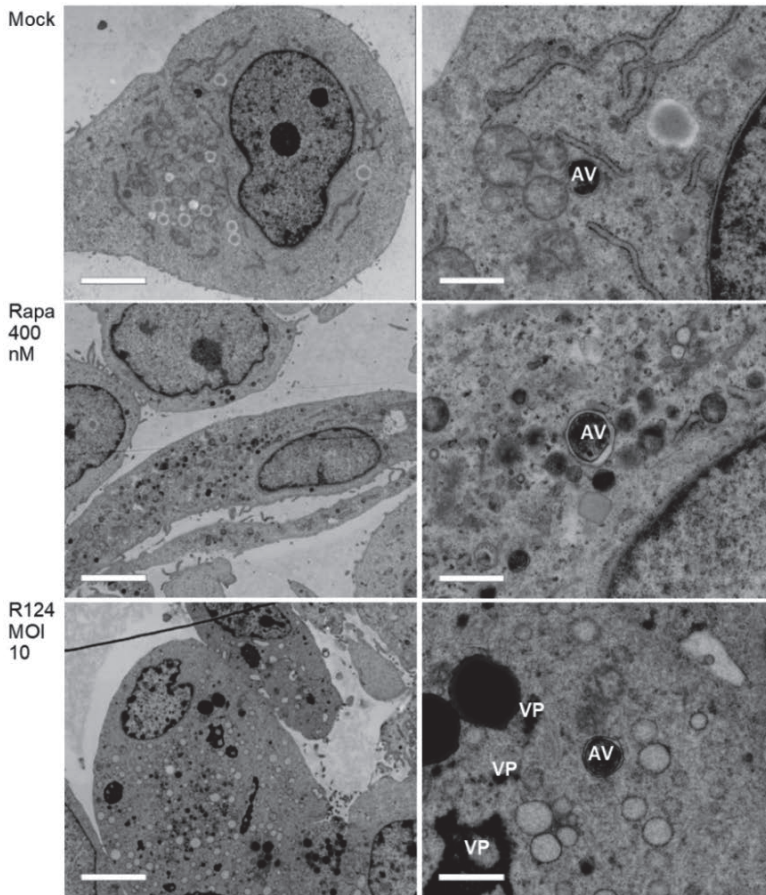


**Figure 7.** Autophagosomes can be observed in R124-infected U87-MG cells. U87-MG glioblastoma cells were left untreated (Mock) or were treated with 400 nM Rapa, or infected with R124 at an MOI of 10. After 48 hours, the cells were fixed, dehydrated, embedded, and ultrathin cell sections were analyzed by electron microscopy. Scale bars represent 4.6 $\mu$ m (left panel), or 920nm (right panel, 5x zoom of left panel cell). AV = autophagic vacuoles; VP = viral particles.

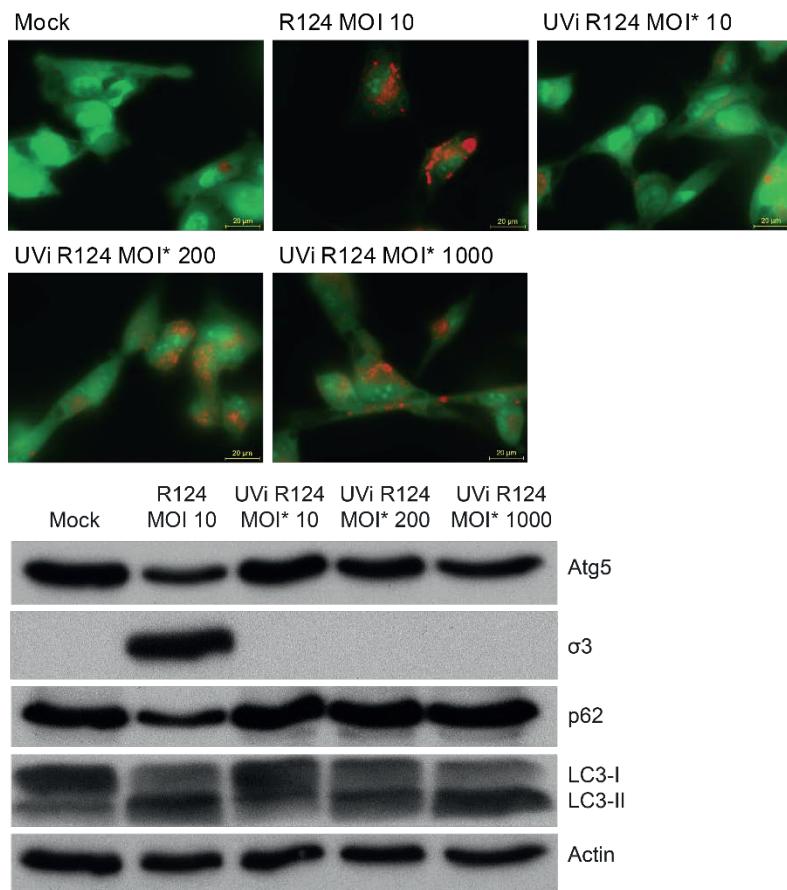


**Figure 8.** High amounts of UV-inactivated reovirus particles are needed to induce Atg5-Atg12 conjugation, LC3-I to LC3-II conversion, and acidic vesicular organelles in U87-MG cells. U87-MG cells were infected with R124 at an MOI of 10, or UV-inactivated R124 particles at an MOI\* of 10, 200, or 1000. After 48 hours, protein lysates were made in RIPA lysis buffer and analyzed for the expression of Atg5,  $\sigma$ 3, p62, LC3, and Actin. Alternatively, cells were incubated with acridine orange and fluorescence microscopy images were taken.

## DISCUSSION

Oncolytic virotherapy using reovirus has entered a variety of clinical trials, which demonstrated both the safety and feasibility of the approach. Its efficacy has been limited in stand-alone therapies [1]. A better understanding of the reovirus-host interaction is crucial to improve therapeutic strategies. Here, we demonstrate that

reovirus induces several key features of autophagy, evident by the appearance of double-membraned vesicles, an increase in acidic vesicles, LC3 conversion, p62 degradation, Atg5-Atg12 conjugation, and the formation of GFP-LC3 puncta in infected cells.

For other members of the Reoviridae family, it has been shown that autophagy enhances their replication. Bluetongue virus stimulates autophagy through the downregulation of the autophagy-inhibiting Akt-TSC2-mTOR pathway and the upregulation of the autophagy-stimulating AMPK-TSC2-mTOR pathway [25]. Autophagy was shown to enhance bluetongue virus replication, as the pharmacological or siRNA-mediated inhibition of autophagy resulted in decreased virus replication, whereas inducing autophagy with Rapamycin (Rapa) led to an increase in viral yields [10]. Similarly, avian reovirus p17 non-structural protein has been shown to trigger autophagy through the activation of PTEN, AMPK, and PKR/eIF2 $\alpha$  signaling pathways [9]. As in the study on bluetongue virus, treatment with Rapa increased avian reovirus progeny, whereas inhibiting the autophagy pathway decreased virus replication. Studies on rotavirus have revealed that its viroporin NSP4 activates autophagy by stimulating the release of calcium from the ER into the cytoplasm, which leads to a CaMKK- $\beta$ - and AMPK-dependent initiation of autophagy [26]. This process relies on the activity of PI3K, Atg3, and Atg5. As for bluetongue virus and avian reovirus, inhibition of autophagy reduced the amount of infectious virus. Interestingly, a recently accepted manuscript showed contradictory findings that rotavirus activity can be reduced by blocking the PI3K-Akt-mTOR signaling pathway and thus stimulating autophagy [27]. Further research is warranted to gain more insight on this complex rotavirus-host interaction. For the interactions between mammalian reovirus and the autophagy machinery, not much is known. There are indications that mammalian reovirus induces autophagy in multiple myeloma cell lines, but the role of autophagy in mammalian reovirus infection remains unclear [11, 12].

Our finding that GFP-LC3 puncta are formed in cells that show reovirus protein expression indicates that autophagy can be induced by the virus. For some viruses, it has been suggested that they use the autophagosome environment as a niche to replicate and/or be shielded from the cytoplasmic antiviral immunity [28-30]. Notably, Figure 1 shows that LC3 and the reovirus outer capsid protein  $\mu$ 1C do not overlap in our experiments, implying that the virus particles may exist in the vicinity of autophagosomes but not reside inside these vesicles. This finding is supported by the electron microscopy pictures, where no virions were detected inside autophagosomal structures.

The process of autophagy is characterized by the formation of autophagosomes, fusion of autophagosomes with lysosomes, and the degradation

of the autolysosomal content [3]. LC3-II is localized to autophagosomes and therefore generally seen as a marker for autophagosome formation [21]. However, an increase in LC3-II can also be the consequence of a delay or a block in autolysosomal degradation. It is crucial to assess whether reovirus induces the full autophagic flux, including lysosomal degradation. For example, Influenza A virus blocks the fusion between autophagosomes and lysosomes with its matrix protein 2 [31]. The conventional method to study autophagic flux is through the use of BafA1. This compound blocks autophagosome-lysosome fusion or lysosomal acidification, and therefore should lead to a block in the degradation of autophagic proteins thus an increase in LC3-II and p62 [21]. It should be mentioned that BafA1 treatment can inhibit the entry steps of reovirus infection [32, 33]. An effect of BafA1 on the reovirus-induced autophagy markers could thus potentially be attributed to an inhibition of viral entry. Therefore, we did not study the effect of adding BafA1 to reovirus-infected cells in our experiments. Nevertheless, it seems likely that reovirus induces the full autophagic flux, as we demonstrated that p62 is degraded upon reovirus infection.

In our experiments, we observed that a part but not all of the autophagic machinery facilitates reovirus replication. Recent publications revealed that genes considered to have a specific role in autophagy can exert additional functions as well [34-36]. This underlines the importance of testing knock-out cell lines for multiple autophagy-related genes before drawing firm conclusions about whether autophagy is involved in the studied process. Our results indicate that the autophagic process is not strictly involved in the replication of reovirus, but that some functions of autophagy-related proteins are important for a productive virus infection. We show that a subset of autophagy-related proteins seems to facilitate reovirus replication: specifically Atg3 and Atg5, which both are essential for the lipidation of LC3. This raises the question as to whether the formation of LC3-II rather than the process of autophagy facilitates the replication of reovirus. As LC3 lipidation does not strictly rely on the expression of Atg13, this would explain the contrasting result for that knock-out. Correspondingly, we noted that the cellular presence of LC3 puncta correlates with the presence of virus protein in the same cell, suggesting that they co-evolve. It remains to be determined whether the LC3 puncta consist of LC3-II or LC3-I. For Coronavirus, it has been demonstrated that virus infection in cell culture induces the formation of double-membraned vesicles coated with LC3-I [37]. However, we found that the levels of LC3-I decrease during reovirus infection, and the levels of LC3-II conversely increase. Therefore, it seems unlikely that LC3-I rather than LC3-II is detected as puncta.

Importantly, both Atg3 and Atg5 have been demonstrated to have additional functions besides facilitating autophagy [34-36]. It has been shown that

vaccinia virus infection induces the formation of Atg3-Atg12, resulting in aberrant autophagosome formation [38]. This conjugate has previously been demonstrated to be involved in basal autophagic flux, mitophagy, and late endosome function [39-41]. It is widely known that reovirus entry relies on the maturation of endosomes, raising the possibility that in the absence of Atg3, entry of the virus is hindered [42, 43]. Future studies are needed to investigate this possibility. Research on non-canonical roles of Atg5 has demonstrated that the Atg5-Atg12 conjugate can alternatively function to inhibit type I IFN production by directly interacting with RIG-I and IPS-1 [44]. Type I IFN is considered a general anti-viral response, and is known to inhibit a productive reovirus infection [45]. Therefore, an Atg5-mediated decrease in type I IFN could explain the observed importance for reovirus replication.

Our findings that an MOI\* of 10 of UV-inactivated reovirus fails to induce LC3 lipidation, Atg5-Atg12 conjugation or an increase in acidic vesicular organelles demonstrate that a productive reovirus infection facilitates the induction of autophagy. It remains to be studied what specific step in the reovirus infection cycle is involved in the induction of autophagy. It has been shown that the apoptosis induction capacity of reovirus relies on  $\sigma 1$  attachment to cell surface molecules [46]. Contrastingly, for necroptosis induction by reovirus, both genomic RNA within incoming virus particles needs to be sensed as well as dsRNA must be formed [47]. Interestingly, for other members of the Reoviridae virus family, non-structural proteins were found to be associated with autophagy induction [27]. Our data indicate that this is not the case for reovirus. Though our results indicate that a productive reovirus infection facilitates the induction of autophagy, the replication process itself seems dispensable as we find that exposure of cells to a much higher MOI\* (200 or 1000) of UV-inactivated virus is able to induce autophagic features. In this respect, it could be speculated that a specific reovirus capsid protein, or a set of proteins, is involved in the induction of autophagy.

## REFERENCES

1. Zhao, X.; Chester, C.; Rajasekaran, N.; He, Z.; Kohrt, H.E. Strategic Combinations: The Future of Oncolytic Virotherapy with Reovirus. *Mol Cancer Ther* **2016**, *15*, 767-773.
2. Strong, J.E.; Coffey, M.C.; Tang, D.; Sabinin, P.; Lee, P.W. The molecular basis of viral oncolysis: usurpation of the Ras signaling pathway by reovirus. *EMBO J* **1998**, *17*, 3351-3362.
3. Lennemann, N.J.; Coyne, C.B. Catch me if you can: the link between autophagy and viruses. *PLoS Pathog* **2015**, *11*, e1004685.
4. Daussy, C.F.; Beaumelle, B.; Espert, L. Autophagy restricts HIV-1 infection. *Oncotarget* **2015**, *6*, 20752-20753.
5. Campbell, G.R.; Spector, S.A. Inhibition of human immunodeficiency virus type-1 through autophagy. *Curr Opin Microbiol* **2013**, *16*, 349-354.
6. Dong, X.; Levine, B., Autophagy and viruses: adversaries or allies? *J Innate Immun* **2013**, *5*, 480-493.
7. Jiang, H.; White, E.J.; Rios-Vicil, C.I.; Xu, J.; Gomez-Manzano, C.; Fueyo, J. Human adenovirus type 5 induces cell lysis through autophagy and autophagy-triggered caspase activity. *J Virol* **2011**, *85*, 4720-4729.
8. Arnoldi, F.; De Lorenzo, G.; Mano, M.; Schraner, E.M.; Wild, P.; Eichwald, C.; Burrone, O.R. Rotavirus increases levels of lipidated LC3 supporting accumulation of infectious progeny virus without inducing autophagosome formation. *PLoS One* **2014**, *9*, e95197.
9. Chi, P.I.; Huang, W.R.; Lai, I.H.; Cheng, C.Y.; Liu, H.J. The p17 nonstructural protein of avian reovirus triggers autophagy enhancing virus replication via activation of phosphatase and tensin deleted on chromosome 10 (PTEN) and AMP-activated protein kinase (AMPK), as well as dsRNA-dependent protein kinase (PKR)/eIF2alpha signaling pathways. *J Biol Chem* **2013**, *288*, 3571-3584.
10. Lv, S.; Xu, Q.; Sun, E.; Yang, T.; Li, J.; Feng, Y.; Zhang, Q.; Wang, H.; Zhang, J.; Wu, D. Autophagy Activated by Bluetongue Virus Infection Plays a Positive Role in Its Replication. *Viruses* **2015**, *7*, 4657-4675.
11. Thirukkumaran, C.M.; Shi, Z.Q.; Luider, J.; Kopciuk, K.; Gao, H.; Bahlis, N.; Neri, P.; Pho, M.; Stewart, D.; Mansoor, A.; Morris, D.G. Reovirus modulates autophagy during oncolysis of multiple myeloma. *Autophagy* **2013**, *9*, 413-414.
12. Thirukkumaran, C.M.; Shi, Z.Q.; Luider, J.; Kopciuk, K.; Gao, H.; Bahlis, N.; Neri, P.; Pho, M.; Stewart, D.; Mansoor, A.; Morris, D.G. Reovirus as a viable therapeutic option for the treatment of multiple myeloma. *Clin Cancer Res* **2012**, *18*, 4962-4972.

13. Dubridge, R.B.; Tang, P.; Hsia, H.C.; Leong, P.M.; Miller, J.H.; Calos, M.P. Analysis of Mutation in Human-Cells by Using an Epstein-Barr-Virus Shuttle System. *Mol Cell Biol* **1987**, *7*, 379-387.
14. Fallaux, F.J.; Kranenburg, O.; Cramer, S.J.; Houweling, A.; Van Ormondt, H.; Hoeben, R.C.; Van Der Eb, A.J. Characterization of 911: a new helper cell line for the titration and propagation of early region 1-deleted adenoviral vectors. *Hum Gene Ther* **1996**, *7*, 215-222.
15. Sou, Y.S.; Waguri, S.; Iwata, J.; Ueno, T.; Fujimura, T.; Hara, T.; Sawada, N.; Yamada, A.; Mizushima, N.; Uchiyama, Y.; Kominami, E.; Tanaka, K.; Komatsu, M. The Atg8 conjugation system is indispensable for proper development of autophagic isolation membranes in mice. *Mol Biol Cell* **2008**, *19*, 4762-4775.
16. Kuma, A.; Hatano, M.; Matsui, M.; Yamamoto, A.; Nakaya, H.; Yoshimori, T.; Ohsumi, Y.; Tokuhiya, T.; Mizushima, N. The role of autophagy during the early neonatal starvation period. *Nature* **2004**, *432*, 1032-1036.
17. Shang, L.; Chen, S.; Du, F.; Li, S.; Zhao, L.; Wang, X. Nutrient starvation elicits an acute autophagic response mediated by Ulk1 dephosphorylation and its subsequent dissociation from AMPK. *Proc Natl Acad Sci U S A* **2011**, *108*, 4788-4793.
18. Hieke, N.; Löffler, A.S.; Kaizuka, T.; Berleth, N.; Bohler, P.; Driessen, S.; Stuhldreier, F.; Friesen, O.; Assani, K.; Schmitz, K.; Peter, C.; Diedrich, B.; Dengjel, J.; Holland, P.; Simonsen, A.; Wesselborg, S.; Mizushima, N.; Stork, B. Expression of a ULK1/2 binding-deficient ATG13 variant can partially restore autophagic activity in ATG13-deficient cells. *Autophagy* **2015**, *11*, 1471-1483.
19. van den Wollenberg, D.J.; Dautzenberg, I.J.; van den Hengel, S.K.; Cramer, S.J.; de Groot, R.J.; Hoeben, R.C. Isolation of reovirus T3D mutants capable of infecting human tumor cells independent of junction adhesion molecule-A. *PLoS One* **2012**, *7*, e48064.
20. Virgin, H.W.; Mann, M.A.; Fields, B.N.; Tyler, K.L. Monoclonal-Antibodies to Reovirus Reveal Structure-Function-Relationships between Capsid Proteins and Genetics of Susceptibility to Antibody Action. *Journal of Virology* **1991**, *65*, 6772-6781.
21. Mizushima, N.; Yoshimori, T.; Levine, B. Methods in mammalian autophagy research. *Cell* **2010**, *140*, 313-326.
22. Reiss, K.; Stencel, J.E.; Liu, Y.; Blaum, B.S.; Reiter, D.M.; Feizi, T.; Dermody, T. S.; Stehle, T. The GM2 glycan serves as a functional coreceptor for serotype 1 reovirus. *PLoS Pathog* **2012**, *8*, e1003078.
23. Kemp, V.; Dautzenberg, I.J.; van den Wollenberg, D.J.; Hoeben, R.C. Autophagy has minor effects on reovirus-induced cytolysis. *Unpublished data*. **2017**.

24. van den Wollenberg, D.J.; Dautzenberg, I.J.; Ros, W.; Lipinska, A.D.; van den Hengel, S.K.; Hoeben, R.C. Replicating reoviruses with a transgene replacing the codons for the head domain of the viral spike. *Gene Ther* **2015**, *22*, 267-279.
25. Lv, S.; Xu, Q.Y.; Sun, E.C.; Zhang, J.K.; Wu, D.L. Dissection and integration of the autophagy signaling network initiated by bluetongue virus infection: crucial candidates ERK1/2, Akt and AMPK. *Sci Rep* **2016**, *6*, 23130.
26. Crawford, S.E.; Hyser, J.M.; Utama, B.; Estes, M.K. Autophagy hijacked through viroporin-activated calcium/calmodulin-dependent kinase kinase-beta signaling is required for rotavirus replication. *Proc Natl Acad Sci U S A* **2012**, *109*, E3405-13.
27. Yin, Y.; Dang, W.; Zhou, X.; Xu, L.; Wang, W.; Cao, W.; Chen, S.; Su, J.; Cai, X.; Xiao, S.; Peppelenbosch, M.P.; Pan, Q. PI3K-Akt-mTOR axis sustains rotavirus infection via the 4E-BP1 mediated autophagy pathway and represents an antiviral target. *Virulence* **2018**, *9*, 83-98.
28. Richards, A.L.; Jackson, W.T. That which does not degrade you makes you stronger: infectivity of poliovirus depends on vesicle acidification. *Autophagy* **2013**, *9*, 806-807.
29. Richards, A.L.; Jackson, W.T. How positive-strand RNA viruses benefit from autophagosome maturation. *J Virol* **2013**, *87*, 9966-9972.
30. Wang, Y.; Duan, Y.; Han, C.; Yao, S.; Qi, X.; Gao, Y.; Maier, H.J.; Britton, P.; Chen, L.; Zhang, L.; Gao, L.; Gao, H.; Shen, N.; Wang, J.; Wang, X. Infectious Bursal Disease Virus Subverts Autophagic Vacuoles To Promote Viral Maturation and Release. *J Virol* **2017**, *91*, e01883-16.
31. Gannage, M.; Dormann, D.; Albrecht, R.; Dengjel, J.; Torossi, T.; Ramer, P.C.; Lee, M.; Strowig, T.; Arrey, F.; Conenello, G.; Pypaert, M.; Andersen, J.; Garcia-Sastre, A.; Munz, C. Matrix protein 2 of influenza A virus blocks autophagosome fusion with lysosomes. *Cell Host Microbe* **2009**, *6*, 367-380.
32. Boulant, S.; Stanifer, M.; Kural, C.; Cureton, D.K.; Massol, R.; Nibert, M.L.; Kirchhausen, T. Similar uptake but different trafficking and escape routes of reovirus virions and infectious subvirion particles imaged in polarized Madin-Darby canine kidney cells. *Mol Biol Cell* **2013**, *24*, 1196-1207.
33. Martinez, C.G.; Guinea, R.; Benavente, J.; Carrasco, L. The entry of reovirus into L cells is dependent on vacuolar proton-ATPase activity. *Journal of Virology* **1996**, *70*, 576-579.
34. Bestebroer, J.; V'Kovski, P.; Mauthe, M.; Reggiori, F. Hidden behind autophagy: the unconventional roles of ATG proteins. *Traffic* **2013**, *14*, 1029-1041.

35. Mauthe, M.; Langereis, M.; Jung, J.; Zhou, X.; Jones, A.; Omta, W.; Tooze, S. A.; Stork, B.; Paludan, S. R.; Ahola, T.; Egan, D.; Behrends, C.; Mokry, M.; de Haan, C.; van Kuppeveld, F.; Reggiori, F. An siRNA screen for ATG protein depletion reveals the extent of the unconventional functions of the autophagy proteome in virus replication. *J Cell Biol* **2016**, *214*, 619-635.
36. Mauthe, M.; Reggiori, F. ATG proteins: Are we always looking at autophagy? *Autophagy* **2016**, *12*, 2502-2503.
37. Reggiori, F.; Monastyrska, I.; Verheije, M.H.; Cali, T.; Ulasli, M.; Bianchi, S.; Bernasconi, R.; de Haan, C.A.; Molinari, M. Coronaviruses Hijack the LC3-I-positive EDEMosomes, ER-derived vesicles exporting short-lived ERAD regulators, for replication. *Cell Host Microbe* **2010**, *7*, 500-508.
38. Moloughney, J.G.; Monken, C.E.; Tao, H.; Zhang, H.; Thomas, J.D.; Lattime, E.C.; Jin, S.V. Vaccinia virus leads to ATG12-ATG3 conjugation and deficiency in autophagosome formation. *Autophagy* **2014**, *7*, 1434-1447.
39. Murrow, L.; Debnath, J. ATG12-ATG3 connects basal autophagy and late endosome function. *Autophagy* **2015**, *11*, 961-962.
40. Radoshevich, L.; Murrow, L.; Chen, N.; Fernandez, E.; Roy, S.; Fung, C.; Debnath, J. ATG12 conjugation to ATG3 regulates mitochondrial homeostasis and cell death. *Cell* **2010**, *142*, 590-600.
41. Murrow, L.; Malhotra, R.; Debnath, J. ATG12-ATG3 interacts with Alix to promote basal autophagic flux and late endosome function. *Nat Cell Biol* **2015**, *17*, 300-310.
42. Mainou, B.A.; Dermody, T.S. Transport to late endosomes is required for efficient reovirus infection. *J Virol* **2012**, *86*, 8346-8358.
43. Thete, D.; Danthi, P. Conformational changes required for reovirus cell entry are sensitive to pH. *Virology* **2015**, *483*, 291-301.
44. Jounai, N.; Takeshita, F.; Kobiyama, K.; Sawano, A.; Miyawaki, A.; Xin, K.Q.; Ishii, K.J.; Kawai, T.; Akira, S.; Suzuki, K.; Okuda, K. The Atg5 Atg12 conjugate associates with innate antiviral immune responses. *Proc Natl Acad Sci U S A* **2007**, *104*, 14050-14055.
45. Shmulevitz, M.; Pan, L.Z.; Garant, K.; Pan, D.; Lee, P.W. Oncogenic Ras promotes reovirus spread by suppressing IFN-beta production through negative regulation of RIG-I signaling. *Cancer Res* **2010**, *70*, 4912-4921.
46. Tyler, K.L.; Squier, M.K.; Rodgers, S.E.; Schneider, B.E.; Oberhaus, S.M.; Grdina, T.A.; Cohen, J.J.; Dermody, T.S. Differences in the capacity of reovirus strains to induce apoptosis are determined by the viral attachment protein sigma 1. *J Virol* **1995**, *69*, 6972-6979.

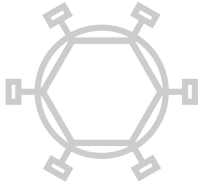
47. Berger, A.K.; Hiller, B.E.; Thete, D.; Snyder, A.J.; Perez, E., Jr.; Upton, J.W.; Danthi, P. Viral RNA at Two Stages of Reovirus Infection Is Required for the Induction of Necroptosis. *J Virol* **2017**, *91*, e02404-16.







# 4



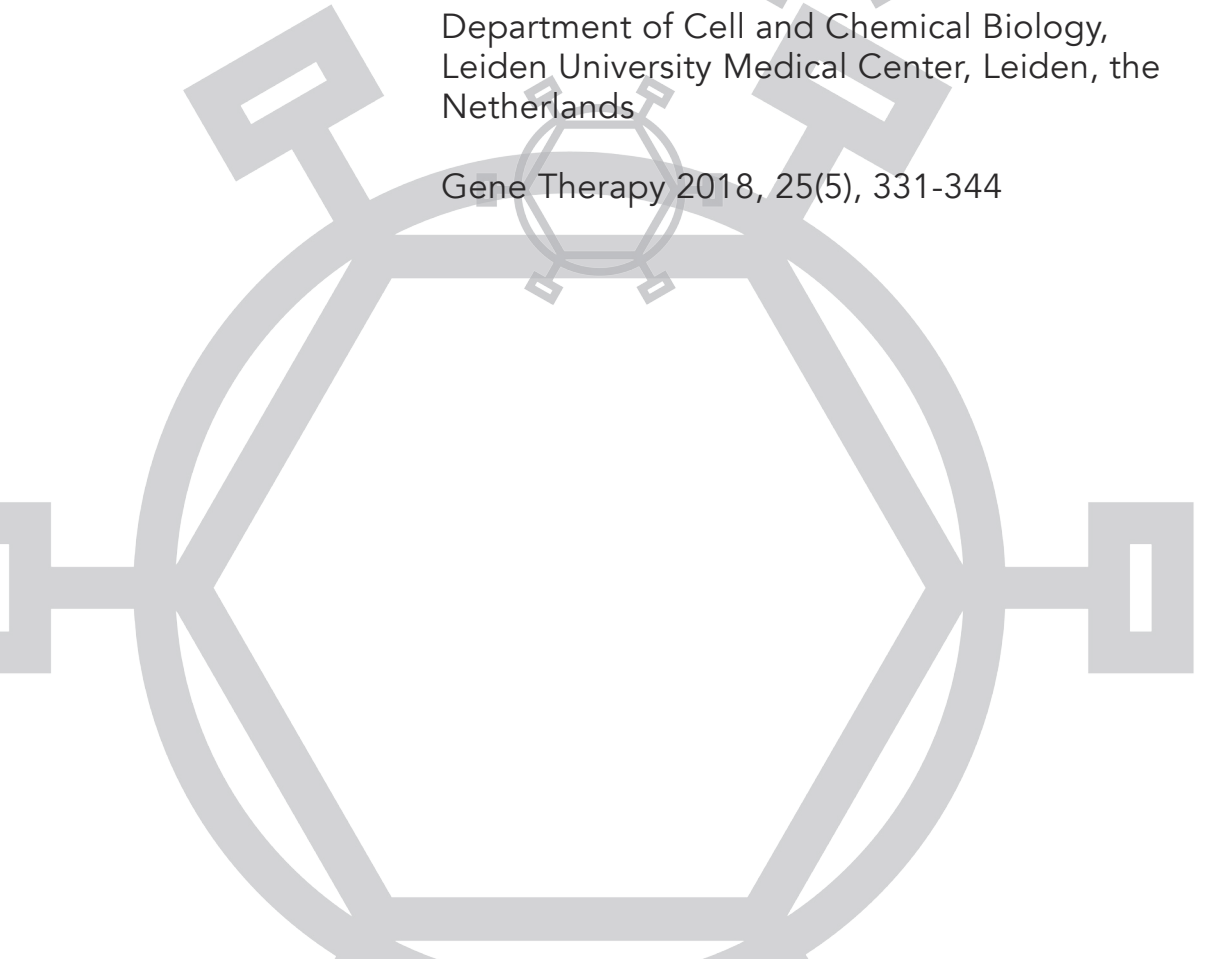
## Characterization of a replicating expanded-tropism oncolytic reovirus carrying the adenovirus E4orf4 gene



Vera Kemp, Iris J.C. Dautzenberg, Steve J. Cramer, Rob C. Hoeben, Diana J.M. van den Wollenberg

Department of Cell and Chemical Biology,  
Leiden University Medical Center, Leiden, the  
Netherlands

Gene Therapy 2018, 25(5), 331-344



## **ABSTRACT**

While the mammalian orthoreovirus Type 3 Dearing (reovirus T3D) infects many different tumor cells, various cell lines resist the induction of reovirus-mediated cell death. In an effort to increase the oncolytic potency, we introduced transgenes into the S1 segment of reovirus T3D. The adenovirus E4orf4 gene was selected as transgene since the encoded E4orf4 protein induces cell death in transformed cells. The induction of cell death by E4orf4 depends in part on its binding to phosphatase 2A (PP2A). In addition to the S1-E4orf4 reovirus, two other reoviruses were employed in our studies. The reovirus rS1-RFA encodes an E4orf4 double-mutant protein that cannot interact with PP2A and the rS1-iLOV virus encoding the fluorescent marker iLOV as a reporter. The replacement of the codons for the junction adhesion molecule-A (JAM-A) binding head domain of the truncated spike protein blocks the entry of these recombinant viruses via the reovirus receptor JAM-A. Instead, these viruses rely on internalization via binding to sialic acids on the cell surface. This expands their tropism and allows infection of JAM-A deficient tumor cells. Here, we not only demonstrate the feasibility of this approach, but also established that the cytolytic activity of these recombinant viruses is largely transgene-independent.

## INTRODUCTION

The lytic replication of mammalian orthoreovirus Type 3 Dearing (reovirus T3D) initiates preferentially cell death in transformed cells, but not in normal diploid cells. The cell's innate sensing of the virus, and more specifically the PKR-dependent inhibition of translation, has been demonstrated to underlie the difference in reovirus sensitivity between cancer cells and healthy cells. In many tumor cells, the pathways that control cell division and other regulatory processes are derailed. Mutations leading to constitutively active RAS signaling occur in approximately 30% of all human cancers and in some cancer types, for instance in pancreatic cancer, the incidence is even higher [1, 2]. The Ras signaling inhibits the PKR response and Ras-transformed cells are generally more sensitive to reovirus-induced apoptosis. This leads to enhanced virus release and spread from the infected cells [3, 4]. These observations led to the initiation of a series of clinical trials in which the wild-type reovirus T3D was administered to patients as viral anti-cancer agent [5]. Reovirus treatment in various cancer types proved to be well tolerated and safe for patients but when used as a monotherapy the anti-tumor efficacy was limited, warranting studies on combinatorial therapies. For such preclinical studies many rodent models are available. Studies in murine models are facilitated by the reovirus' capacity to replicate in human as well as in murine cells. This allows studies on the effect of immune modulation in immune-competent mouse tumor models [6].

Not all tumor cells are sensitive to reovirus infection and subsequent oncolysis. While some tumor cells resist infection by reoviruses due to the absence of the reovirus receptor junction adhesion molecule-A (JAM-A) at the cell surface, other cells resist reoviruses at a post-entry level. In several head and neck cancer cell lines, reovirus infection did not efficiently initiate cell death. In a panel of squamous cell carcinomas of the head and neck (SCCHN), the variation in sensitivity to reovirus infection was not linked to differences in EGFR/Ras/MAPK pathways [7]. In HT1080 fibrosarcoma cells, reovirus T3D exposure causes a persistent infection despite an activating N-Ras mutation. In the persistently reovirus-infected HTR1 cell line the apoptotic pathway is not completely abolished, since chemical-induced apoptosis and exposure to E1B-defective adenoviruses still result in apoptotic cell death [8].

To overcome the resistance to reovirus infection and oncolysis, we employed the plasmid-based reverse genetics system to generate replication-competent transgene-containing reoviruses. Recently, we and others demonstrated the feasibility of this approach by replacing the sequence coding for the JAM-binding head domain of the reovirus attachment protein  $\sigma 1$  by genes encoding the green fluorescent reporter proteins iLOV or UnaG [9, 10].

The location of the transgene in segment S1 of reovirus was based on our observation that the *jln* mutants obtained by bioselection of the reovirus T3D on JAM-A deficient U118-MG cells acquired the capacity to infect cells independent of the presence of the reovirus receptor JAM-A on the cell surface. One of the mutants, *jln-3*, harbors a single point mutation in the S1 segment, that leads to a Gly196Arg substitution in the tail region of the  $\sigma 1$  spike protein close to the region involved in sialic acid binding. This mutation allows the *jln* mutants to employ sialic acids on the cell surface as primary receptors and we demonstrated that the head-domain of the  $\sigma 1$  protein was not required for entry of the *jln* mutants [11]. Therefore, the codons in S1 that encode the head domain can be replaced by a heterologous transgene.

Several therapeutic proteins are candidates to be expressed by replicating reovirus vectors. One suitable candidate is the human adenovirus type 2 (HAdV-2) E4 open reading frame 4 (E4orf4) protein. This small 14 kDa protein is encoded by a fragment of only 345 nucleotides in length. The E4orf4 protein induces p53-independent apoptosis in transformed cells, but not in normal cells [12, 13]. This effect of E4orf4, however, is cell line dependent, since it can induce caspase-independent cell death in some other transformed cell lines [14]. Induction of cell death by E4orf4 is dependent on the association of E4orf4 with the B $\alpha$  subunit of protein phosphatase 2A (PP2A). PP2A is an abundant cellular serine/threonine phosphatase that targets proteins implicated in many cell growth and signaling pathways [15]. Binding of E4orf4 to PP2A inhibits ATP-utilizing chromatin assembly and modifying factor (ACF) containing chromatin remodeling complexes, causing alterations in the cell's chromatin, leading to cell death [16]. Amino acid substitutions in the E4orf4 protein that inhibit its binding to PP2A prevent cell death induction in H1299 lung carcinoma cells. One such E4orf4 mutant harbors mutations that result in two amino acid substitutions: R81A and F84A (RFA for short) [12].

E4orf4 can also trigger a cytoplasmic-induced cell death, caused by interaction with Src family kinases (SFKs). The E4orf4-Src interaction is detected when E4orf4 is overexpressed alone, and outside the context of an adenovirus infection. In adenovirus-infected cells the E4orf4-Src association is rarely observed, since E4orf4 mainly resides in the nucleus and is therefore not available to Src [17, 18]. The changes in the RFA mutant do not affect the region involved in Src binding and therefore the RFA protein may still induce cytoplasmic programmed cell death.

The most studied reovirus-induced cell death mechanism is the apoptotic pathway [19-24]. As is mentioned before, induction of apoptosis is enhanced in reovirus-infected Ras-transformed cells and may stimulate virus release and spread of the virus to neighboring cells. The signaling events involved in the induction of reovirus-mediated cell death are both cell-type dependent and reovirus strain-specific [25, 26]. Necrosis, a caspase-independent cell death pathway, is controlled

by the sialic acid binding capacity of reovirus  $\sigma 1$  protein and requires the production of viral RNAs [27]. Our transgene-containing recombinant reoviruses rely on enhanced binding to sialylated glycans on the host cells, which could induce the caspase-independent necrosis type of cell death. This supported our hypothesis that combining reovirus infection of tumor cells with E4orf4 protein expression may increase the oncolytic potency of reovirus T3D for tumor types that resist wild-type reovirus T3D-mediated cell death.

Here, we generated reoviruses containing the wild-type E4orf4 gene, a virus carrying the gene encoding the double mutant of E4orf4 (RFA) and, as control, our previously generated reovirus containing the iLOV gene, and tested these in various cell types that resisted wild-type reovirus-induced cell death.

## MATERIALS AND METHODS

### *Cell lines and viruses*

The cell lines 911 [28], human glioblastoma cell line U118-MG, chicken hepatoma cell line LMH, p53-deleted human non-small-cell lung carcinoma cell line H1299, human bladder carcinoma cell line UMUC-3, and the normal human foreskin fibroblasts VH10 and VH25 [29] were cultured in high glucose Dulbecco's Modified Eagle's Medium (DMEM, Invitrogen, Life Technologies, Bleiswijk, the Netherlands), supplemented with 8% fetal bovine serum (FBS, Invitrogen) and with antibiotics penicillin and streptomycin (pen/strep). LMH cells were cultured on dishes coated with 0.1% gelatin (Sigma-Aldrich Chemie BV, Zwijndrecht, the Netherlands). PC-3M-Pro4/Luc cells (Pro4-Luc cells in text) are highly metastatic human prostate cancer cells obtained from the Department of Urology of the Leiden University Medical Center [30]. Pro4-Luc cells are cultured in high glucose DMEM 8% FBS, pen/strep and 400  $\mu\text{g}/\text{ml}$  G418 (Santa Cruz, Bio-Connect BV, Huissen, the Netherlands).

The 911-Flag.PP2A cells were generated by stable transfection of 911 cells with plasmid pcDNA3-FLAG.PP2A.B $\alpha$  (kindly provided by Prof. P. Branton, Department of Biochemistry, McGill University, Montreal, Quebec, Canada [12]) and selected on medium containing 800  $\mu\text{g}/\text{ml}$  G418. Cell line 911-Flag.PP2A was derived from one colony (#1) and further propagated after initial selection in high glucose DMEM 8% FBS, pen/strep and 400  $\mu\text{g}/\text{ml}$  G418. Cell line 911scFvHis is a 911-cell derivative and expresses a single-chain antibody on its surface that is capable of binding His-tags. This cell line was used for the first propagation of recombinant reoviruses, and was cultured in high glucose DMEM 8% FBS, pen/strep and 400  $\mu\text{g}/\text{ml}$  G418. The T7-RNA polymerase-expressing cell line BSR-T7 [31] was provided by Prof. K.K. Conzelmann (Ludwig-Maximilians-University Munich, München, Germany) and cultured in high glucose DMEM, 8% FBS, pen-strep and 400  $\mu\text{g}/\text{ml}$  G418 [29]. All cells were cultured in an atmosphere of 5% CO<sub>2</sub> at 37°C. The identity

of the human cell lines used in this study was verified by short tandem repeat analyses and comparison with the STR databases at the Forensic Laboratory for DNA Research, Department of Human Genetics, Leiden University Medical Center. All cell lines used are regularly tested for mycoplasma with the MycoAlert mycoplasma detection kit (Lonza Benelux BV, Breda, the Netherlands).

The *wt*-T3D virus strain R124 was isolated from reovirus T3D stock VR-824 from the American Type Culture Collection by two rounds of plaque purification and propagated on 911 cells. In the text, R124 is referred to as *wt*-R124. *Jin-3* mutant reovirus was obtained by bioselection of *wt*-R124 on U118-MG cells as previously described [11] and further propagated on 911 cells. Recombinant reovirus rS1His-2A-iLOV (referred to as rS1-iLOV in this manuscript) was generated as described previously [9].

### *Plasmid constructs and recombinant reoviruses*

#### PBacT7 constructs with S1His-2A-HA.E4orf4 and S1His-2A-HA.RFA

The S1His-2A-HA.E4orf4 segment was designed *in silico* and a DNA copy was synthesized by Eurofins Genomics (Ebersberg, Germany). The total length of this synthetic segment is 1419 bp (Figure 1). The segment sequence was assembled to contain the following features: 1) nt 1 to 768 from the S1 segment of reovirus mutant *jin-3*; this includes the 5'-untranslated region (UTR), entire  $\sigma$ 1s ORF, and the first 252 amino acids of the *jin-3*  $\sigma$ 1, including the codons for the G196R change near the sialic acid binding domain [11]; 2) the codons for a 6xHis-tag (18 bp) which was placed in frame with the  $\sigma$ 1 open reading frame; 3) the codons for the porcine teschovirus-1 2A sequence (66 bp + 3 additional bp); 4) the HA-tagged E4orf4 encoding sequence (372 bp); 5) a stop codon, and 6) the 3'-UTR of the S1 segment from nt 1219 to 1416 of reovirus T3D, which includes the A-, B, and C-box elements implicated in encapsidation of the reovirus plus strand RNA in the viral capsid [32, 33].

The synthetic S1His-2A-HA.E4orf4 fusion construct was inserted in a pEX-A2 plasmid by Eurofins Genomics (to generate pEX-S1His-2A-HA.E4orf4). The S1His-2A-HA.E4orf4 part was further PCR amplified from this construct using forward primer T7\_compl\_S1For (5'-TAATACGACTCACTATAGCTATTGGTCGGATGGATCCTCGCCTACG T-3') and reverse primer S1EndR (5'-GATGAAATGCCCCAGTGC-3') with Pfu polymerase (Fermentas, Fisher Scientific, Landsmeer, the Netherlands). The underlined sequences are the parts complementary to the sequence in the pEX-S1His-2A-HA.E4orf4 construct. The PCR product was digested with restriction endonuclease *SacII* and purified with SureClean (Bioline; GC Biotech BV, Alphen aan den Rijn, the Netherlands) according to the manufacturer's protocol. The PCR product was inserted in the plasmid pBACT7 backbone of pBacT7-S1T3D [34]. Plasmid pBacT7-S1T3D was obtained at Addgene (plasmid 33282). The *wt* S1T3D was

removed by digestion with *Sma*I and *Sac*II and the pBACT7 backbone was isolated from a 1% agarose gel and purified by JetSorb (Genomed; ITK Diagnostics BV, Uithoorn, the Netherlands) according to the manufacturer's protocol. The *Sac*II-digested S1His-2A-HA.E4orf4-containing PCR product was inserted in the *Sma*I- and *Sac*II-digested pBACT7 DNA with T4 DNA ligase (Fisher Scientific, Landsmeer, the Netherlands), resulting in construct pBT7-S1His-2A-HA.E4orf4.

To obtain the RFA mutant of E4orf4 that no longer binds to PP2A as a result of amino acid substitutions R81A and F84A, plasmid pBT7-S1His-2A-HA.E4orf4 was used as input for site-directed ligase-independent mutagenesis (SLIM) PCR with forward primer RFAmutE4O4\_For (5'-GATCTGTTTGTACGCCACCTGGGCTTGCT CAGGAAATATGAC-3') and reverse primer RFAmutE4O4\_Rev (5'-GTCATATTCCTGAA GCAAGCCCAGGTGGCGGCGTGACAAACAGATC-3'). Underlined are the nucleotides encoding the substituted amino acids R81A and F84A in the mutated E4orf4 protein. The SLIM PCR was performed with the following components; 100 ng pBT7-S1His-2A-HA.E4orf4, 5  $\mu$ l 10x KOD buffer, 1 mM MgSO<sub>4</sub>, 20 pmol of each primer (RFAmutE4O4\_For and RFAmutE4O4\_Rev), 250  $\mu$ M dNTP's, 1U KOD polymerase (Novagen; Merck-Millipore, Amsterdam, the Netherlands) and molecular biology-grade water to a final volume of 50  $\mu$ l. Cycling parameters: 2 min 94°C, 30 cycles 15 sec 94°C - 30 sec 58°C - 10 min 68°C and one final extension step of 10 min 68°C. The input plasmid was digested by adding 2  $\mu$ l DpnI (Fermentas, Fisher Scientific, Landsmeer, the Netherlands) to the reaction and incubation for 2 hours at 37°C. An aliquot of 10  $\mu$ l was used to transform chemically competent Top10 bacteria (Invitrogen, Fisher Scientific, Landsmeer, the Netherlands). DNA was extracted from colonies with GeneJet Plasmid Miniprep kit (Fisher Scientific, Landsmeer, the Netherlands) according to the manual and sent for sequencing to the Leiden Genome Technology Center (Leiden University Medical Center, Leiden, the Netherlands) to confirm the presence of the mutations, resulting in construct pBT7-S1His-2A-HA.RFA.

#### Reoviruses rS1-E4orf4 and rS1-RFA

Recombinant reoviruses were generated from both plasmids, pBT7-S1His-2A-HA.E4orf4 and pBT7-S1His-2A-HA.RFA as previously described [9]. In short, pBT7-S1His-2A-HA.E4orf4 or pBT7-S1His-2A-HA.RFA were transfected with TRANSIT-LT1 transfection reagent (Mirus, Sopachem BV, Ochten, the Netherlands) in BSR-T7 cells, together with four other plasmids containing the remaining reovirus segments (obtained through AddGene): pT7-L1T1L (plasmid 33286), pT7-L2-M3T3D (plasmid 33300), pT7-L3-M1T3D (plasmid 33301) and pT7-M2-S2-S3-S4T3D (plasmid 33302) [35]. Two days post transfection, the cells were harvested and lysed by three cycles of freeze-thawing and cell debris was cleared from supernatant by centrifugation.

Initial propagation was done in 911scFvHis cells until first signs of cytopathic effect (CPE) before further expanding the reoviruses on 911 cells. Official recombinant virus names rS1His-2A-HA.E4orf4 and rS1His-2A-HA.RFA are abbreviated to rS1-E4orf4 and rS1-RFA in this manuscript.

Accession number of the HA $\Delta$ V-2 E4orf4 protein: YP\_001551773.

#### *RNA isolation and S1 RT-PCR*

Cells (911,  $1 \times 10^5$  per well) in 24-well plates were infected with rS1-E4orf4 or rS1-RFA. Since we had no indication of the titer of the early passaged batches, 1/20th part of the isolated reoviruses P1 was used for exposure to 911 cells. Total RNA was extracted, 24 hours post infection (hpi), with the Absolutely RNA miniprep kit (Stratagene, Agilent Technologies, Amstelveen, the Netherlands) from the infected cells according to the manual. cDNA was synthesized with the S1EndR primer (5'-GATGAAATGCCCCAGTGC-3') and SuperScript III reverse transcriptase (Invitrogen, Life Technologies, Bleiswijk, the Netherlands). For the S1 PCR the following primers were used; S1For: 5'- GCTATTGGTCGGATGGATCCTCG-3' and S1EndR with GoTag polymerase (Promega, Leiden, the Netherlands). The PCR products were purified with SureClean (Bioline, GC Biotech BV, Alphen aan den Rijn, the Netherlands) for the subsequent sequence reactions with primers S1For, S1EndR and S1Trunc\_For: 5'-GACTGTGTTTGATTCTATCAACTC-3'. Sequence analysis was performed in the Leiden Genome Technology Center (Leiden University Medical Center, Leiden, the Netherlands).

#### *Western blot analysis*

Cell lysates were prepared in RIPA lysis buffer (50 mM Tris pH 7.5, 150 mM NaCl, 0.1% SDS, 0.5% DOC, 1% NP40) supplemented with protease inhibitors (complete mini tablets, Roche Diagnostics, Almere, the Netherlands). Protein concentrations in the lysates were measured by Bradford assay (Biorad, Veenendaal, the Netherlands).

For detection of the HA-tagged E4orf4 and RFA proteins in lysates, equal amounts of protein (30  $\mu$ g) were loaded into the slots of a 15% polyacrylamide-SDS gel after addition of western sample buffer (final concentrations: 10% glycerol, 2% SDS, 50 mM Tris-HCl pH 6.8, 2.5%  $\beta$ -mercaptoethanol and 0.025% bromophenol blue). The proteins were transferred to Immobilon-PSQ (Merck-Millipore, Amsterdam, the Netherlands) and the blot was divided for staining with  $\beta$ -Actin antibody (ImmunO clone C4, MP Biomedicals, Eindhoven, the Netherlands) and HA.11 monoclonal antibody (Biolegend, ITK Diagnostics BV, Uithoorn, the Netherlands) for detection of the HA-tag. A Goat-anti-Mouse HRP-conjugated secondary antibody was used for detection and the signals were visualized by standard chemiluminescence techniques.

Reovirus proteins were detected by loading equal amounts of lysate (20 µg) into slots of a 12% polyacrylamide-SDS gel after addition of western sample buffer. The proteins were transferred to Immobilon-FL (Merck-Millipore, Amsterdam, the Netherlands) for detection with the Odyssey system (LI-COR Biotechnology, Westburg, Leusden, the Netherlands). The blot was divided for staining with mouse Vinculin antibody hVIN-1 (Sigma-Aldrich Chemie BV, Zwijndrecht, the Netherlands) and a combination of mouse anti-σ3 4F2 (Developmental Studies Hybridoma Bank, University of Iowa, Iowa City, USA) and rabbit anti-P2A peptide serum ABS31 (Merck-Millipore, Amsterdam, the Netherlands). For the detection of the primary antibodies, the IRDye 800CW Donkey-anti-Rabbit IgG and IRDye 680RD Donkey-anti-Mouse IgG (LiCor, Westburg BV, Leusden, the Netherlands) were used, prior to analyzing the signals with the Odyssey.

#### *Immunoprecipitation (IP) assay*

Cell line 911-Flag.PP2A was infected with rS1-E4orf4 or rS1-iLOV at an MOI of 1 (in a 6-well plate). As controls, 911-Flag.PP2A cells were PEI-transfected with plasmid pEGFP-N2, plasmid pcDNA.HA.E4orf4, and plasmid pcDNA.HA.RFA (3 µg plasmid DNA per well). Lysates were made in Giordano buffer containing NP40 (50 mM Tris·HCl pH 7.4, 250 mM NaCl, 0.1% Triton X-100, 5 mM EDTA and 0.5% NP40) at 24 hpi and 48 hours post transfection. A small amount of lysate was set aside for protein detection in whole cell extracts (WCE).

Remaining cell lysates were used in the IP procedure, with anti-flag M2 affinity gel beads (Sigma-Aldrich Chemie BV, Zwijndrecht, the Netherlands) according to the manufacturer's protocol. In short, equilibrated anti-flag beads in Giordano buffer were added to the different lysates and tumbled for 2 hours at 4°C. The beads were washed 3x with Giordano buffer to remove unbound proteins, and subsequently 2x sample buffer without β-mercaptoethanol (125 mM Tris·HCl pH 6.8, 4% SDS, 20% glycerol and 0.01% bromophenol blue) was added. The samples were boiled for 5 minutes before loading on a 15% polyacrylamide-SDS gel. IP proteins in lysates were detected using anti-HA HA.11 (Biolegend, ITK Diagnostics BV, Uithoorn, the Netherlands). The blot with WCE was divided for staining with the same anti-HA antibody and monoclonal anti-flag M2 antibody (Sigma-Aldrich Chemie BV, Zwijndrecht, the Netherlands). After the incubation with the anti-flag antibody, the membranes were re-stained with the anti-σ3 4F2 antibody. For the detection of the primary antibodies, IRDye 680RD Donkey-anti-Mouse IgG was used, prior to analyzing the signals with the Odyssey (infection panel) or Goat-anti-Mouse HRP-conjugated secondary antibody for detection with the standard chemiluminescence technique (transfection panel).

### *Transfections*

Transfection controls in Western detection for HA.E4orf4 and HA.RFA proteins in 911 cells and in 911-flag.PP2A IP assay were generated using 25 kDa linear polyethyleneimine (PEI) at a concentration of 1 mg/ml (pH 7.4). For transfection of the 911 cell line, cells were grown in 24-well plates in 400  $\mu$ l fresh DMEM containing 8% FBS/well and 1  $\mu$ g DNA (either plasmid pCDNA.HA.E4orf4 or plasmid pCDNA.HA.RFA) mixed with 3  $\mu$ g PEI in 100  $\mu$ l Opti-MEM (Invitrogen, Life Technologies, Bleiswijk, the Netherlands). For the IP controls, 911-flag.PP2A cells in 1.5 ml DMEM, 8% FBS in 6 well plates were transfected using 3  $\mu$ g DNA (pCDNA.HA.E4orf4, pCDNA.HA.RFA or pEGFP-N2 plasmids) and 9  $\mu$ g PEI in 250  $\mu$ l Opti-MEM. The next day the cells received fresh DMEM with 8% FBS and were allowed to recover for 48 hours before the cells were harvested and lysed.

### *Viability (WST) assays*

WST-1 reagent (Roche, Woerden, the Netherlands) was used to assay the viability of cells after reovirus infections. In a 96-well plate  $5 \times 10^3$  cells/well (in triplicate) were exposed to different reoviruses (rS1-E4orf4, -RFA, -iLOV, *jin-3* and wt-R124) at an MOI of 5 (Figure 4) or MOI of 30 (Figure 5B) in DMEM containing 2% FBS, or mock-infected. For the assay 5  $\mu$ l of WST-1 reagent, which is half of the amount suggested by the manufacturer, was added to each well which already contained 100  $\mu$ l medium, at the indicated days post infection. The percentage survival was calculated by dividing the OD<sub>450</sub> values of the reovirus-exposed cells by the values of the mock-treated cells for each cell line, and multiplying this by 100%. Cultures with survival values below 1% were considered all dead and adjusted to 1% for plotting the data in log scale.

### *Caspase 3/7 assay*

H1299 and 911 cells, grown in 96-well plates at  $5 \times 10^3$  cells/well were exposed to the reovirus variants wt-R124, *jin-3*, rS1-E4orf4, rS1-RFA or rS1-iLOV, each at an MOI of 30, or mock-infected. All conditions were tested in triplicate. Caspase activity was measured 24 hpi using the Caspase-Glo 3/7 assay (Promega, Leiden, the Netherlands) according to the manufacturer's protocol. For the detection, a PerkinElmer's VictorX3 (PerkinElmer, Groningen, the Netherlands) multilabel plate reader was used.

### *Statistics*

For the WST-1 assays the percentages survival were transformed to log kill with this formula:  $\log \text{ kill} = \log(100/\text{survival} (\%))$ . Subsequently multiple t tests were performed on the transformed data with corrections for multiple comparisons using the Holm-

Sidak method in GraphPad Prism version 7.0. The generated results (log kill and adjusted P values for comparisons) are summarized in separate tables.

## RESULTS

### *Generation of recombinant reoviruses*

To augment the oncolytic potency of reoviruses we have chosen to explore the possibility of incorporating a therapeutic transgene in their genome. Our previous results demonstrated that the S1 segment, encoding the reovirus attachment protein  $\sigma 1$ , is a suitable location for inserting a gene encoding for a small fluorescent protein, called iLOV, without loss of virus replication [9]. The engineered recombinant reoviruses can no longer bind to the reovirus receptor junction adhesion molecule-A (JAM-A) but are thought to rely on enhanced binding to sialylated glycans on the cell surface. The removal of the codons for the JAM-A interacting head domain of the reovirus attachment protein  $\sigma 1$ , allows for the insertion of small transgenes without exceeding the size of the wild-type T3D S1 segment. As a potentially clinically relevant protein in the context of anti-tumor features, we chose the HAdV-2 E4orf4. Protein E4orf4 induces p53-independent cell death in tumor cells and not in normal diploid cells. The size of the E4orf4 cDNA is 345 bp in length and therefore fits in the S1 segment to replace the sequence encoding the JAM-A binding domain. To detect E4orf4 in cells, the codons for an HA-tag were fused with the amino terminus of the E4orf4 gene, increasing the insert size with 27 nucleotides. The addition of the HA-tag to the amino terminus of HAdV-2 E4orf4 does not affect its function [12]. We employed the porcine teschovirus-1 2A element to allow separation of the truncated and C-terminal His-tagged  $\sigma 1$  from the HA-tagged E4orf4 protein, similar to the strategy previously used to generate the iLOV reporter virus (Figure 1). Similarly, we generated a derivative virus in which four point mutations in the E4orf4 gene substitute two amino acids at position 81 and 84 (R81A/F84A). This 'RFA' virus is unable to bind to PP2A.

To produce the recombinant reoviruses rS1-E4orf4 and rS1-RFA, the plasmids with the modified S1 segments together with four plasmids encoding the other nine genome segments of reovirus were transfected into BSR-T7 cells as previously described [9]. Newly assembled recombinant reoviruses from the transfected BSR-T7 cells were propagated on 911 cells containing an artificial receptor for the His-tag (911scFvHis), yielding passage 1 (P1) of the recombinant reovirus. For further propagation the 911 cell line was used.

The genetic integrity of the recombinant reoviruses was checked by sequencing the RT-PCR product of the isolated viral S1 RNA. The expected nucleotide changes in the RFA mutant are present (positions 1120-1121 CG in E4orf4 to GC in

RFA and at positions 1129-1130 TT in E4orf4 to GC in RFA) and no other mutations were found in either the S1-E4orf4 or in the S1-RFA segments (Figure 2A).

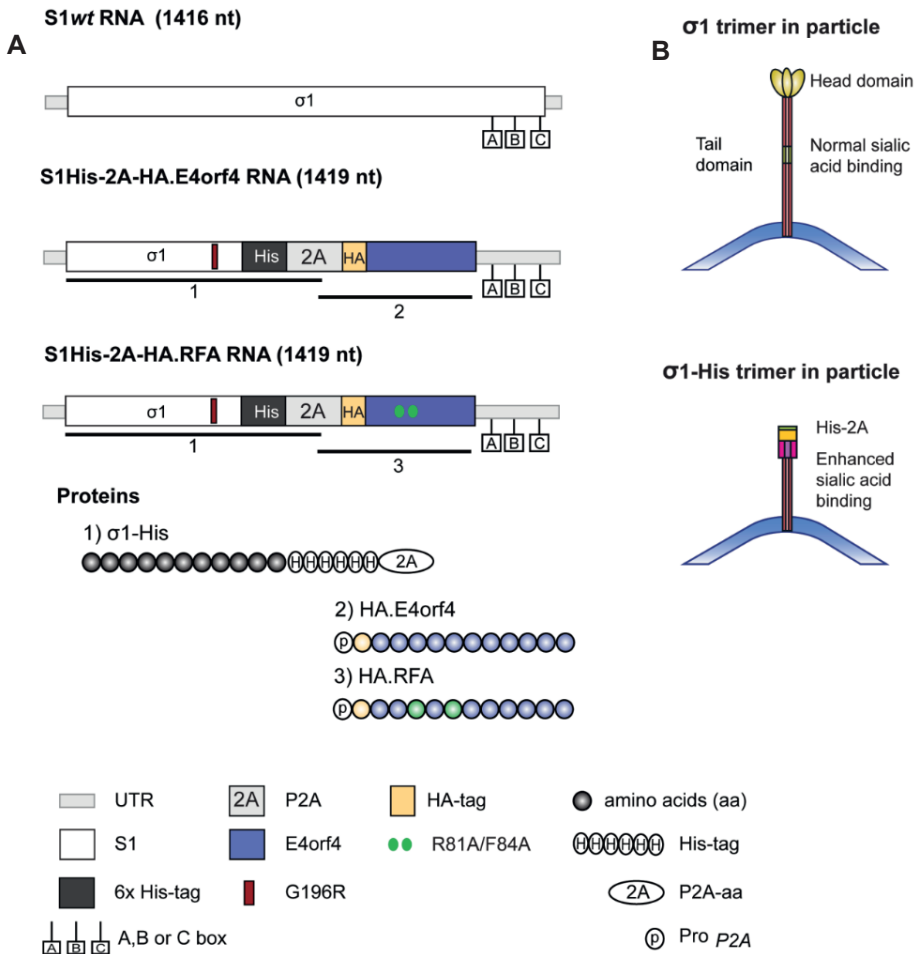


**Figure 1.** Schematic representation of the modified S1 gene segment. A) S1wt RNA compared with S1His-2A-HA.E4orf4 and the double mutant S1His-2A-HA.RFA RNA. Protein HA.RFA cannot bind to Protein Phosphatase 2A. The  $\sigma$ 1-His protein is present in the particle, the HA-tagged proteins (E4orf4 or the double mutant RFA) only in infected cells. Modified reovirus S1 contains a point mutation in the sequence coding for the  $\sigma$ 1 tail resulting in a G196R amino acid change. This change allows the virus to enter host cells by enhanced binding to sialic acids and compensates for the loss of the head domain. B) Simplified depiction of the wt  $\sigma$ 1 trimer and the truncated  $\sigma$ 1-His trimer in the capsid of a reovirus particle.

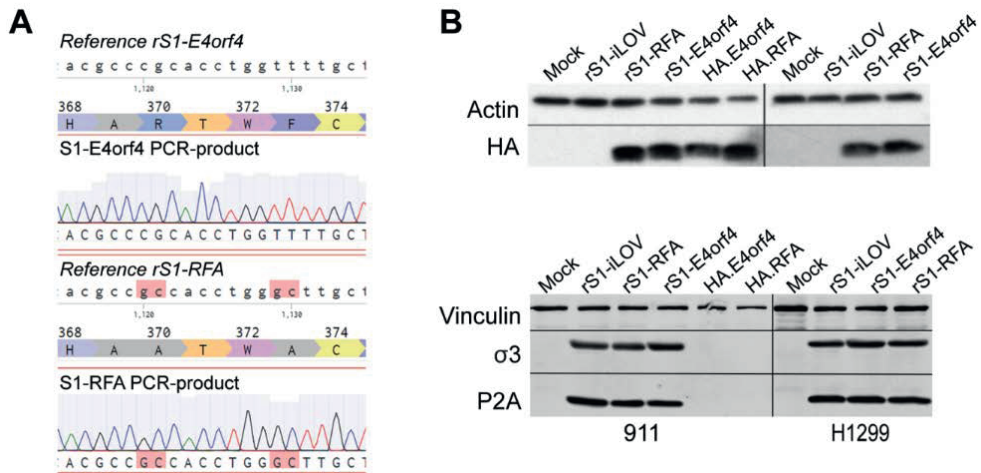


**Figure 2.** Confirmation of S1His-2A-HA.E4orf4 and -HA.RFA sequence and protein expression in cell lysates. A) Alignment of E4orf4 and RFA RT-PCR sequencing results with the reference sequences. The amino acid sequence is depicted in the reference panels. The nucleotide mutations in the S1His-2A-HA.RFA sequence responsible for the amino acid changes R to A and F to A are marked in red boxes. The amino acid numbering 368 to 374 is derived from the complete  $\sigma 1$ -His-2A-HA.E4orf4/RFA protein. Alignments are generated with Benchling (Benchling Inc., San Francisco, USA). B) Protein detection by western blotting in 911 (left part) and H1299 (right part) cell lysates. 911 and H1299 cells were mock-infected or infected with recombinant reoviruses (at an MOI of 1) rS1-iLOV, rS1-E4orf4 or rS1-RFA. As positive controls for detection of HA-tagged proteins, 911 cells were transfected with pcDNA.HA.E4orf4 (HA.E4orf4) and pcDNA.HA.RFA (HA.RFA). RIPA lysates were generated 48 hours after infection/transfection. Upper panel: detection of HA-tagged E4orf4 or RFA proteins. Actin staining was included as loading control. Lower panel: detection of viral proteins  $\sigma 3$  (4F2 antibody) and  $\sigma 1$ -His (P2A antibody) in lysates of infected cells. Loading control: vinculin.

To study the genetic stability of the recombinants, the viruses were serially passaged 10 times in 911 cells. In P10 of a rS1-E4orf4 reovirus batch we detected the presence of a minor population that contained a deletion in the S1-E4orf4 segment. Sequence analysis revealed the loss of 47 nucleotides at the 3' end of the E4orf4 sequence, resulting in a shift in location of the stop codon and a 6 nucleotide deletion in the A-box of S1 (Figure S1). In the E4orf4 protein this resulted in a loss of 5 amino acids at the C-terminus and two amino acid changes compared to the full-length E4orf4 protein. The C-terminus of E4orf4 in different adenovirus strains is the

least conserved region of the protein, in contrast to the highly conserved binding sites for PP2A and Src. In the deletion mutant found, the binding sites of PP2A and Src are not affected (Figure S2). The same deletion mutant emerged in high passage number batches of several independent transfection experiments to generate rS1-E4orf4 reovirus in BSR-T7 cells. Therefore, we decided to use for all experiments a low passage number of rS1-E4orf4 reovirus in which only trace amounts of the deletion mutant were detectable by RT-PCR of the S1-E4orf4 segment. Remarkably, no deletion mutants were detected in batches of rS1-RFA reoviruses.

To verify that the modified S1 segments were expressed and the E4orf4 proteins were produced in infected cells, 911 and H1299 cells were exposed to rS1-E4orf4 and rS1-RFA reoviruses at an MOI of 1. As positive controls, 911 cells transfected with plasmid pcDNA.HA.E4orf4 or plasmid pcDNA.HA.RFA were included (Figure 2B). HA-tagged proteins (14 kDa) were detected 48 hours post infection (hpi) in both the 911 and H1299 cell lines infected with rS1-E4orf4, rS1-RFA and in the plasmid-transfected 911 cells. No HA-tag could be detected in cells infected with the rS1-iLOV reovirus carrying the iLOV gene as reporter. On a separate blot, the same cell lysates were incubated with an antibody directed against reovirus  $\sigma 3$  (41 kDa) to show the presence of replicating reovirus and a P2A antibody to detect the recombinant truncated  $\sigma 1$  (30 kDa) proteins. P2A and  $\sigma 3$  were detected in the cell lysates of cells infected with the three recombinant reoviruses, but not in uninfected cells or transfected 911 cells.

Detection of  $\sigma 3$  and P2A in lysates of rS1-E4orf4 and rS1-RFA infected 911 and H1299 cells showed that the two recombinant reoviruses infect and replicate in both cell lines. In addition, detection of the HA-tagged proteins demonstrated the efficient expression of the E4orf4 and RFA transgenes in cells upon infection with the recombinant reoviruses.

#### *E4orf4 binds to PP2A in context of reovirus infection*

To confirm that the adenovirus E4orf4 protein expressed in the context of a reovirus infection can bind to the B55 $\alpha$  subunit of cellular protein phosphatase 2A (PP2A), 911 cells expressing flag-tagged PP2A (911-Flag.PP2A) were infected with the rS1-E4orf4, rS1-RFA and rS1-iLOV reoviruses. In a co-immunoprecipitation assay, E4orf4 was found to interact with the flag-tagged PP2A in lysates of the rS1-E4orf4 infected cells (Figure 3). This interaction was also evident in 911-Flag.PP2A cells transfected with a plasmid encoding the HA-tagged E4orf4 protein. In contrast, in 911-Flag.PP2A cells infected with rS1-RFA or transfected with the double mutant HA.RFA plasmid, no association was visible on the Flag-IP blot. These results demonstrate the capacity of E4orf4 to interact with PP2A-B55 $\alpha$  in the context of a reovirus infection.

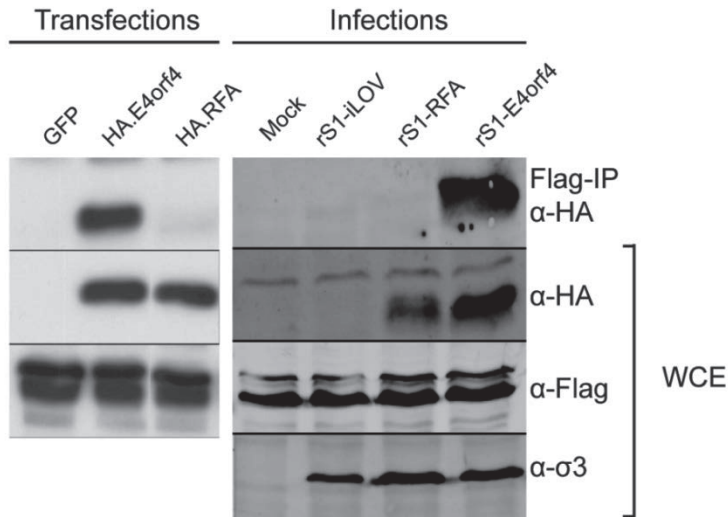


**Figure 3.** Detection of E4orf4 - PP2A interaction in reovirus rS1-E4orf4 infected 911-Flag.PP2A cells. HA.E4orf4 was co-immunoprecipitated using anti-flag antibodies to confirm the association of Flag.PP2A with E4orf4 in the context of reovirus rS1-E4orf4 infection. 911-Flag.PP2A cells were mock-infected or infected with rS1-iLOV, rS1-RFA and rS1-E4orf4 viruses at an MOI of 1. As controls 911-Flag.PP2A cells were transfected with pcDNA.HA.E4orf4 (HA.E4orf4) and pcDNA.HA.RFA (HA.RFA). As a negative control pEGFP-N2 (GFP) is included. Lysates were made 24 hours post infection (hpi) or 48 hours post transfection. Blots with whole cell extracts (WCE) were subjected to HA-antibody staining to show presence of HA-tagged E4orf4 and RFA proteins in lysates of infected and transfected cells. Expression of Flag-tagged PP2A in WCE was detected with anti-flag antibody and presence of reovirus protein in infected cells was detected using anti- $\sigma$ 3.

#### *E4orf4 reoviruses induce cell death in most, but not all tumor cell lines tested*

To test to what extent the recombinant reoviruses containing either iLOV, E4orf4 or RFA as transgenes are capable of inducing cell death in tumor cell lines, we used an assay based on cleavage of the tetrazolium salt WST-1 by living cells to quantify residual cell viability upon reovirus infection. Cells were exposed to the three recombinant reoviruses rS1-iLOV, rS1-E4orf4 and rS1-RFA, *wt*-R124, and *jin*-3 mutant reovirus at an MOI of 5 and cell viability was measured 5 days post infection (dpi) (Figure 4A). In the permissive 911 cells all viruses induce cell death, with *jin*-3 and *wt*-R124 reoviruses being more efficient than the recombinant viruses. The JAM-A negative glioblastoma cell line U118-MG could be very efficiently killed by *jin*-3 but resisted *wt*-R124 infection. In addition, all three recombinant reoviruses induced cell

death in U118-MG cells to a similar extent. A comparable result was obtained for the chicken hepatoma cell line LMH. Chicken cells do not express a cellular receptor that can be used by mammalian reoviruses and therefore resist *wt*-R124 infection. The three recombinant reoviruses are comparably effective (10% cell survival or less) in induction of cell death in LMH cell cultures as *jin-3* (~20% cell survival). In the JAM-A negative human bladder cancer cell line UMUC-3 the recombinant reoviruses induce cell death but these cells are less sensitive to *jin-3* and fully resist *wt*-R124 infection. Of all cell lines tested here, only the JAM-A positive Pro4-Luc cells are not sensitive to infection by the recombinant reoviruses or *wt*-R124. However, these cells are efficiently infected and killed by *jin-3*.

An overview of the cell lines used with information on the JAM-A status and susceptibility to *wt*-R124 infection as well as a motivation for the cell lines used, is summarized in the supplementary data (Table S1). To confirm that reoviruses rS1-E4orf4 and rS1-RFA can enter the five cell lines, we exposed cells to rS1-RFA and rS1-E4orf4 at an MOI of 2 and checked for reovirus  $\sigma 3$  at 1 and 24 hpi in a western blot assay. In the cell lysates an increase in reovirus  $\sigma 3$  is detected 24 hpi compared to 1 hpi suggesting that indeed the viruses can enter and start to replicate in the cells. Even in the Pro4-Luc cells that resist oncolysis by both rS1-RFA and rS1-E4orf4 an increase in reovirus  $\sigma 3$  is evidently detected (Figure S3). In the cell lines LMH and UMUC-3 the amount of reovirus  $\sigma 3$  protein after 24 hours is lower than that in the other cell lines. It is possible that in LMH and UMUC-3 the replication process is slower, since 5 dpi the cells do respond to induction of cell death (Figure 4A).

Expression of the E4orf4 transgene after reovirus-mediated gene transfer into cells should not affect the viability of normal non-transformed cells. Cultures of the normal diploid skin fibroblast VH10, VH25 and control 911 cells were exposed to rS1-E4orf4, rS1-RFA, *jin-3* and *wt*-R124 at an MOI of 5. At 4 dpi, a WST-1-based cell viability assay was performed. In both fibroblast cell lines no reduction in cell viability was detected upon *jin-3*, *wt*-R124 and the two recombinant reoviruses containing E4orf4 or RFA (Figure 4B).

The results of the cell viability assays suggest that all three recombinant reoviruses tested are potent in inducing cell death in the tumor cell lines. A comparison of the mean log kill of rS1-E4orf4 to rS1-RFA or rS1-iLOV confirms that E4orf4 has no added effect on induction of cell death in the tested cell lines (Table 1). This suggests that the recombinant reoviruses with truncated  $\sigma 1$  protein and enhanced sialic acid binding capability are, by themselves, potent inducers of cell death in various tumor cells, while normal human diploid fibroblasts are not affected by these viruses.

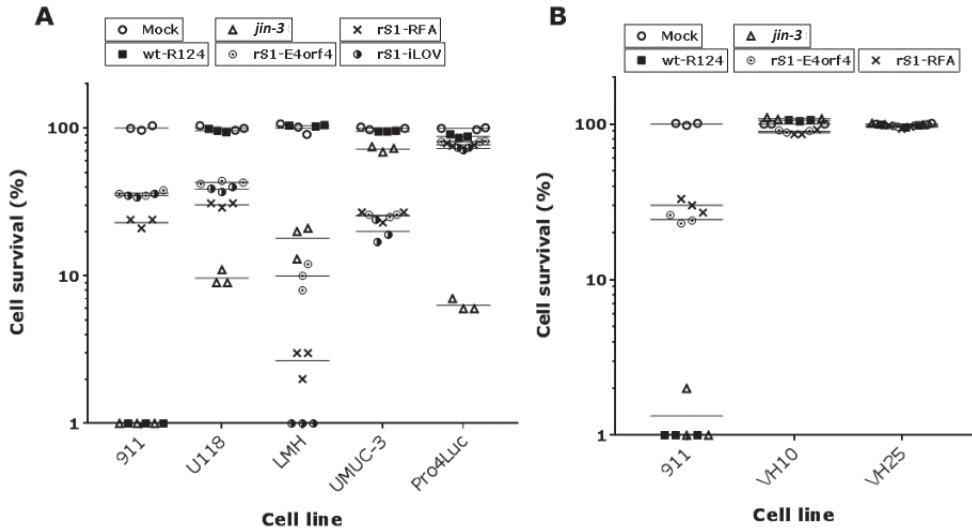


**Figure 4.** Cell viability assay in various tumor cell lines and normal fibroblasts after exposure to recombinant reoviruses, *jin-3*, or wt-R124. A) Cultures of various cell lines (*i.e.* 911, U118-MG, LMH, UMUC-3, and Pro4-Luc) are mock-treated or exposed in triplicate to one of the five reoviruses; wt-R124, *jin-3*, rS1-E4orf4, rS1-RFA or rS1-iLOV at an MOI of 5. WST-1 reagent was added 5 days post infection (dpi). B) Cells (911 and normal fibroblast cell lines VH10 and VH25) are mock-treated or exposed in triplicate to 4 reoviruses; wt-R124, *jin-3*, rS1-E4orf4 or rS1-RFA at an MOI of 5. WST-1 reagent was added 4 dpi. Cell survival (%) was calculated as the percentage of OD<sub>450</sub> values of the infected cells over the mock-treated cells and plotted in a log scale on the Y-axis using GraphPad Prism 7.0d.

Cell line	Mean log kill			Mean log kill		
	S1-E4orf4	S1-RFA	Adjusted <i>P</i>	S1-E4orf4	S1-iLOV	Adjusted <i>P</i>
911	0.44	0.64	0.003	0.44	0.46	0.273
U118-MG	0.37	0.52	<0.001	0.37	0.41	0.047
LMH	1.01	1.58	0.005	1.01	2.00	<0.001
UMUC-3	0.59	0.59	0.964	0.59	0.70	0.124
Pro4Luc	0.09	0.11	0.028	0.09	0.14	0.007

**Table 1.** Mean log kill calculations belonging to Figure 4a.

*Addition of E4orf4 in reovirus recombinants does not increase caspase 3/7 activity in both H1299 and 911 cells*

Diverse mechanisms of cell death can be triggered by E4orf4 proteins. Several studies using the human non-small-cell lung carcinoma cell line H1299 show that transfection of a plasmid containing E4orf4 results in the induction of caspase 3/7 activity, but this activation is not required for the induction of cell death. In these cells the caspase inhibitor CrmA did not inhibit E4orf4-induced cell death [12, 14, 36]. We first evaluated the wt-R124 reovirus-induced cell death of H1299 cells, as there is a marked discrepancy in the effect of reovirus on these cells in the available literature data [26, 37].

The H1299 and 911 cells were exposed to the 5 different reovirus variants at an MOI of 30. At 5 dpi, the cell viability was measured (Figure 5A). The viability of H1299 cells exposed to wt-R124 was reduced to ~45% compared to uninfected cells. Recombinant reovirus rS1-E4orf4 and rS1-iLOV decreased viability of the exposed H1299 cells to ~60%, and rS1-RFA to ~40%. The reovirus mutant *jin-3* was the most potent inducer of cell death in H1299 cells (< 1%). In 911 cells all 5 reoviruses reduce the cell viability to ~10% or less. From these data we conclude that in H1299 cells the E4orf4 protein does not contribute to an increased oncolytic potency of the rS1-E4orf4 virus in comparison to wt-R124 reovirus. This is evident from the comparison of the mean log kill upon exposure of H1299 cells to the rS1-E4orf4 to rS1-RFA or rS1-iLOV viruses (Table 2).

In a subsequent experiment we measured the induction of caspase 3/7 activity in both H1299 and 911 cell lines upon infection with the different reoviruses (Figure 5B). In 911 cells, both wt-R124 and mutant *jin-3* strongly induced caspase 3/7 activity compared to mock-treated cells (a 12-fold and 14-fold increase, respectively). All three recombinant reoviruses (rS1-E4orf4, rS1-RFA, and rS1-iLOV) displayed only a 4-fold increase over mock-treated cells. In reovirus-infected H1299 cells induction of caspase 3/7 activity was for all five virus variants much lower; for wt-R124 there was only a very small increase compared to mock-treated cells, *jin-3* and the three recombinant reoviruses increased the caspase activity approximately 2-fold compared to mock-infected cells. Apparently, insertion of E4orf4 in reovirus did not lead to an additional increase in caspase 3/7 activity in H1299 cells. The 2-fold increase of caspase 3/7 activity in H1299 cells did not correlate to induction of cell death, since reovirus mutant *jin-3* effectively killed H1299 cells while the three recombinant reoviruses were as effective as wt-R124 in cell lysis.

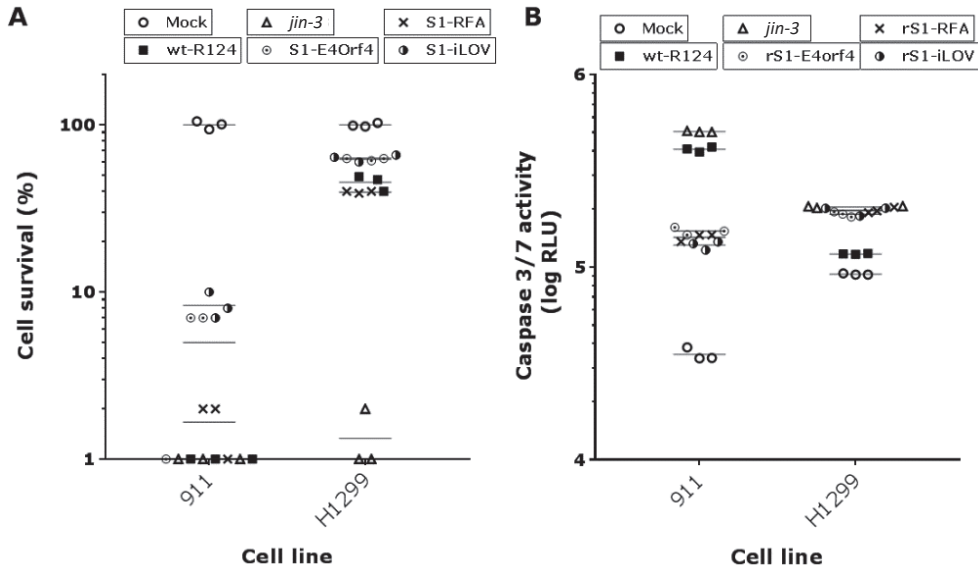


**Figure 5.** Caspase 3/7 activity and cell viability in H1299 and 911 cells after exposure to recombinant reoviruses, *jin-3*, or wt-R124. A) Cells (911 and H1299) were mock-treated or exposed in triplicate to five reoviruses; wt-R124, *jin-3*, rS1-E4orf4, rS1-RFA or rS1-iLOV at an MOI of 30. WST-1 reagent was added 5 days post infection. Cell survival (%) was calculated as the percentage of OD<sub>450</sub> values of the infected cells over the mock-treated cells and plotted in a log scale on the Y-axis. B) Cells (911 and H1299) were mock-treated or exposed in triplicate to five reoviruses; wt-R124, *jin-3*, rS1-E4orf4, rS1-RFA or rS1-iLOV at an MOI of 30. Caspase 3/7 activity was measured 24 hours post infection. Caspase activity is plotted on the Y-axis in log relative light units (log RLU). Graphs are generated using GraphPad Prism 7.0d.

Cell line	Mean log kill			Mean log kill		
	S1-E4orf4	S1-RFA	Adjusted <i>P</i>	S1-E4orf4	S1-iLOV	Adjusted <i>P</i>
911	1.44	1.80	0.292	1.44	1.08	0.487
H1299	0.21	0.40	<0.001	0.21	0.20	0.639

**Table 2.** Mean log kill calculations belonging to Figure 5a.

## DISCUSSION

Oncolytic virus therapy is a powerful approach for cancer treatment. Already a large number of clinical studies demonstrated the feasibility and safety of the approach [5, 38, 39]. Nevertheless, the anti-tumor response of oncolytic virus therapy needs improvement. Such enhancements may come from combining the administration of

the oncolytic viruses with immunomodulation or conventional anti-cancer treatments such as radiation or chemotherapy. In addition, the oncolytic virus may be modified to enhance tumor cell selectivity (tumor targeting), tumor cell infectivity (expanding the virus' tropism), or by including a transgene that may enhance anti-tumor efficacy. Such approaches have been extensively evaluated in a wide variety of preclinical and clinical studies involving adenoviruses [40, 41]. Here we demonstrated the feasibility of generating replication-competent, expanded-tropism reoviruses carrying a heterologous transgene for enhancing its cytolytic activity.

Previously, we demonstrated the feasibility of genetically retargeting reoviruses to an artificial receptor by inclusion of a receptor-binding ligand at the carboxyl terminus of the viral spike protein [42]. Furthermore, using bioselection we identified several *j1n* mutants that were able to infect wt reovirus-resistant JAM-A deficient cells. The mutations in the *j1n* viruses clustered in the region of the  $\sigma$ 1-spike protein's shaft that is involved in sialic acid binding [11]. The enhanced-affinity sialic acid binding most probably underlies the viruses' capacity to infect cells independent of JAM-A expression.

This enhanced tropism for binding to sialic acids allows for the replacement of JAM-A interacting sequences in the head domain by heterologous sequences as we previously showed by insertion of a small reporter gene encoding the iLOV reporter that exhibits a green fluorescence protein [9]. In the study reported here we generated two new recombinant reoviruses that encode the HAdV-2 E4orf4 protein as well as the E4orf4 'RFA' mutant protein, which cannot interact with the B $\alpha$  subunit of protein phosphatase 2A (PP2A). We showed that inclusion in the reovirus S1 segment of the codons for the HAdV-2 E4orf4 protein or its double mutant 'RFA', yields replication-competent recombinant reoviruses. In cell lysates of rS1-E4orf4 or rS1-RFA infected 911 and H1299 cells, HA.E4orf4 and HA.E4orf4.RFA could be detected (Figure 2B). Moreover, we confirmed that the wt E4orf4 protein can bind the B $\alpha$  subunit of PP2A also in reovirus-infected cells.

The use of the rS1-RFA reovirus was based on loss of interaction between the RFA protein and PP2A. It should be noted that this is not an inert control as this protein retains the capacity to bind to Src family kinases [17]. Src kinases are tyrosine phosphatases that are involved in many cellular processes such as cell growth and differentiation. They interact with many cellular proteins including cell surface receptors [43]. Src kinase binds directly to the arginine-rich motif of E4orf4 and leads to tyrosine phosphorylation of E4orf4. This eventually results in caspase-independent induction of cytoplasmic cell death [44]. The E4orf4 mutant RFA can still bind Src kinase and cause cell death independent of binding to PP2A. Although the E4orf4 protein is mainly present in the nucleus during an adenovirus infection

and interaction with Src kinase is rarely observed, overexpression of E4orf4 in the cytoplasm, outside the context of an adenovirus infection, leads to binding of Src kinase and programmed cell death [15,16].

In rS1-E4orf4 virus infected cells, like in transfection experiments, E4orf4 is present in both the nucleus and cytoplasm (data not shown). Therefore, we also included the rS1-iLOV as an additional control in our studies. In our recombinant reoviruses only the N-terminal part of  $\sigma 1$  (*i.e.* the first 252 amino acids) is present. Our previous data with rS1-iLOV showed that this virus was able to induce cell death in several transformed cell lines that resisted *wt*-R124 cell killing. In another study an attenuated T3D reovirus mutant was found in persistently infected HT1080 cells, and this virus harbored a stop codon in S1 resulting in a truncated  $\sigma 1$  protein after the first 251 amino acids. This reovirus could still induce cell death in tumor cell lines, although with a slightly reduced efficiency. Furthermore, this reovirus was severely attenuated in SCID mice [45]. Our data demonstrate that our recombinant reoviruses with the truncated  $\sigma 1$  proteins are potent inducers of cell death in the tumor cell lines U118-MG, LMH and UMUC-3, but not in normal fibroblasts. The only cancer cell line of our panel that resists all three of our recombinant reoviruses is the Pro4-Luc cell line, but these cells are efficiently killed by *jin-3* (Figure 4).

In none of the cell lines tested, inclusion of transgenes encoding the E4orf4 protein or its RFA derivative did enhance the induction of cell death in infected cells compared to reovirus carrying the iLOV transgene. In many studies that evaluate the HAdV-2 E4orf4-induced cell death, H1299 cells were used as the model [12, 14, 36]. To explore if E4orf4 or RFA expression in the context of our recombinant reovirus infection could have an enhanced effect over *wt*-R124, *jin-3* or iLOV containing reovirus, we also used H1299 cells (Figure 5). However, infection with rS1-E4orf4 and rS1-RFA did not further decrease the viability of H1299 cells compared to rS1-iLOV. The most potent inducer of cell death in H1299 cells was *jin-3*. All five reovirus variants strongly reduce the viability of 911 cells after infection. We further checked whether caspase 3/7 activity was increased upon E4orf4 expression in H1299 cells. According to literature, caspase 3/7 activity was increased in H1299 cells in plasmid transfection experiments with E4orf4-containing plasmids, but addition of a caspase inhibitor did not inhibit the induction of cell death [14]. In cell lines 911 and H1299 a different caspase response was observed upon infection with the five reoviruses. Both *wt*-R124 and *jin-3* showed a great increase in caspase 3/7 activity in 911 cells but this effect is much less in H1299 cells. The three recombinant reoviruses, however, exhibit a moderate induction of caspase 3/7 in 911 cells (4-fold increase over mock). In H1299 cells the fold induction over mock is similar in cells exposed to *jin-3* and the recombinant reoviruses; approximately 2-fold. In the context of reovirus, E4orf4 does neither increase caspase 3/7 activity in infected H1299 cells

nor in 911 cells. The 2-fold induction of caspase 3/7 activity in H1299 cells did not correlate with the induction of cell death as observed in the WST-1 assay, since *jin-3*, which exerted a similar caspase induction, kills H1299 cells more effectively than the recombinant reoviruses.

In some cell types, binding of the reovirus  $\sigma 1$  protein to sialic acids induces a non-apoptotic cell death pathway, *i.e.* necrosis, much more efficiently than reoviruses lacking sialic acid binding capacity [27]. In other cell types, binding to sialic acids induces more potent apoptotic cell death [46]. Our finding that reoviruses with enhanced sialic acid binding capacity seem to induce pronounced cell death but with relatively limited caspase activity in 911 cells, are consistent with the results by Hiller *et al.* [27], who showed that reoviruses capable of binding to sialic acid induce a caspase-independent form of cell death. The presence of the JAM-A binding domain in  $\sigma 1$  of reovirus mutant *jin-3* could explain the enhanced induction of caspase 3/7 activity in 911 cells, and confirms the findings of Connolly *et al.* [46], that indicate that the JAM-A binding domain is involved in activation of NF- $\kappa$ B and subsequent induction of apoptosis.

For oncolytic viruses to be applicable in the clinic they need to be efficacious as well as genetically stable. While the viruses generated in this study are generally stable when propagated in the 911 production cell line, reovirus deletion mutants in batches of rS1-E4orf4 were occasionally detected. Most notably a 47-nucleotide deletion in rS1-E4orf4 batches that spans the last 24 nucleotides of the 3' part of the E4orf4 sequence, leads to relocation of the stop codon and disrupts the A-box in the S1 segment. The three boxes – A, B and C - (Figure 1) included in the transgene containing S1 sequence are thought to be important for packaging of the segment into the virions [32]. However, the described disruption of the A-box resulted in a replicating virus, indicating that the A-box is trivial for efficient viral genome packaging. The resulting E4orf4 protein in the deletion mutant is 5 amino acids shorter at the C-terminus and has two amino acid changes (valine and serine to tyrosine and glutamic acid, respectively) compared to the full-length E4orf4 protein (Figure S1). The C-terminus of E4orf4 proteins from different adenoviruses is quite variable, therefore we assume that our E4orf4 deletion mutant would not interfere with the interaction of the protein to its binding partners, PP2A and Src. In the E4orf4 proteins of the different adenovirus strains the binding domains of both PP2A and Src are highly conserved and these domains are unchanged in the deletion mutant of E4orf4 present in the rS1-E4orf4 batches (Figure S2). Remarkably, in batches with rS1-RFA reoviruses, deletion mutants were never observed upon serial propagation, even though the nucleotide substitutions are located at some distance ( $\sim 70$  nt) from the breakpoint.

In rS1-iLOV batches, also deletion mutants were detected in high passage number batches [9]. The mutations in these batches were larger and affected the function of the iLOV protein. They also located at the 3' end of the transgene sequence. In two different mutants found in rS1-iLOV batches, the nucleotides recognized as the A-box were completely deleted. In the E4orf4 deletion mutant reoviruses only 6 nucleotides of the A-box were deleted, further confirming that the A-box is dispensable for packaging of the S1 segment in reovirus particles.

In high passage number rS1-iLOV batches, no full-length S1-iLOV was detected, suggesting that the deletion mutants had a selective advantage over the iLOV-containing viruses. In the rS1-E4orf4 virus batches, even at a high passage number, the full-length S1-E4orf4 segment remained dominantly present.

It is most likely that the deletions occur at a viral RNA level and not by rearrangements of the plasmids used for reovirus generation. In an independent experiment where we used limiting dilutions after one single round of propagation on 911 cells we detected two different deletion mutants only upon continued passaging (data not shown), strongly suggesting that the deletions occurred during the replication of the reovirus RNA genomes during propagation.

No additional deletions or point mutations were found in the S1 sequence of the three recombinant reoviruses. This suggests that the point mutation underlying the *jln-3* phenotype is stable and that no additional mutations are required for effective replication of the recombinant reoviruses in the 911 helper cell line.

It remains to be established whether the recombinant reoviruses are effective *in vivo*. New variants that efficiently replicate, spread, and enhance anti-tumor immunity *in situ* may be required. It is encouraging that we can combine forward and reverse genetics approaches to generate such variants.

Since the recombinant reoviruses with truncated  $\sigma 1$  spikes are potent inducers of cell death by themselves, adding transgenes that encode proteins that amplify oncolysis may be obsolete. A better choice may be to use the available capacity for including foreign transgenes encoding immunostimulatory proteins or cancer vaccine peptides. This will combine the reovirus-induced cell death and possible release of tumor antigens in the tumor environment with the stimulation of an anti-cancer immune response.

## SUPPLEMENTARY FIGURES



**Figure S1.** Partial alignment of the E4orf4 deletion mutant (Del mut) sequence with full-length E4orf4 (HADV-2) sequence. The deletion is highlighted in pink-shaded boxes. The A-box is marked and spans nucleotides 1242-1252. The stop codons are marked with \* in the yellow-shaded background. Abbreviations: Nucl - Nucleotide sequence; AA - amino acid translation. Alignments are generated with Benchling (Benchling Inc., San Francisco, USA).

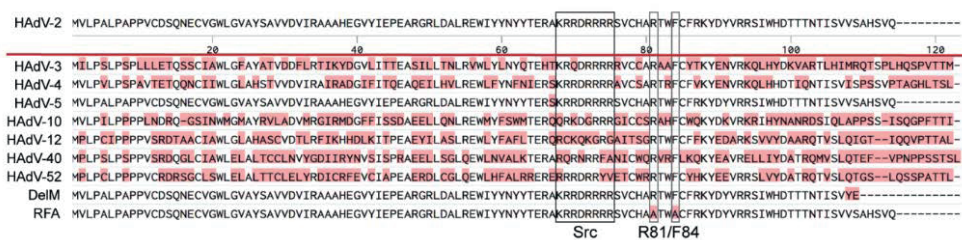


**Figure S2.** Alignment of E4orf4 proteins of various adenovirus types with deletion mutant E4orf4 (DelM) and the RFA protein. Mismatches are annotated with pink-shaded boxes. The conserved Src binding domain and conserved amino acids R81 and F84 are marked with black squares. Alignments are generated with Benchling (Benchling Inc., San Francisco, USA). Accession numbers used in the alignments of E4orf4 proteins are: HAdV-3 AET87291; HAdV-4 YP\_068051; HAdV-5 AP\_000229; HAdV-10 BAM66773; HAdV-12 CAB57853.1; HAdV-40 AMQ95251; HAdV-52 ABK35062. HAdV-2 E4orf4 is used in our recombinant reovirus and serves as the alignment template; Accession number YP\_001551773.

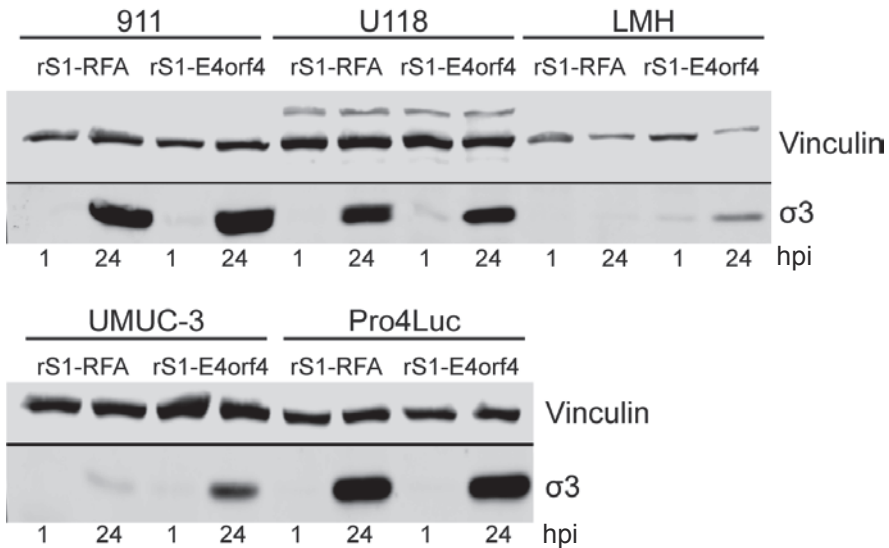


**Figure S3.** Indication of reovirus replication by comparing reovirus  $\sigma 3$  protein levels at 1 hour and 24 hours post infection (hpi). Cell lines 911, U118-MG (U118), LMH, UMUC-3, and Pro4-Luc were exposed to recombinant reoviruses rS1-RFA and rS1-E4orf4 at an MOI of 2 in 2 wells per virus for each cell line, in a 24-well plate. Giordano lysates were made 1 hour or 24 hours post infection. For the 24 hour timepoint, fresh medium was added to the cells in the well 1 hour post exposure. Equal volumes (1/4 of the total volume) of lysates were loaded into the slots of a 10% polyacrylamide-SDS gel. The proteins were transferred to Immobilon-FL. The blot was divided for staining with mouse Vinculin antibody (hVIN-1) and mouse anti- $\sigma 3$  (4F2). For detection of the primary antibodies, IRDye 680RD Donkey-anti-Mouse IgG were used, prior to analyzing the signals with the Odyssey.

4

## REFERENCES

1. Fernández-Medarde, A.; Santos, E. Ras in Cancer and Developmental Diseases. *Genes & Cancer* **2011**, *2*, 344-58.
2. Shin, S.M.; Choi, D.K.; Jung, K.; Bae, J.; Kim, J.S.; Park, S.W. *et al.* Antibody targeting intracellular oncogenic Ras mutants exerts anti-tumour effects after systemic administration. *Nature communications* **2017**, *8*, 15090.
3. Smakman, N.; Van Den Wollenberg, D.J.M.; Borel Rinkes, I.H.M.; Hoeben, R.C.; Kranenburg, O. Sensitization to apoptosis underlies KrasD12-dependent oncolysis of murine C26 colorectal carcinoma cells by reovirus T3D. *J Virol* **2005**, *79*, 14981-5.
4. Marcato, P.; Shmulevitz, M.; Pan, D.; Stoltz, D.; Lee, P.W.K. Ras Transformation Mediates Reovirus Oncolysis by Enhancing Virus Uncoating, Particle Infectivity, and Apoptosis-dependent Release. *Mol Ther* **2007**, *15*, 1522-30.
5. Zhao, X.; Chester, C.; Rajasekaran, N.; He, Z.; Kohrt, H.E. Strategic Combinations: The Future of Oncolytic Virotherapy with Reovirus. *Mol Cancer Ther* **2016**, *15*, 767-73.
6. Gong, J.; Sachdev, E.; Mita, A.C.; Mita, M.M. Clinical development of reovirus for cancer therapy: An oncolytic virus with immune-mediated antitumor activity. *World J Methodol* **2016**, *6*, 25-42.
7. Twigger, K.; Roulstone, V.; Kyula, J.; Karapanagiotou, E.M.; Syrigos, K.N.; Morgan, R. *et al.* Reovirus exerts potent oncolytic effects in head and neck cancer cell lines that are independent of signalling in the EGFR pathway. *BMC cancer* **2012**, *12*, 368.
8. Kim, M.; Egan, C.; Alain, T.; Urbanski, S.J.; Lee, P.W.; Forsyth, P.A. *et al.* Acquired resistance to reoviral oncolysis in Ras-transformed fibrosarcoma cells. *Oncogene* **2007**, *26*, 4124-34.
9. Van Den Wollenberg, D.J.; Dautzenberg, I.J.; Ros, W.; Lipinska, A.D.; Van Den Hengel, S.K.; Hoeben, R.C. Replicating reoviruses with a transgene replacing the codons for the head domain of the viral spike. *Gene Ther* **2015**, *22*, 51-63.
10. Eaton, H.E.; Kobayashi, T.; Dermody, T.S.; Johnston, R.N.; Jais, P.H.; Shmulevitz, M. African Swine Fever Virus NP868R Capping Enzyme Promotes Reovirus Rescue during Reverse Genetics by Promoting Reovirus Protein Expression, Virion Assembly, and RNA Incorporation into Infectious Virions. *J Virol* **2017**, *91*.
11. Van Den Wollenberg, D.J.M.; Dautzenberg, I.J.C.; Van Den Hengel, S.K.; Cramer, S.J.; De Groot, R.J.; Hoeben, R.C. Isolation of reovirus T3D mutants capable of infecting human tumor cells independent of junction adhesion molecule-A. *PLoS ONE* **2012**, *7*, e48064.

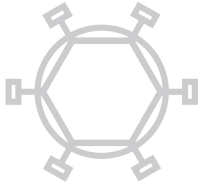
12. Marcellus, R.C.; Chan, H.; Paquette, D.; Thirlwell, S.; Boivin, D.; Branton, P.E. Induction of p53-independent apoptosis by the adenovirus E4orf4 protein requires binding to the Balpha subunit of protein phosphatase 2A. *J Virol* **2000**, *74*, 7869-77.
13. Branton, P.E.; Roopchand, D.E. The role of adenovirus E4orf4 protein in viral replication and cell killing. *Oncogene* **2001**, *20*, 7855-65.
14. Livne, A.; Shtrichman, R.; Kleinberger, T. Caspase activation by adenovirus e4orf4 protein is cell line specific and is mediated by the death receptor pathway. *J Virol* **2001**, *75*, 789-98.
15. Janssens, V.; Goris, J. Protein phosphatase 2A: a highly regulated family of serine/threonine phosphatases implicated in cell growth and signalling. *Biochem J* **2001**, *353*, 417-39.
16. Brestovitsky, A.; Sharf, R.; Mittelman, K.; Kleinberger, T. The adenovirus E4orf4 protein targets PP2A to the ACF chromatin-remodeling factor and induces cell death through regulation of SNF2h-containing complexes. *Nucleic Acids Res* **2011**, *39*, 6414-27.
17. Champagne, C.; Landry, M.C.; Gingras, M.C.; Lavoie, J.N. Activation of adenovirus type 2 early region 4 ORF4 cytoplasmic death function by direct binding to Src kinase domain. *J Biol Chem* **2004**, *279*, 25905-15.
18. Miron, M.J.; Blanchette, P.; Groitl, P.; Dallaire, F.; Teodoro, J.G.; Li, S. *et al.* Localization and importance of the adenovirus E4orf4 protein during lytic infection. *J Virol* **2009**, *83*, 1689-99.
19. Oberhaus, S.M.; Dermody, T.S.; Tyler, K.L. Apoptosis and the cytopathic effects of reovirus. *Curr Top Microbiol Immunol* **1998**, *233*, 23-49.
20. Connolly, J.L.; Dermody, T.S. Virion disassembly is required for apoptosis induced by reovirus. *J Virol* **2002**, *76*, 1632-41.
21. Richardson-Burns, S.M.; Kominsky, D.J.; Tyler, K.L. Reovirus-induced neuronal apoptosis is mediated by caspase 3 and is associated with the activation of death receptors. *J Neurovirol* **2002**, *8*, 365-80.
22. Clarke, P.; Richardson-Burns, S.M.; DeBiasi, R.L.; Tyler, K.L. Mechanisms of apoptosis during reovirus infection. *Curr Top Microbiol Immunol* **2005**, *289*, 1-24.
23. Danthi, P.; Hansberger, M.W.; Campbell, J.A.; Forrest, J.C.; Dermody, T.S. JAM-A-independent, antibody-mediated uptake of reovirus into cells leads to apoptosis. *J Virol* **2006**, *80*, 1261-70.
24. Dionne, K.R.; Zhuang, Y.; Leser, J.S.; Tyler, K.L.; Clarke, P. Daxx Upregulation within the Cytoplasm of Reovirus-Infected Cells Is Mediated by Interferon and Contributes to Apoptosis. *J Virol* **2013**, *87*, 3447-60.

25. Berger, A.K.; Danthi, P. Reovirus activates a caspase-independent cell death pathway. *MBio* **2013**, *4*, e00178-13.
26. Simon, E.J.; Howells, M.A.; Stuart, J.D.; Boehme, K.W. Serotype-Specific Killing of Large Cell Carcinoma Cells by Reovirus. *Viruses* **2017**, *9*.
27. Hiller, B.E.; Berger, A.K.; Danthi, P. Viral gene expression potentiates reovirus-induced necrosis. *Virology* **2015**, *484*, 386-94.
28. Fallaux, F.J.; Kranenburg, O.; Cramer, S.J.; Houweling, A.; van Ormondt, H.; Hoeben, R.C. *et al.* Characterization of 911: a new helper cell line for the titration and propagation of early region 1-deleted adenoviral vectors. *Hum Gene Ther* **1996**, *7*, 215-22.
29. Pereg, Y.; Shkedy, D.; de Graaf, P.; Meulmeester, E.; Edelson-Averbukh, M.; Salek, M. *et al.* Phosphorylation of Hdmx mediates its Hdm2- and ATM-dependent degradation in response to DNA damage. *Proc Natl Acad Sci USA* **2005**, *102*, 5056-61.
30. Buijs, J.T.; Rentsch, C.A.; van der Horst, G.; van Overveld, P.G.M.; Wetterwald, A.; Schwaninger, R. *et al.* BMP7, a Putative Regulator of Epithelial Homeostasis in the Human Prostate, Is a Potent Inhibitor of Prostate Cancer Bone Metastasis in Vivo. *The American Journal of Pathology* **2007**, *171*, 1047-57.
31. Buchholz, U.J.; Finke, S.; Conzelmann, K-K. Generation of Bovine Respiratory Syncytial Virus (BRSV) from cDNA: BRSV NS2 Is Not Essential for Virus Replication in Tissue Culture, and the Human RSV Leader Region Acts as a Functional BRSV Genome Promoter. *J Virol* **1999**, *73*, 251-9.
32. Roner, M.R.; Roehr, J. The 3' sequences required for incorporation of an engineered ssRNA into the Reovirus genome. *Virol J* **2006**, *3*, 1.
33. Roner, M.R.; Steele, B.G. Features of the mammalian orthoreovirus 3 Dearing I1 single-stranded RNA that direct packaging and serotype restriction. *J Gen Virol* **2007**, *88*, 3401-12.
34. Kobayashi, T.; Antar, A.A.R.; Boehme, K.W.; Danthi, P.; Eby, E.A.; Guglielmi, K.M. *et al.* A Plasmid-Based Reverse Genetics System for Animal Double-Stranded RNA Viruses. *Cell Host Microbe* **2007**, *1*, 147-57.
35. Kobayashi, T.; Ooms, L.S.; Ikizler, M.; Chappell, J.D.; Dermody, T.S. An improved reverse genetics system for mammalian orthoreoviruses. *Virology* **2010**, *398*, 194-200.
36. Li, S.; Szymborski, A.; Miron, M.J.; Marcellus, R.; Binda, O.; Lavoie, J.N. *et al.* The adenovirus E4orf4 protein induces growth arrest and mitotic catastrophe in H1299 human lung carcinoma cells. *Oncogene* **2009**, *28*, 390-400.
37. Terasawa, Y.; Hotani, T.; Katayama, Y.; Tachibana, M.; Mizuguchi, H.; Sakurai, F. Activity levels of cathepsins B and L in tumor cells are a biomarker for

- efficacy of reovirus-mediated tumor cell killing. *Cancer Gene Ther* **2015**, *22*, 188-97.
38. Galanis, E.; Markovic, S.N.; Suman, V.J.; Nuovo, G.J.; Vile, R.G.; Kottke, T.J. *et al.* Phase II Trial of Intravenous Administration of Reolysin(®) (Reovirus Serotype-3-dearing Strain) in Patients with Metastatic Melanoma. *Mol Ther* **2012**, *20*, 1998-2003.
  39. Karapanagiotou, E.M.; Roulstone, V.; Twigger, K.; Ball, M.; Tanay, M.; Nutting, C. *et al.* Phase I/II trial of carboplatin and paclitaxel chemotherapy in combination with intravenous oncolytic reovirus in patients with advanced malignancies. *Clin Cancer Res* **2012**, *18*, 2080-9.
  40. Wold, W.S.; Toth, K. Adenovirus vectors for gene therapy, vaccination and cancer gene therapy. *Curr Gene Ther* **2013**, *13*, 421-33.
  41. Schiza, A.; Wenthe, J.; Mangsbo, S.; Eriksson, E.; Nilsson, A.; Totterman, T.H. *et al.* Adenovirus-mediated CD40L gene transfer increases Teffector/Tregulatory cell ratio and upregulates death receptors in metastatic melanoma patients. *J Transl Med* **2017**, *15*, 79.
  42. Van Den Wollenberg, D.J.M.; Van Den Hengel, S.K.; Dautzenberg, I.J.C.; Cramer, S.J.; Kranenburg, O.; Hoeben, R.C. A strategy for genetic modification of the spike-encoding segment of human reovirus T3D for reovirus targeting. *Gene Ther* **2008**, *15*, 1567-78.
  43. Parsons, S.J.; Parsons, J.T. Src family kinases, key regulators of signal transduction. *Oncogene* **2004**, *23*, 7906-9.
  44. Robert, A.; Miron, M.-J.; Champagne, C.; Gingras, M.-C.; Branton, P.E.; Lavoie, J.N. Distinct cell death pathways triggered by the adenovirus early region 4 ORF 4 protein. *J Cell Biol* **2002**, *158*, 519-28.
  45. Kim, M.; Garant, K.A.; zur Nieden, N.I.; Alain, T.; Loken, S.D.; Urbanski, S.J. *et al.* Attenuated reovirus displays oncolysis with reduced host toxicity. *Br J Cancer* **2011**, *104*, 290-9.
  46. Connolly, J.L.; Barton, E.S.; Dermody, T.S. Reovirus binding to cell surface sialic acid potentiates virus-induced apoptosis. *J Virol* **2001**, *75*, 4029-39.



# 5



## Arming oncolytic reovirus with GM-CSF gene to enhance immunity



Vera Kemp<sup>1</sup>, Diana J.M. van den Wollenberg<sup>1</sup>, Marcel G.M. Camps<sup>2</sup>, Thorbald van Hall<sup>3</sup>, Priscilla Kinderman<sup>3</sup>, Nadine Pronk-van Montfoort<sup>3</sup>, Rob C. Hoeben<sup>1</sup>

1. Department of Cell and Chemical Biology, Leiden University Medical Center, 2333 ZA Leiden, the Netherlands

2. Department of Immunohematology and Blood Transfusion, Leiden University Medical Center, 2333 ZA Leiden, the Netherlands

3. Department of Medical Oncology, Leiden University Medical Center, 2333 ZA Leiden, the Netherlands

Cancer Gene Therapy 2019, doi: 10.1038/s41417-018-0063-9

**ABSTRACT**

Oncolytic reovirus administration has been well tolerated by cancer patients in clinical trials. However, its anti-cancer efficacy as a monotherapy remains to be augmented. We and others have previously demonstrated the feasibility of producing replication-competent reoviruses expressing a heterologous transgene. Here, we describe the production of recombinant reoviruses expressing murine (mm) or human (hs) GM-CSF (rS1-mmGMCSF and rS1-hsGMCSF, respectively). The viruses could be propagated up to 10 passages while deletion mutants occurred only occasionally. In infected cell cultures, the secretion of GM-CSF protein (up to 481 ng/10<sup>6</sup> cells per day) was demonstrated by ELISA. The secreted mmGM-CSF protein was functional in cell culture, as demonstrated by the capacity to stimulate the survival and proliferation of the GM-CSF dependent dendritic cell (DC) line D1, and by its ability to generate DCs from murine bone marrow cells. Importantly, in a murine model of pancreatic cancer we found a systemic increase in DC and T-cell activation upon intra-tumoral administration of rS1-mmGMCSF. These data demonstrate that reoviruses expressing functional GM-CSF can be generated and have the potential to enhance anti-tumor immune responses. The GM-CSF reoviruses represent a promising new agent for use in oncolytic virotherapy strategies.

## INTRODUCTION

Oncolytic viruses represent a promising tool in experimental anti-cancer treatment strategies. The features that determine the malignancy and outgrowth of cancer cells are often associated with an increased sensitivity to viral infections [1]. Many of the current strategies to improve the potential of oncolytic viruses are focused on the modulation and stimulation of a long-lasting adaptive anti-cancer immune response. Talimogene laherparepvec (T-VEC), the first oncolytic virus that was approved for treatment of a subset of melanoma patients, is a Herpes Simplex Virus that has been genetically modified to express GM-CSF [2, 3]. The approval of T-VEC may pave the way for clinical application of other oncolytic viruses.

Mammalian orthoreovirus Type 3 Dearing, hereafter called reovirus, is a non-enveloped virus carrying a segmented double-stranded RNA genome with a total size of 23.5 kB. Reovirus has the natural preference to replicate in and kill tumor cells, and therefore is studied as an oncolytic agent for a variety of cancer types [4]. Treatment with the reovirus product Reolysin (Pelareorep) is well tolerated, but the efficacy and effects on progression-free and overall survival remain to be augmented.

One of the approaches to increase the anti-cancer potency of oncolytic viruses is through incorporating therapeutic transgenes in the virus backbone. Genetic modification of dsRNA viruses can be challenging but the development of a plasmid-based reverse genetics system has allowed researchers worldwide to make adaptations to the reovirus genome [5]. We have previously demonstrated that this system can be used to incorporate a small transgene in the reovirus backbone. We successfully replaced the S1 segment-encoded head domain of the reovirus spike protein  $\sigma_1$ , which is responsible for binding to the reovirus receptor junction adhesion molecule-A (JAM-A), for the small fluorescent protein iLOV [6], generating the recombinant reovirus rS1-iLOV. The mutation that causes the G196R substitution in the spike protein, which was identified in the *jln-3* reovirus mutant that is able to infect a variety of cancer cell lines that lack the JAM-A receptor [7], was incorporated in the same segment to allow for sialic acid dependent but JAM-A independent viral entry. More recently, we published the generation and characterization of two additional recombinant reoviruses, rS1-E4orf4 and rS1-RFA [8]. In the rS1-E4orf4 virus, the S1 head domain was replaced for a gene encoding E4orf4, an adenovirus-derived protein that is involved in the induction of tumor cell selective non-classical apoptosis [9, 10]. This cell death induction partially depends on E4orf4 binding to phosphatase 2A (PP2A). The other reovirus, rS1-RFA, encodes a double mutant (RFA) of E4orf4 that is unable to bind PP2A. We showed that truncation of  $\sigma_1$  seems to result in improved tumor cell killing, but that the expression of E4orf4 does not enhance the oncolytic potential [8]. Based on these results, we speculated that it

would be a more effective approach to generate a reovirus that leads to the synthesis of a secreted immune-modulating protein instead of a protein that acts *in cis*, *i.e.* only in the infected cell.

Here, we describe the generation and characterization of two reoviruses, rS1-mmGMCSF and rS1-hsGMCSF which harbor the codons for murine or human GM-CSF, respectively. GM-CSF is widely used to generate dendritic cells (DCs) *in vitro*. It promotes the survival and function of both monocyte-derived DCs [11] as well as CD8 $\alpha^+$  DCs [12]. By enhancing DC maturation, and stimulating cross-presentation of tumor antigens, GM-CSF can boost subsequent anti-tumor immune responses. We demonstrate the secretion and the functionality of GM-CSF upon viral infection *in vitro*. Importantly, treatment of mice bearing pancreatic tumors with rS1-mmGMCSF systemically increased the percentage of activated DCs and effector T-cells compared to treatment with the control reovirus rS1-iLOV. These results show the successful production of a recombinant reovirus expressing a functional transgene that could be of clinical value.

## **MATERIALS AND METHODS**

### *Cell lines*

The human embryonic retinoblast-derived cell line '911' [13] was cultured in high glucose Dulbecco's Modified Eagle Medium (DMEM) (Invitrogen, Breda, the Netherlands), supplemented with penicillin, streptomycin (pen-strep) and 8% fetal bovine serum (FBS) (Invitrogen, Breda, the Netherlands). The polyclonal 911scFvHis cell line was established by lentiviral transduction of 911 cells with the pLV-scFvHis-IRES-Neo vector as described before [14]. The KPC3 cell line are low passage cells derived from a primary tumor in KPC mice [15] and were cultured in Iscove's Modified Dulbecco's Medium (IMDM) (Gibco, Life technologies, Fisher Scientific) supplemented with 8% FCS (Gibco, Life technologies, Fisher Scientific, cat. nr 10270-106), pen-strep and glutamine. The T7 RNA polymerase-expressing cell line BSR-T7 [16] was kindly provided by K. Conzelmann. The 911scFvHis and BSR-T7 cell lines were cultured in DMEM containing 8% FBS, pen-strep and 400  $\mu$ g/ml G418. The growth factor dependent dendritic cell (DC) line D1 was cultured in IMDM (Lonza) containing 50  $\mu$ M  $\beta$ -mercaptoethanol (Sigma-Aldrich), 2 mM GlutaMAX (Fisher Scientific), 100 IU/ml penicillin (Sandoz), and 10% FCS (Sigma-Aldrich), supplemented with 30% conditioned supernatant derived from murine GM-CSF producing NIH/3T3 cells (hereafter referred to as R1 sup) [17, 18]. All cell lines were cultured in a 5% CO<sub>2</sub> atmosphere at 37°C.

### *Reoviruses*

The wild-type T3D strain R124 was isolated by plaque purification from a heterogeneous reovirus T3D stock and propagated as described previously [7]. The *jin-3* mutant reovirus was isolated from U118-MG cells upon infection with wild-type (wt) T3D [7]. The genomes of the R124 and *jin-3* viruses were fully sequenced [7]. Infectious virus titers were quantified by plaque assays read-out on 911 cells. All experiments were performed using cesium chloride (CsCl) purified virus stocks, unless indicated otherwise. For purification, a freeze-thaw lysate containing virus particles was incubated with 0.1% Triton (Sigma-Aldrich, Zwijndrecht, the Netherlands) and 25 units/mL Benzonase (Santa Cruz, Bio-Connect B.V. Huissen, the Netherlands) for 15 minutes on ice followed by 15 minutes at 37°C. After two extractions with Halotec CL10 (FenS B.V. Goes, the Netherlands), the cleared lysate was loaded onto a discontinuous CsCl gradient (1.45 and 1.2 g/cm<sup>3</sup> in phosphate-buffered saline (PBS)). After centrifugation in a SW28 rotor (Beckman Coulter, Woerden, the Netherlands) at 95,000 g for 4 hours (hrs) at 16°C, the lower band containing the infectious particles was harvested and desalted in an Amicon Ultra 100K device according to the manufacturer's protocol (Millipore, Merck Chemicals BV, Amsterdam, the Netherlands). The CsCl-purified reoviruses were recovered in reovirus storage buffer (RSB: 10 mM Tris·HCl pH 7.5, 150 mM NaCl, 10 mM MgCl<sub>2</sub>·6H<sub>2</sub>O, 5% sucrose), aliquoted and stored at 4°C until use. The amount of particles was calculated based on the OD<sub>260</sub> values. The recombinant reoviruses expressing transgenes are described in a separate Materials and Methods section.

### *Plasmid constructs*

The S1 segments encoding the murine or (codon-optimized) human GM-CSF gene were designed *in silico* and the DNA was synthesized by Eurofins Genomics (Ebersberg, Germany). Prior to the GM-CSF sequences, a porcine teschovirus-1 2A (P2A) sequence was incorporated. Behind the GM-CSF sequences, the S1 3'-untranslated region (UTR) consisted of the C-box and the remaining 3' end sequence of S1. The P2A-GMCSF sequences were flanked by a 5' NcoI site and inserted in the pEX-A2 plasmid by Eurofins Genomics. This NcoI site allowed the exchange of the NcoI-SacII 614 bp fragment (containing sequences P2A-GM-CSF-3'-UTR S1) from the pEX-GMCSF constructs with the NcoI-SacII 584 bp fragment (removing the P2A-iLOV-3'-UTR sequences) of plasmid pBT7-S1His-2A-iLOV [6], using standard cloning techniques. This results in the plasmids: pBacT7-S1His-2A-mmGMCSF, pBacT7-S1His-2A-hsGMCSF and pBacT7-S1His-2A-hsGMCSFco.

The structure of the S1-His-2A-mmGMCSF (1407 bp) and S1His-2A-hsGMCSF(co) (1416 bp) constructs is shown in Figure 1: they contain 1) nt 1-768 of the reovirus *jin-3* S1 segment, including the 5'-UTR, the entire  $\sigma 1s$  ORF, and the

codons for the first 252 amino acids of the *jin-3*  $\sigma 1$  protein which harbor the G196R change near the sialic acid binding region; 2) the codons (18 bp) for a 6x His-tag that are in frame with the  $\sigma 1$  ORF; 3) the codons (66 + 3 additional bp) for the P2A sequence; 4) the sequence encoding the murine (423 bp) or (codon-optimized) human (432 bp) GM-CSF protein; 5) a stop codon; and 6) the 3'-UTR (nt 1219-1416) of the reovirus T3D S1 segment, including the C-box but not the A- and B-boxes. The A-, B-, and C-boxes have been implicated in packaging of the positive RNA strand in the viral capsid [19].

### *Recombinant reoviruses*

The reovirus expressing iLOV (rS1His-2A-iLOV, hereafter referred to as rS1-iLOV) was previously generated as described [6]. Reoviruses expressing murine (rS1His-2A-mmGMCSF) or human GM-CSF (rS1His-2A-hsGMCSF) are here referred to as rS1-mmGMCSF and rS1-hsGMCSF. The reovirus expressing the codon-optimized variant of hsGM-CSF (rS1His-2A-hsGMCSFco) is referred to as rS1-hsGMCSFco. All three recombinant viruses were constructed by transfection of  $2.5 \times 10^5$  BSR-T7 cells with the following plasmids: pT7-M2-S3-S4T3D (Addgene, plasmid #33302), pT7-L3-M1T3D (Addgene, plasmid #33301), pT7-L2-M3T3D (Addgene, plasmid #33300), pT7-L1T1L (Addgene, plasmid #33286), and pBacT7-S1His-2A-mm/hsGMCSF (2  $\mu$ g per plasmid, total of 10  $\mu$ g DNA). TransIT-LT1 (Mirus, Sopachem BV, Ochten, the Netherlands) was used as a transfection reagent. The cells were harvested 72 hours post transfection, lysed by three cycles of freezing and thawing, and subsequently added to 911scFvH cells to promote amplification of the produced viruses. The 911scFvH cells were harvested two weeks post infection, and lysed by three cycles of freezing and thawing. Individual virus clones were obtained by limiting dilution of the reoviruses originated from the first passage on 911scFvH cells. RNA was isolated 48 hours post infection from cells infected with the individual clones using the Absolutely RNA miniprep kit (Stratagene, Agilent Technologies, Amstelveen, the Netherlands). An RT-PCR was performed to analyze the stability of the S1 segments with the following primers: S1EndR (GATGAAATGCCCCAGTGC) for S1 cDNA synthesis, and S1For (GCTATTGGTCGGATGGATCCTCG) and S1EndR for the S1 PCR, using Pfu polymerase (Fermentas, FisherScientific, Landsmeer, the Netherlands). The resulting PCR product was analyzed by gel electrophoresis, and further purified for analysis by Sanger Sequencing at the Leiden Genome Technology Center (Leiden University Medical Center, Leiden, the Netherlands). The clones with an S1 segment containing GM-CSF were further propagated for up to 10 passages to study the stability of the clones. Infectious virus titers were determined by TCID<sub>50</sub> assays on 911 cells. All experiments were performed with CsCl-purified virus stocks, unless

indicated otherwise. Virus batches were stored in RSB supplemented with 0.1% BSA (RSB/0.1%BSA).

#### *GM-CSF ELISAs*

911scFvH cells were infected with rS1-mmGMCSF, rS1-hsGMCSFco or *jln-3* at an MOI of 1. After several time points, the levels of murine GM-CSF (mmGM-CSF) or human GM-CSF (hsGM-CSF) were determined using Quantikine® ELISA immunoassay kits (R&D Systems, Abingdon, United Kingdom) according to the manufacturer's instructions. The experiments were repeated twice to validate the results obtained. For the *in vivo* experiments, levels of mmGM-CSF in serum and tumor tissue from treated C57BL/6 mice were determined using the same kit.

#### *mmGM-CSF functionality in vitro*

To study the functionality of rS1-mmGMCSF-induced secreted murine GM-CSF *in vitro*, we used bone marrow cells from C57BL/6 mice. Supernatants from rS1-mmGMCSF or rS1-iLOV (negative control) infected 911 cells were pre-exposed to short-wave UV irradiation for 15 minutes to inactivate any virus that may be present. The absence of infectious virus was confirmed by TCID<sub>50</sub> assay on 911 cells ( $\leq 10$  pfu/mL). GM-CSF concentrations were determined by ELISA. Freshly isolated bone marrow cells were cultured in IMDM containing 50  $\mu$ M  $\beta$ -ME, 2mM GlutaMAX, penicillin, and 10% FCS, supplemented with rS1-mmGMCSF supernatant (sup) at 5 ng/ml GM-CSF or an equal volume of negative control rS1-iLOV sup. As a positive control, R1 sup was used at the same concentration of GM-CSF [17, 18]. Medium was refreshed at day-3 and -6. Finally, after 9 days of culturing, the cells were analyzed by flow cytometry. Used antibodies were anti-MHCII (clone M5/114.15.2, eBioscience, cat. nr. 12-5321-82), anti-CD11b (clone M1/70, eBioscience, cat. nr. 48-0112-82), anti-CD11c (clone N418, eBioscience, cat. nr. 47-0114-82), and anti-CD86 (clone GL1, eBioscience, cat. nr. 17-0862-82). The experiment was repeated twice to confirm the results.

Alternatively, the DC line D1 [17] was exposed to various concentrations of GM-CSF. Survival and proliferation of this cell line is dependent on the presence of growth factors such as GM-CSF. As for the experiment with bone marrow cells, supernatants from rS1-mmGMCSF or rS1-iLOV (negative control) infected 911 cells were pre-treated with short-wave UV irradiation for 15 minutes to inactivate any reovirus that may be present. The absence of infectious virus was confirmed by TCID<sub>50</sub> assay on 911 cells ( $\leq 10$  pfu/mL). GM-CSF concentrations were determined by ELISA, and D1 cells were exposed to culture medium containing rS1-mmGMCSF at 1 or 5 ng/ml GM-CSF. As a positive control, D1 cells were treated with medium containing R1 sup at the same concentrations. Cells were monitored daily for

viability by light microscopy, and a WST-1 cell proliferation assay (Roche, Woerden, the Netherlands) was performed after 3 days according to the manufacturer's protocol. The experiment was repeated twice to validate the results obtained.

### *Animal experiments*

The mouse experiments were controlled by the animal welfare committee (IvD) of the Leiden University Medical Center and approved by the national central committee of animal experiments (CCD) under the permit number AVD116002015271, in accordance with the Dutch Act on Animal Experimentation and EU Directive 2010/63/EU. The 8-10 weeks of age male C57BL/6 mice (Charles River, L'Arbresle Cedex, France) were inoculated subcutaneously with  $1 \times 10^5$  low passage KPC3 cells in PBS/0.1%BSA in a total volume of 100  $\mu$ L per injection. Tumor volume was measured twice weekly using a caliper and calculated (tumor volume = width x length x height). At tumor volume of 50-200 mm<sup>3</sup> the tumors were treated intratumorally with  $1 \times 10^7$  pfu of rS1-iLOV or rS1-mmGMCSF, or as control, reovirus storage buffer (RSB), all in a total volume of 30  $\mu$ L per injection. All treatments were repeated on day-2 and day-3 after the first treatment. Six days after the first treatment, mice were sacrificed and tumors, tumor-draining lymph nodes (TDLNs), and spleens were collected for analyses.

### *RT-qPCR analysis of tumors*

To check for the presence of viral genome product S4, and virus-induced CXCL10 and/or mmGM-CSF expression in the tumors, reverse transcription-quantitative PCR (RT-qPCR) analysis was performed. A proportion of the tumors was snap-frozen in liquid nitrogen, and stored at -80°C until use. Of each tumor, 10-30 mg was taken up in 500  $\mu$ L LBP lysis buffer (NucleoSpin Plus kit, Macherey-Nagel™) in an RNase-free Eppendorf tube. The tissue was disrupted by addition of a sterile 5mm stainless steel bead and placing the tubes in a TissueLyser system for 5 minutes at high-speed 30 Hz. Subsequently, RNA isolation was performed according to the NucleoSpin Plus protocol with the minor modification that all centrifugation steps were performed at 10,000 rpm. For S4 analysis, 150 ng of RNA was used to generate cDNA with primer S4EndR (GATGAATGAAGCCTGTCCACGTC). For CXCL10 and mmGM-CSF analysis, 500 ng of RNA was used to generate cDNA using the High-Capacity RNA-to-cDNA™ Kit (Thermo Fisher, cat. nr. 4387406) according to the manufacturer's protocol. The qPCRs were performed with Biorad IQ™ SYBR® Green Supermix (cat. nr. 170-8886) and the following primers: S4Q Forw (CGCTTTTGAAGGTCGTGTATCA) and S4Q Rev (CTGGCTGTGCTGAGATTGTTTT), CXCL10 Forw (ACGAACTTAACCACCATCT) and CXCL10 Rev (TAAACTTTAACTACCCATTGATACATA), GM-CSF Forw (CTAACATGTGTGCAGACCCG) and GM-CSF Rev (GGCTGTCTATGAAATCCGCA), household gene Mzt2 For

(TCGGTGCCCATATCTCTGTC) and Mzt2 Rev (CTGCTTCGGGAGTTGCTTTT), and household gene Ptp4a2 For (AGCCCCTGTGGAGATCTCTT) and Ptp4a2 Rev (AGCATCACAACTCGAACCA). The used PCR program contained the following steps: 1) 3 minutes 95°C; 2) 40x a) 10 seconds 96°C, b) 30 seconds 60°C, and c) plate read; 3) 10 seconds 95°C; 4) Melt curve 65-95°C with increment of 0.2°C every 10 seconds, and plate read. Expression of CXCL10 and mmGM-CSF genes was normalized to reference genes Mzt2 and Ptp4a2 in Biorad CFX Manager 3.1 software. Reovirus S4 <sup>10</sup>log copy numbers were determined based on a standard curve, generated with serial dilutions of plasmid pcDNA\_S4. Calculations of copy numbers were performed according to a described formula for rotavirus NSP3 quantification [20]. All samples were measured in duplicate.

#### *Flow cytometric analysis of tissues*

To examine the effect of treatment on the immune composition of the tumors, TDLNs, and spleens, these tissues were analyzed by flow cytometry. The tumor tissue was cut into pieces and Liberase TL (Roche, 05401020001) was added. After 15 minutes incubation at 37°C, the reaction was stopped by the addition of medium. The mixture was transferred to a cell strainer and gently dissociated until a single cell suspension was obtained. Cells were incubated with Zombie Aqua™ Fixable Viability Dye (Biolegend, cat. nr. 423101) in PBS at room temperature and 2.4G2 FcR blocking (BD Biosciences, cat. nr. 553141) in FACS buffer prior to antibody stainings for flow cytometry analyses. Used antibodies are anti-CD3 (clone 145-2C11, BD Biosciences, cat. nr. 562286), anti-CD4 (clone RM4-5, Biolegend, cat. nr. 100547), anti-CD8 (clone 53-6.7, eBioscience, cat. nr. 56-0081-82), anti-CD45.2 (clone 104, eBioscience, cat. nr. 47-0454-82), anti-CD62L (clone MEL-14, Biolegend, cat. nr. 104436), anti-CD69 (clone H1.2F3, Biolegend, cat. nr. 104507), anti-CD25 (clone PC61, Biolegend, cat. nr. 102012), anti-KLRG1 (clone 2F1, eBioscience, cat. nr. 25-5893-82), anti-CD8α (clone S3-6.7, Biolegend, cat. nr. 100734), anti-CD86 (clone GL-1, eBioscience, cat. nr. 12-0862-82), anti-CD11c (clone N418, Biolegend, cat. nr. 117310), anti-CD11b (clone M1/70, Invitrogen, cat. nr. 48-0112-82). Samples were fixed in 1% PFA (Pharmacy Leiden University Medical Center, the Netherlands) and acquired on a BD Fortessa X20 Flow Cytometer. Flow cytometry data were analyzed by FlowJo software (version 10).

#### *Statistical analysis*

All statistical analyses were performed using GraphPad Prism software (version 7). Data represent means and standard deviations. For the flow cytometry data, the means of the groups were compared with analysis of variance (ANOVA) including Holm-Sidak's multiple comparisons test. For the RT-qPCR data, the means of the

groups were compared by multiple Mann-Whitney tests. Significant differences are indicated by asterisks, with p values < 0.05 shown as \*, < 0.01 as \*\*, < 0.001 as \*\*\*, and < 0.0001 as \*\*\*\*. N.s. indicates non-significant differences.

## RESULTS

### *Generation of the rS1-mmGMCSF and rS1-hsGMCSF reoviruses*

Previously, we described a method for the generation and characterization of recombinant reoviruses. The strategy was based on the replacement of the JAM-A binding head domain of the S1 segment by a sequence containing the codons for a His-tag, a 2A peptide-bond skipping sequence, and a small transgene [6, 8]. This modification results in reoviruses with truncated  $\sigma 1$ -spikes in their capsids. We utilized the mutation leading to the G196R substitution in the S1 segment to allow the virus to enter cells independent from JAM-A, through facilitating enhanced sialic acid binding. The first recombinant virus we produced harbors a transgene encoding the small plant-derived green fluorescent protein iLOV [6]; subsequently, we generated a reovirus with S1 carrying a transgene coding for the adenovirus-derived apoptotic E4orf4 protein [8]. Based on the results of experiments with these viruses we decided to generate a recombinant reovirus encoding an immunostimulatory rather than a direct cytolytic product. We chose GM-CSF, which nicely fits within the limited space available in the S1 genome segment of reovirus (max. 522 bp). Figure 1 shows the structure of the previously and newly constructed S1 segments: they contain nt 1-768 of the reovirus *jin-3* S1 segment harboring the G196R change near the sialic acid binding region, a 6x His-tag, the porcine teschovirus-1 2A sequence, the transgene sequence encoding the heterologous protein – iLOV, E4orf4, RFA, human (432 bp) GM-CSF (hsGM-CSF) or murine (425 bp) GM-CSF (mmGM-CSF) – including a stop codon, and the 3'-UTR of the reovirus T3D S1 segment. In contrast to S1His-2A-iLOV, -E4orf4, and -RFA, the 3'-UTR region in GM-CSF encoding S1 segments contains the C-box but lacks the A- and B-boxes. The A-, B-, and C-boxes have been implicated in packaging of the positive RNA strand in the viral capsid [19].

Using a plasmid-based reverse genetics system, we attempted to generate reoviruses armed with these S1 segments encoding mmGM-CSF or hsGM-CSF. To this end, BSR-T7 cells were transfected with plasmids encoding the different reovirus segments. After 72 hours, the cells were harvested and the lysates were added to 911scFvH cells for further viral replication. Two weeks later, clear cytopathic effect (CPE) was seen (Figure 2), indicating that infectious virus was produced.

### *Stability of S1-mmGMCSF and S1-hsGMCSF*

The 911scFvH cells were harvested and a limiting dilution assay was performed to obtain individual virus clones. Then, 911scFvH cells were infected with the clones,

RNA was isolated for use in an RT-PCR procedure to amplify the S1 segment. The S1 PCR product was analyzed to detect the presence of the S1 segment carrying the GM-CSF transgene. For rS1-mmGMCSF, the migration of the PCR product in agarose electrophoresis confirmed the expected size of the recombinant segment. Sequencing validated the presence of complete S1-His-2A-mmGMCSF. Upon further propagation up to passage #10, the clone continued to express the full-length segment, showing that we obtained a clone that stably expresses the full-length S1His-2A-mmGMCSF transgene (Figure 3A). Further experiments were performed with a passage #10 virus batch of rS1-mmGMCSF.

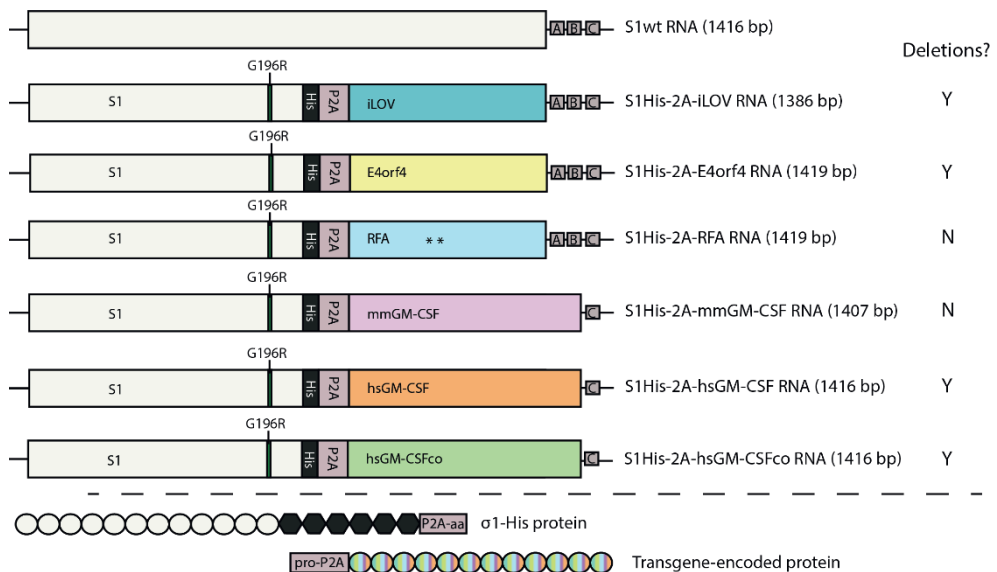


**Figure 1.** Structure of the S1 segments in the various recombinant reoviruses. The S1 segments of the recombinant reoviruses contain nt 1-768 of the reovirus *jin-3* S1 segment, including the mutation underlying the G196R change near the sialic acid binding region; the codons for the 6x His-tag in frame with the  $\sigma 1$  ORF; the codons for the porcine teschovirus-1 2A (P2A) sequence; the transgene encoding the heterologous protein – iLOV, E4orf4, RFA, murine GM-CSF (mmGM-CSF), human GM-CSF (hsGM-CSF), or codon-optimized hsGM-CSF (hsGM-CSFco) – including a stop codon; and the 3'-UTR (nt 1219-1416) of the reovirus T3D S1 segment. In contrast to S1His-2A-iLOV, -E4orf4, and -RFA, the 3'UTR region in the GM-CSF encoding S1 segments contains the C-box but not the A- and B-boxes. The occurrence or absence of deletion mutants is indicated by Y (yes) or N (no), respectively. The use of the P2A sequence results in the separate synthesis of a  $\sigma 1$ -His-tagged spike protein and the transgene-encoded protein.

For rS1-hsGMCSF, all virus clones showed a S1 PCR product smaller than the expected size of S1His-2A-hsGMCSF (Figure 3B), indicating the generation of deletion mutants. Three deletion mutants were sequenced and found to have lost the hsGM-CSF sequences. Similar results were obtained in a number of repeated experiments (data not shown). In an attempt to improve transgene preservation, we constructed an alternative S1 plasmid harboring a codon-optimized hsGM-CSF sequence, S1His-2A-hsGMCSFco. We repeated the procedure by transfection of BSR-T7 cells and subsequent infection of 911scFvH cells, and analyzed the S1His-2A-hsGMCSFco RT-PCR product after RNA isolation of infected 911scFvH cells. As before, deletion mutants seemed to be present in all clones (Figure 3C). However, a predominant band at the expected full-length size was evident, indicating that the complete S1His-2A-hsGMCSFco RNA sequence is encoded by the virus. Sequencing of this PCR product confirmed the integrity of the fragment and the presence of an intact S1 segment carrying His, P2A and the complete human GM-CSF gene.

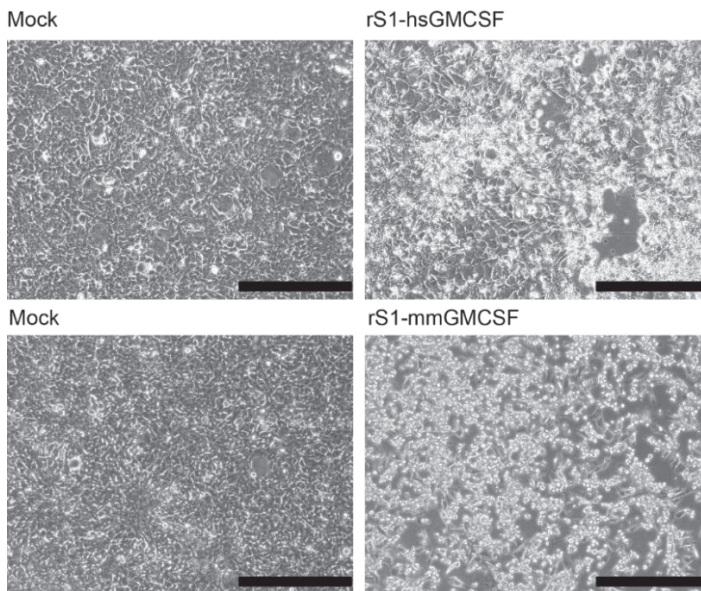


**Figure 2.** Reoviruses rS1-mmGMCSF and rS1-hsGMCSF retrieved from transfected BSR-T7 cells induce CPE in infected 911scFvHis cells. BSR-T7 cells were transfected with plasmids encoding the different reovirus segments. The S1 segment was replaced for a S1His-2A-mmGMCSF or -hsGMCSF segment. After 72 hours, the cells were harvested, and 911scFvH cells were exposed to the cleared lysates for further viral replication. Two weeks later, clear CPE was seen, indicating that infectious virus was produced. Scale bars represent 100  $\mu$ m.

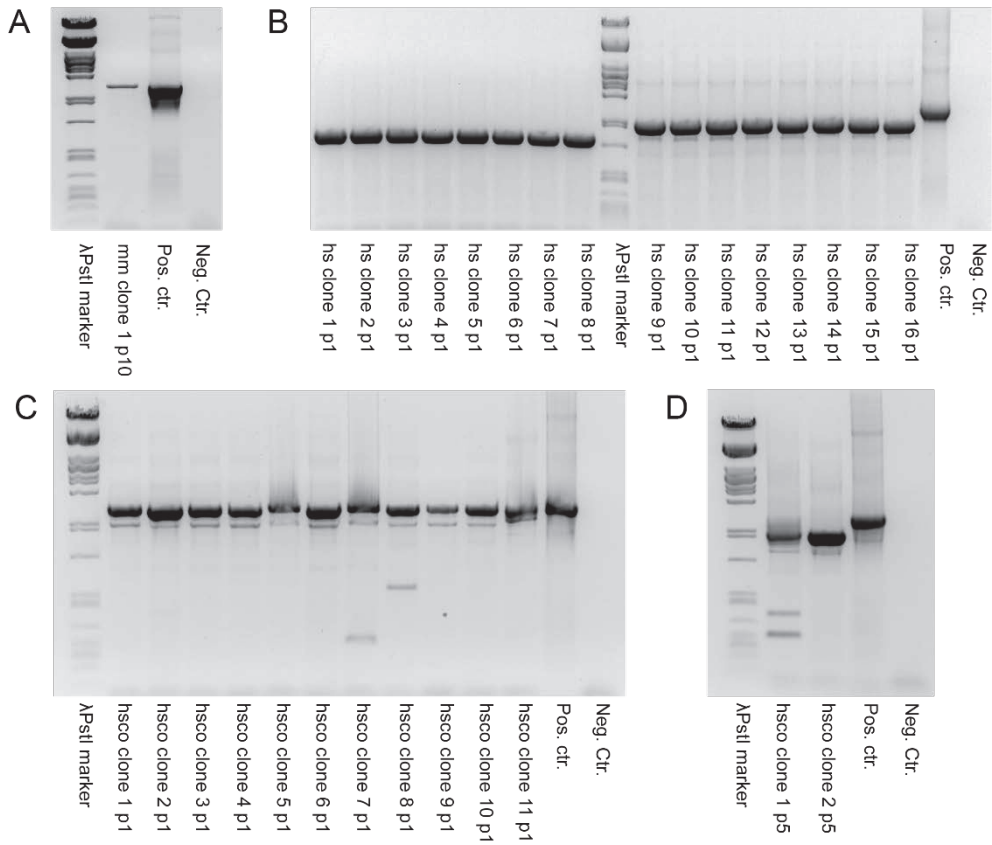


**Figure 3.** Reovirus rS1-mmGMCSF but not rS1-hsGMCSF(co) S1 segments are stable during prolonged propagation. 911scFvH cells were infected with individual clones of rS1-mmGMCSF, rS1-hsGMCSF, or rS1-hsGMCSFco for analysis of the S1 segment by RT-PCR. A) One rS1-mmGMCSF clone was propagated for 10 passages in total and RNA was extracted for RT-PCR analysis of the S1 segment. A band at the expected size of S1His-2A-mmGMCSF was detected, and confirmed to be full-length S1His-2A-mmGMCSF by sequencing. In the PCR, plasmid pBacT7S1His-2A-mmGMCSF was used as a positive control and Milli-Q water as a negative control. B) All the rS1-hsGMCSF PCR products consisted of shorter fragments than that of the full-length S1His-2A-hsGMCSF size. In the PCR, plasmid pBacT7S1His-2A-hsGMCSF was used as a positive control and Milli-Q water as a negative control. C) In the PCR products of rS1-hsGMCSFco clones, a predominant full-length size fragment and a shorter fragment are detected. In the PCR, plasmid pBacT7S1His-2A-hsGMCSFco was used as a positive control and Milli-Q water as a negative control. D) Upon prolonged propagation of the rS1-hsGMCSFco clones, only the shorter PCR products could be detected in the S1 RT-PCR.

For rS1-hsGMCSFco, also three S1 PCR products of deletion mutants were sequenced. The deletion mutants were found to have lost hsGM-CSFco sequences. These deletion mutants overgrew the virus population upon further propagation (Figure 3D). Therefore, we continued with low passage (#2) rS1-hsGMCSFco clones for further experiments. An overview of all deletion mutants is depicted in Figure 4.

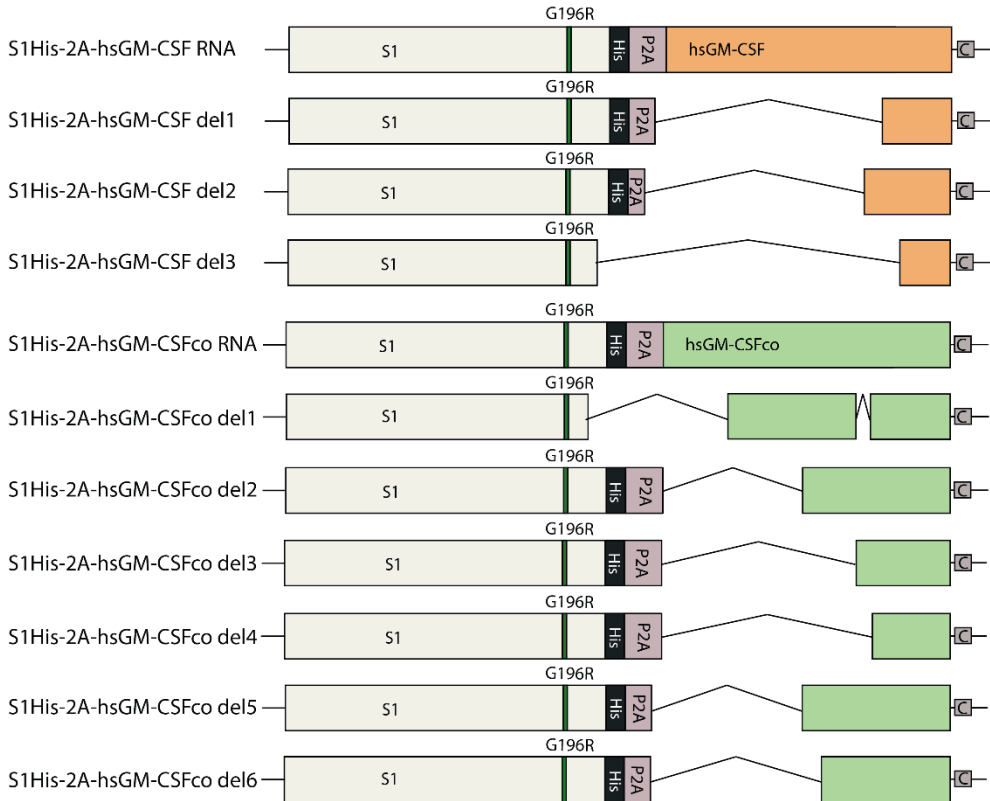


**Figure 4.** Overview of the deletion mutants. For rS1-hsGMCSF(co), the deletion mutants were sequenced. The various deletions are indicated by black angulated lines. Varying parts of the transgene and occasionally reovirus-derived sequences were lost.

*Secretion of mmGM-CSF and hsGM-CSF from infected 911 cells*

To see whether the reovirus clones induce the secretion of GM-CSF from infected cell cultures, 911 cells were infected with rS1-mmGMCSF, rS1-hsGMCSFco, or *jin-3*. Supernatants were collected at several time points post infection, and analyzed for the presence of mmGM-CSF or hsGM-CSF by ELISA. A clear induction of GM-CSF

secretion was observed, increasing in time (Figure 5A-B). This indicates that the mmGM-CSF or hsGM-CSFco sequences present in the S1 segments are effectively expressed, stimulating the production and secretion of GM-CSF protein.

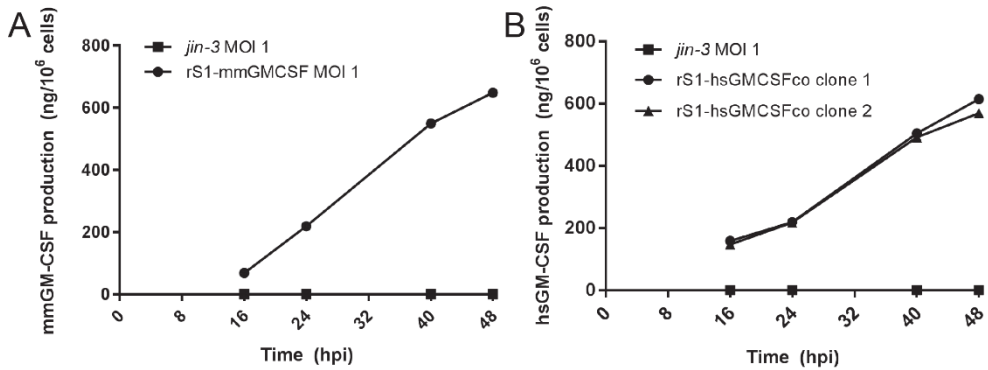


**Figure 5.** Infection of 911 cells with rS1-mmGMCSF/rS1-hsGMCSF leads to secretion of detectable GM-CSF in the supernatant. 911 cells were infected with A) a p#10 CsCl-purified rS1-mmGMCSF batch at an MOI of 1, or B) a p#2 freeze-thaw (FT) batch of rS1-hsGMCSFco at unknown MOI (20  $\mu$ l of a 5 ml T25 harvest). As a control, cells were infected with A) a CsCl-purified batch of *jin-3* or B) FT batch of *jin-3* at an MOI of 1. At 16, 24, 40, and 48 hours post infection (hpi), the supernatant was collected for each condition and analyzed for the presence of mmGM-CSF/hsGM-CSF by ELISA. A clear induction of GM-CSF secretion is apparent, increasing in time.

#### Functionality of secreted mmGM-CSF in vitro

GM-CSF is known to stimulate the generation of bone marrow derived dendritic cells (BMDCs) from murine bone marrow cells [2]. To address the question whether the secreted mmGM-CSF from infected cells is functional, murine bone marrow leukocytes isolated from C57BL/6 mice were exposed to supernatant of rS1-mmGMCSF infected 911scFvH cells (referred to as rS1-mmGMCSF sup) at a concentration of 5 ng/ml mmGM-CSF. As a positive control, we used conditioned medium from GM-CSF producing NIH/3T3 cells [17] (referred to as R1 sup) at the same concentration of mmGM-CSF. As a negative control, the same volume of supernatant from rS1-iLOV infected 911scFvH cells (referred to as rS1-iLOV sup) was added. Prior to the treatment, the rS1-iLOV and rS1-mmGMCSF supernatants had been irradiated with UV light to inactivate any reovirus that may be present. After 9 days of culture, the bone marrow leukocytes were analyzed for dendritic cell (DC) markers by flow cytometry. We found multiple sub-populations of CD11c<sup>+</sup> cells, differing in their expression level of CD11b and MHC-II. The results are shown in

Figure 6A-B, demonstrating that mmGM-CSF is very efficient at generating CD11b<sup>INT</sup>, MHC-II<sup>INT</sup> cells, indicative for immature DCs, and of CD11b<sup>INT</sup>, MHC-II<sup>HIGH</sup> cells, indicative for mature DCs [21]. The secreted mmGM-CSF even outcompetes the control R1 supernatant at generating CD11c<sup>+</sup> sub-populations. Furthermore, both cell populations clearly expressed the co-stimulatory marker CD86, the mature DCs (Figure 6D) to a higher level than the immature DCs (Figure 6C), implying they are activated DCs. The control rS1-iLOV supernatant did not induce the generation of CD11c<sup>+</sup> cells.

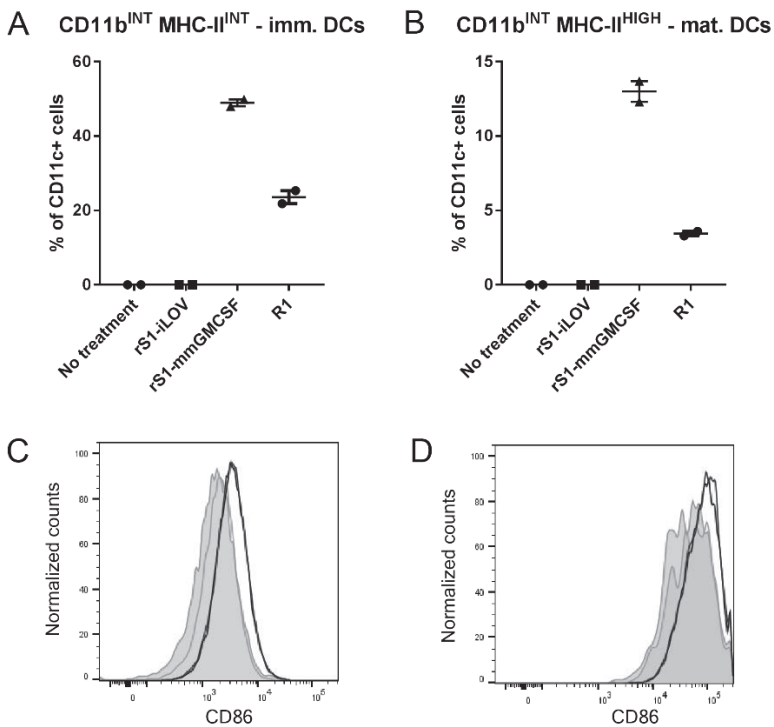


**Figure 6.** Secreted mmGM-CSF induces the maturation and activation of dendritic cells (DCs) from bone marrow cells. Bone marrow cells were exposed to D1 medium supplemented with UV-irradiated supernatants from rS1-mmGMCSF or rS1-iLOV (negative control) infected 911 cells at 5 ng/ml GM-CSF or an equal volume of negative control rS1-iLOV sup. As a positive control, R1 sup was used at 5 ng/ml of GM-CSF. After 3 and 6 days, the treatments on the cells were refreshed. The cells were analyzed by flow cytometry after 9 days of treatment. Shown are A) the percentages of CD11b<sup>LOW</sup> MHC-II<sup>INT</sup> cells in the CD11c<sup>+</sup> population, B) the percentages of CD11b<sup>LOW</sup> MHC-II<sup>HIGH</sup> cells in the CD11c<sup>+</sup> population, C) the CD86 expression

in the CD11b<sup>LOW</sup> MHC-II<sup>INT</sup> CD11c<sup>+</sup> population, and D) the CD86 expression in the CD11b<sup>LOW</sup> MHC-II<sup>HIGH</sup> CD11c<sup>+</sup> population. The experiment was repeated twice to confirm the results. Error bars indicate standard deviation (SD).

Alternatively, the growth factor dependent murine DC line D1 was used [17]. The cells were treated with rS1-mmGMCSF sup at concentrations of 1 and 5 ng/ml mmGM-CSF. As a positive control, R1 sup was taken along at the same concentrations of mmGM-CSF. As a negative control, cells were treated with the same volume of rS1-iLOV sup. After 3 days, the proliferative capacity of the cells was measured by a WST-1 assay. The proliferative capacity of the D1 cells was increased in the presence of both concentrations of rS1-mmGMCSF and R1 sup, but not rS1-iLOV sup (Figure 7). This implies that there is functional mmGM-CSF present in the rS1-mmGMCSF sup, which stimulates the survival and proliferation of D1 cells.

Altogether, these data clearly show that the produced and secreted mmGM-CSF from infected cells is functional *in vitro*, *i.e.* it efficiently triggers the generation of immature and mature DCs from murine bone marrow cells, and it stimulates the survival and proliferation of the murine DC line D1.

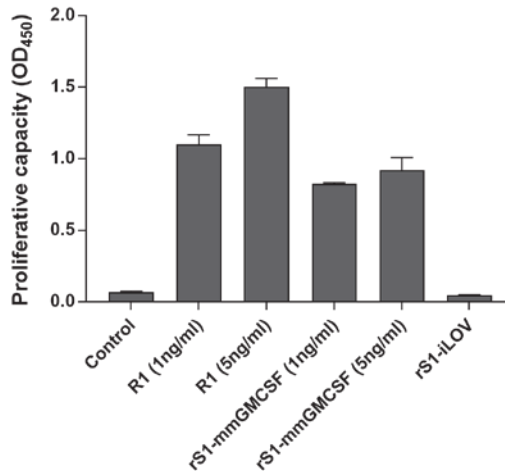


**Figure 7.** Secreted mmGM-CSF facilitates the proliferation of murine DC line D1. D1 cells were cultured in the presence of rS1-mmGMCSF sup or R1 sup at 1 or 5 ng/mL mmGM-CSF. As negative controls, they were left untreated or the same volume of rS1-iLOV sup was added. After 3 days, the proliferative capacity of the cells was examined by a WST-1 assay. Error bars indicate standard deviation (SD). Both rS1-mmGMCSF sup and R1 sup caused an increase in D1 proliferative capacity.

*Activity of rS1-mmGMCSF in KPC3 mouse pancreatic tumor model*

To study the functionality of the mmGM-CSF gene *in vivo*, we made use of a murine subcutaneous pancreatic ductal adenocarcinoma (PDAC) implantation model in C57BL/6 mice using a low-passage KPC-derived tumor cell line [15]. Mice were treated three times (day-0, day-2, and day-3) with intra-tumoral injections containing  $1 \times 10^7$  pfu of rS1-mmGMCSF or control reovirus rS1-iLOV, or sham treatment (reovirus storage buffer). Six days after the first injection (day-6), the mice were sacrificed and the tumors, tumor-draining lymph nodes (TDLNs), and spleens were collected for analysis.

To examine the expression of viral genome products and of virally induced CXCL10 and/or mmGM-CSF in the tumors, a RT-qPCR analysis was performed for the viral S4 genome segment, CXCL10, and for mmGM-CSF mRNA expression. CXCL10 is an IFN-induced chemokine that is often expressed in virus-infected tissues, and therefore an indirect measure of viral infection. Compared to the sham-treated mice, the majority of mice treated with reoviruses had a detectable increase in S4 RNA and CXCL10 mRNA expression in the tumors (Figure 8A-B). Compared to control and rS1-iLOV treated mice, the majority of rS1-mmGMCSF treated mice showed a clear increase in mmGM-CSF mRNA expression (Figure 8C). Some virus-treated mice showed a (nearly) undetectable increase in S4 or mmGM-CSF expression (data points not shown). To study the effects of mmGM-CSF, mice were only included in subsequent analyses when S4 (for rS1-iLOV and rS1-mmGMCSF treatments) or mmGM-CSF (for rS1-mmGMCSF treatment) expression deviated more than 2 standard deviations (SD) above the mean of the sham-treated group. In total, 4 mice were excluded (non-responders). These results indicate that the reoviruses successfully replicated in the KPC3 tumors, and that rS1-mmGMCSF induced the expression of mmGM-CSF inside the tumor tissue.

To specifically address the functionality of the mmGM-CSF gene, we analyzed the immune composition and activation of immune cells in the tumors, TDLNs, and spleens by flow cytometry. No significant differences were observed in the immune infiltrate of tumor tissue between rS1-iLOV and rS1-mmGMCSF. GM-CSF is known to enhance the recruitment, maturation and activation of DCs. In doing so, it can trigger a specific anti-tumor immune response by priming CD4<sup>+</sup> and/or CD8<sup>+</sup> T-cells. Our analyses of the tumors revealed an increase in co-stimulatory marker CD86 and cross-presentation marker CD8 $\alpha$  on CD11c<sup>+</sup> cells (Figure 9A-B) upon both virus treatments. The increase in CD86 expression was even more pronounced on the CD8 $\alpha$ <sup>+</sup> subset of CD11c<sup>+</sup> cells, indicating the activation of cross-presenting DCs (Figure 9C).

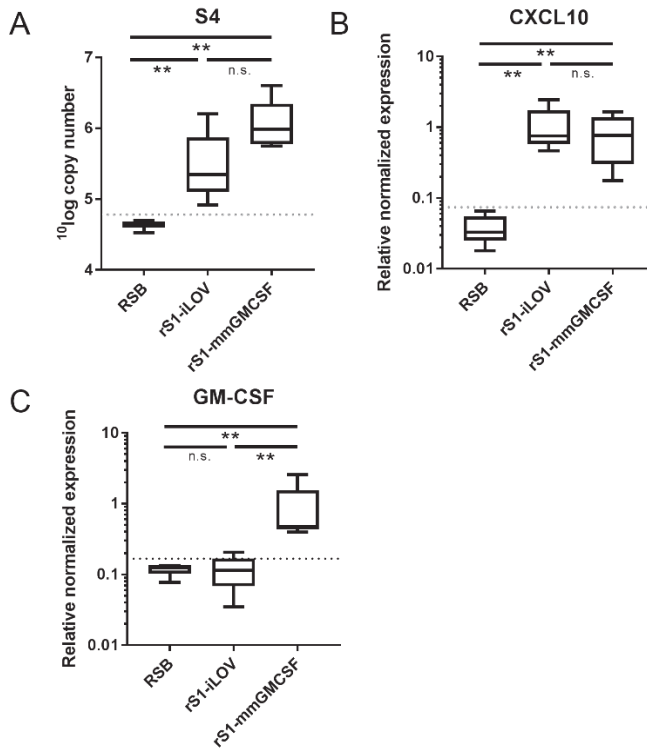


**Figure 8.** Gene expression of mmGM-CSF and S4 in tumor-bearing mice treated with rS1-mmGMCSF or rS1-iLOV. Mice were treated at day-0, day-2, and day-3 with intra-tumoral injections of  $10^7$  pfu rS1-mmGMCSF or control reovirus rS1-iLOV, or sham treatment (reovirus storage buffer). At day-6, the mice were sacrificed, and the tumors were collected for (RT-) qPCR analysis of A) reovirus segment S4 RNA, B) CXCL10 mRNA, and C) mmGM-CSF mRNA expression. For S4,  $10^{10}$  log copy numbers are shown, calculated based on a standard curve of S4 plasmid. For CXCL10 and mmGM-CSF, normalized expression to reference genes Mzt2 and Ptp4a2 is shown. All samples were measured in duplicate. Data are represented as box plots with whiskers indicating minimum and maximum values. Both rS1-mmGMCSF and rS1-iLOV induced S4 RNA and CXCL10 mRNA expression, and rS1-mmGMCSF specifically increased mmGM-CSF mRNA expression. Significant differences are illustrated by asterisks, with p values < 0.05 shown as \*, and < 0.01 as \*\*. N.s. indicates non-significant differences.

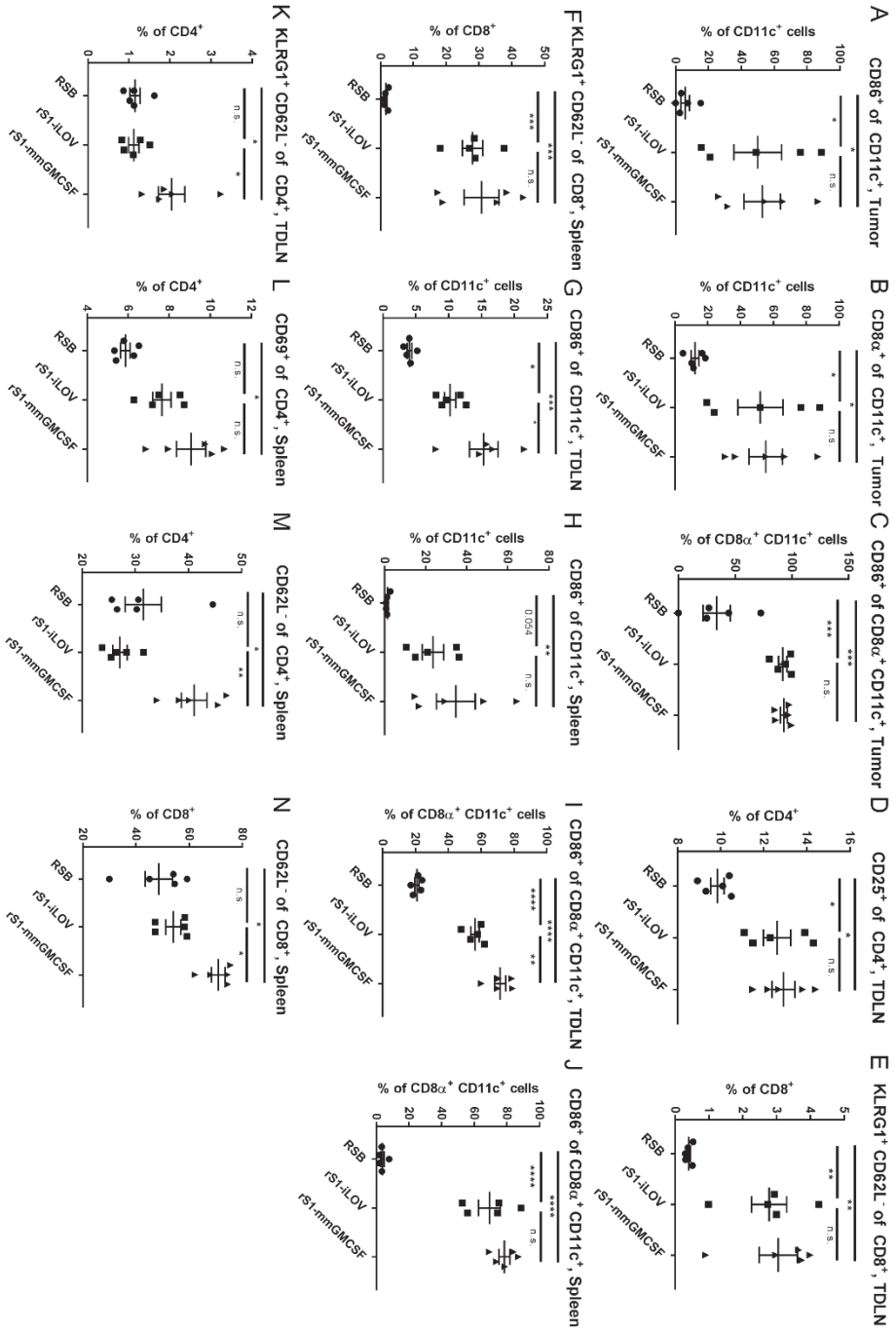


**Figure 9.** Effects of rS1-mmGMCSF on the immune composition in treated mice. Mice were treated at day-0, day-2, and day-3 with intra-tumoral injections of  $10^7$  pfu rS1-mmGMCSF or control reovirus rS1-iLOV, or sham treatment (reovirus storage buffer). At day-6, the mice were sacrificed and the tumors, tumor-draining lymph nodes (TDLNs), and spleens were collected for flow cytometric analysis. Shown are the percentages of A)  $CD86^+$  of  $CD11c^+$  cells in the tumor, B)  $CD8\alpha^+$  of  $CD11c^+$  cells in the tumor, C)  $CD86^+$  of  $CD8\alpha^+CD11c^+$  cells in the tumor, D)  $CD25^+$  of  $CD4^+$  cells in the TDLN, E)  $KLRG1^+ CD62L^-$  of  $CD8^+$  cells in the TDLN, F)  $KLRG1^+ CD62L^-$  of  $CD8^+$  cells in the spleen, G)  $CD86^+$  of  $CD11c^+$  cells in the TDLN, H)  $CD86^+$  of  $CD11c^+$  cells in the spleen, I)  $CD86^+$  of  $CD8\alpha^+CD11c^+$  cells in the TDLN, J)  $CD86^+$  of  $CD8\alpha^+CD11c^+$  cells in the spleen, K)  $KLRG1^+ CD62L^-$  of  $CD4^+$  cells in the TDLN, L)  $CD69^+$  of  $CD4^+$  cells in the spleen, M)  $CD62L^-$  of  $CD4^+$  cells in the spleen, and N)  $CD62L^-$  of  $CD8^+$  cells in the spleen. Error bars indicate SEM. Significant differences are indicated by asterisks, with p values  $< 0.05$  shown as \*,  $< 0.01$  as \*\*,  $< 0.001$  as \*\*\*, and  $< 0.0001$  as \*\*\*\*. N.s. indicates non-significant differences.

Interestingly, we noted several effects on the immune profile at distant locations, *i.e.* the tumor-draining lymph nodes (TDLNs) and the spleens. Both viruses triggered an increase in activation marker CD25 on  $CD4^+$  T-cells in the TDLNs (Figure 9D). In both TDLNs and spleens, activation marker KLRG1 was increased and naïve T-cell marker CD62L was decreased on  $CD8^+$  cells (Figure 9E-F). These findings indicate the systemic activation of  $CD4^+$  and  $CD8^+$  T-cells, suggesting the formation of effector T-cell responses. Like in the tumors, CD86 expression was increased on  $CD11c^+$  cells in the TDLNs and spleens (Figure 9G-H), and even more pronounced on the  $CD8\alpha^+$  subset of  $CD11c^+$  cells (Figure 9I-J), indicating the activation of cross-presenting DCs.

Importantly, mice treated with rS1-mmGMCSF showed a significantly higher increase in  $CD86^+ CD8\alpha^+ CD11c^+$  cells in the TDLNs compared to rS1-iLOV treated mice (Figure 9G), highlighting a systemic immune-modulating effect specific for rS1-mmGMCSF. We also noticed an increase in  $KLRG1^+ CD62L^- CD4^+$  effector T-cells in the TDLNs specifically upon rS1-mmGMCSF treatment (Figure 9K), implying an increase in activation of  $CD4^+$  T-cells in the TDLNs. Furthermore, elevated levels of activation marker CD69 on  $CD4^+$  T-cells, and loss of naïve T-cell marker CD62L on  $CD4^+$  and  $CD8^+$  cells were observed in the spleens of rS1-mmGMCSF treated mice (Figure 9L-N), suggesting that effector T-cell responses are formed in the spleen as well. These findings suggest that rS1-mmGMCSF administration activates T-cell responses in TDLNs and spleens.

Altogether, our findings demonstrate that rS1-mmGMCSF treatment induces the expression of functional mmGM-CSF in this murine model for pancreatic cancer which systemically influences the maturation and activation status of immune cells.

## DISCUSSION

Oncolytic viruses represent promising candidates for anti-cancer therapy, inducing both cancer cell death as well as triggering an immune response that could be directed against the tumor as well as the virus [1]. In 2015, the first oncolytic virus therapy was approved for cancer treatment in the United States (U.S.), namely T-VEC, a Herpes Simplex Virus carrying copies of the GM-CSF gene [3]. The U.S. Food and Drug Administration (FDA) approved the usage of T-VEC for patients with advanced melanoma that cannot be surgically removed (completely). This approval may pave the way for other oncolytic viruses to reach the clinic.

Oncolytic virotherapy using reovirus has entered a variety of clinical trials, which demonstrated both the safety and feasibility of the approach. However, its clinical efficacy has been limited in stand-alone therapies [4]. Genetic modification of reovirus can be challenging, due to its segmented dsRNA genomic nature and a relatively limited packaging capacity. We and others have previously demonstrated the feasibility of generating recombinant reoviruses expressing small transgenes such as iLOV [6], UnaG [22], E4orf4, and RFA [8]. We showed that the JAM-A binding region of the viral S1 segment can be replaced by a small transgene. A mutation in the sialic acid binding area of S1 offered the viruses an alternative entry route through enhanced sialic acid binding. We showed that the viruses with a truncated  $\sigma 1$  spike all seemed potent cancer-killing viruses, and that encoding the cell death inducing E4orf4 protein did not further increase oncolysis [8]. We postulated that encoding an oncolytic transgene may be obsolete. Combined with the current dogma that anti-tumor immunity is crucial for an oncolytic virotherapy to be clinically potent, it may be a better choice to incorporate a transgene encoding an immunostimulatory protein to enhance anti-tumor immune responses. Interestingly, during the previous production of the iLOV-encoding reovirus (rS1-iLOV), we encountered a deletion mutant virus that had deleted the A- and B-boxes [6]. The A-, B-, and C-boxes are thought to be important for packaging of the positive RNA strand in the viral capsid [19]. Therefore, we hypothesized that the A- and B-boxes are dispensable for efficient packaging of S1 into reovirus particles. As a result of this, the available space for transgene insertion increases from 451 to 522 bp.

Here, we describe the successful construction of recombinant reoviruses carrying a gene encoding murine (mm) or human (hs) GM-CSF. We demonstrate that the viruses trigger GM-CSF secretion *in vitro* upon infection of cell lines. This shows that encoding a secretory protein after a 2A sequence in the reovirus S1 segment can lead to efficient intracellular routing of the protein and release from the cell. Furthermore, we show that the produced mmGM-CSF is functional *in vitro*, as it facilitates the proliferation of cells that depend on GM-CSF for their survival, and it efficiently triggers the generation of immature and mature dendritic cells (DCs) from

murine bone marrow cells. Importantly, our data reveal the functionality of the mmGM-CSF gene *in vivo* as well, evident from specific increases in DC activation and the generation of effector T-cells at distant locations in a KPC3 mouse tumor model.

During the production of rS1-hsGMCSF, we encountered the appearance of deletion mutants. Expressing a codon-optimized copy of the hsGM-CSF gene (hsGM-CSFco) allowed us to rescue reoviruses expressing full-length S1-hsGMCSFco. Nevertheless, limiting dilutions of the virus stock revealed that the S1 deletions were present from the first passage on in all of the virus clones. In the batches with the early passage number, both full-length S1-hsGMCSFco and deleted variants were detected by S1 RT-PCR. Upon further propagation, we noticed that the deletion mutants rapidly overgrew the reovirus cultures, thereby losing the viruses harboring full-length S1-hsGMCSFco. This implies that the deletion mutant has a growth advantage over the intact rS1-hsGMCSFco. Therefore, we postulated that either the hsGM-CSFco gene or the hsGM-CSF protein has negative effects on viral replication. As we grow our viruses on 911 cells, which are human cells, it could be that they are sensitive to the produced hsGM-CSF, and therefore better facilitate the replication of the deletion mutant that does not lead to production of hsGM-CSF. However, attempts to generate a genetically stable rS1-hsGMCSFco virus on a non-human cell line were unsuccessful, suggesting that the generation of deletion mutants is not due to sensitivity of the producer cell line to the hsGM-CSF. Further inspection of the sequences surrounding the deletions did not provide evidence for involvement of either splicing or homology-directed mechanisms (data not shown). It seems most likely that the cause of the deletions lies at the RNA level, possibly in the RNA structure of the segment. For our experiments with rS1-hsGMCSFco, we used a passage#2 virus in which predominantly the full-length S1His-2A-hsGMCSFco is still present.

The scope of this study was to generate recombinant reoviruses encoding GM-CSF and determine whether a reovirus-encoded GM-CSF gene has functionality both *in vitro* and *in vivo*. While the short duration of our performed animal study did not allow to examine any potential effects on tumor volume or survival, future studies are recommended to determine whether the GM-CSF expressing reovirus can further stimulate (local and distant) tumor reduction and/or improve survival of tumor-bearing mice. Notably, the KPC3 tumor model has a very low abundance of T-cells [15], which may impede (the detection of) immune-mediated intra-tumoral effects. A higher immunogenic model could be a better choice to look at virus- and GM-CSF induced effects on tumor reduction.

## REFERENCES

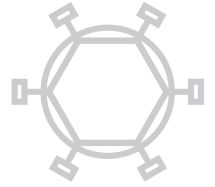
1. Keller, B.A.; Bell, J.C. Oncolytic viruses-immunotherapeutics on the rise. *J Mol Med (Berl)* **2016**, *94*, 979-91.
2. Hu, J.C.; Coffin, R.S.; Davis, C.J.; Graham, N.J.; Groves, N.; Guest, P.J.; Harrington, K.J.; James, N.D.; Love, C.A.; McNeish, I. *et al.* A phase I study of OncoVEXGM-CSF, a second-generation oncolytic herpes simplex virus expressing granulocyte macrophage colony-stimulating factor. *Clin Cancer Res* **2006**, *12*, 6737-47.
3. Pol, J.; Kroemer, G.; Galluzzi, L. First oncolytic virus approved for melanoma immunotherapy. *Oncoimmunology* **2016**, *5*, e1115641.
4. Zhao, X.; Chester, C.; Rajasekaran, N.; He, Z.; Kohrt, H.E. Strategic Combinations: The Future of Oncolytic Virotherapy with Reovirus. *Mol Cancer Ther* **2016**, *15*, 767-73.
5. Komoto, S.; Kawagishi, T.; Kobayashi, T.; Ikizler, M.; Iskarpatyoti, J.; Dermody, T.S.; Taniguchi, K. A plasmid-based reverse genetics system for mammalian orthoreoviruses driven by a plasmid-encoded T7 RNA polymerase. *J Virol Methods* **2014**, *196*, 36-9.
6. van den Wollenberg, D.J.; Dautzenberg, I.J.; Ros, W.; Lipinska, A.D.; van den Hengel, S.K.; Hoeben, R.C. Replicating reoviruses with a transgene replacing the codons for the head domain of the viral spike. *Gene Ther* **2015**, *22*, 267-79.
7. van den Wollenberg, D.J.; Dautzenberg, I.J.; van den Hengel, S.K.; Cramer, S.J.; de Groot, R.J.; Hoeben, R.C. Isolation of reovirus T3D mutants capable of infecting human tumor cells independent of junction adhesion molecule-A. *PLoS One* **2012**, *7*, e48064.
8. Kemp, V.; Dautzenberg, I.J.C.; Cramer, S.J.; Hoeben, R.C.; van den Wollenberg, D.J.M. Characterization of a replicating expanded tropism oncolytic reovirus carrying the adenovirus E4orf4 gene. *Gene Therapy* **2018**, *25*, 331-34.
9. Branton, P.E.; Roopchand, D.E. The role of adenovirus E4orf4 protein in viral replication and cell killing. *Oncogene* **2001**, *20*, 7855-65.
10. Marcellus, R.C.; Chan, H.; Paquette, D.; Thirlwell, S.; Boivin, D.; Branton, P.E. Induction of p53-independent apoptosis by the adenovirus E4orf4 protein requires binding to the Balph subunit of PP2A. *J Virol* **2000**, *74*, 7869-7877.
11. Xu, Y.; Zhan, Y.; Lew, A.M.; Naik, S.H.; Kershaw, M.H. Differential Development of Murine Dendritic Cells by GM-CSF versus Flt3 Ligand Has Implications for Inflammation and Trafficking. *The Journal of Immunology* **2007**, *179*, 7577-7584.
12. Zhan, Y.; Carrington, E.M.; van Nieuwenhuijze, A.; Bedoui, S.; Seah, S.; Xu, Y.; Wang, N.; Mintern, J.D.; Villadangos, J.A.; Wicks, I.P.; Lew, A.M. GM-CSF

- increases cross-presentation and CD103 expression by mouse CD8(+) spleen dendritic cells. *Eur J Immunol* **2011**, 41, 2585-95.
13. Fallaux, F.J.; Kranenburg, O.; Cramer, S.J.; Houweling, A.; Van Ormondt, H.; Hoeben, R.C.; Van Der Eb, A.J. Characterization of 911: a new helper cell line for the titration and propagation of early region 1-deleted adenoviral vectors. *Hum Gene Ther* **1996**, 7, 215-22.
  14. van den Wollenberg, D.J.; van den Hengel, S.K.; Dautzenberg, I.J.; Cramer, S.J.; Kranenburg, O.; Hoeben, R.C. A strategy for genetic modification of the spike-encoding segment of human reovirus T3D for reovirus targeting. *Gene Ther* **2008**, 15, 1567-78.
  15. Lee, J.W.; Komar, C.A.; Bengsch, F.; Graham, K.; Beatty, G.L. Genetically Engineered Mouse Models of Pancreatic Cancer: The KPC Model (LSL-Kras(G12D/+); LSL-Trp53(R172H/+); Pdx-1-Cre), Its Variants, and Their Application in Immuno-oncology Drug Discovery. *Curr Protoc Pharmacol* **2016**, 73, 14.39.1-14.39.20.
  16. Buchholz, U.J.; Finke, S.; Conzelmann, K.K. Generation of bovine respiratory syncytial virus (BRSV) from cDNA: BRSV NS2 is not essential for virus replication in tissue culture, and the human RSV leader region acts as a functional BRSV genome promoter. *J Virol* **1999**, 73, 251-9.
  17. Winzler, C.; Rovere, P.; Rescigno, M.; Granucci, F.; Penna, G.; Adorini, L.; Zimmermann, V.S.; Davoust, J.; Ricciardi-Castagnoli, P. Maturation Stages of Mouse Dendritic Cells in Growth Factor-dependent Long-Term Cultures. *The Journal of Experimental Medicine* **1997**, 185, 317-328.
  18. Boross, P.; van Montfoort, N.; Stapels, D.A.; van der Poel, C.E.; Bertens, C.; Meeldijk, J.; Jansen, J.H.; Verbeek, J.S.; Ossendorp, F.; Wubbolts, R.; Leusen, J.H. Fcγ-chain ITAM signaling is critically required for cross-presentation of soluble antibody-antigen complexes by dendritic cells. *J Immunol* **2014**, 193, 5506-14.
  19. Roner, M.R.; Roehr, J. The 3' sequences required for incorporation of an engineered ssRNA into the Reovirus genome. *Virology* **2006**, 3, 1.
  20. Mijatovic-Rustempasic, S.; Tam, K.I.; Kerin, T.K.; Lewis, J.M.; Gautam, R.; Quayle, O.; Gentsch, J.R.; Bowen, M.D. Sensitive and specific quantitative detection of rotavirus A by one-step real-time reverse transcription-PCR assay without antecedent double-stranded-RNA denaturation. *J Clin Microbiol* **2013**, 51, 3047-54.
  21. Helft, J.; Bottcher, J.; Chakravarty, P.; Zelenay, S.; Huotari, J.; Schraml, B.U.; Goubau, D.; Reis e Sousa, C. GM-CSF Mouse Bone Marrow Cultures Comprise a Heterogeneous Population of CD11c(+)MHCII(+) Macrophages and Dendritic Cells. *Immunity* **2015**, 42, 1197-211.

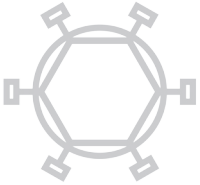
22. Eaton, H.E.; Kobayashi, T.; Dermody, T.S.; Johnston, R.N.; Jais, P.H.; Shmulevitz, M. African Swine Fever Virus NP868R Capping Enzyme Promotes Reovirus Rescue during Reverse Genetics by Promoting Reovirus Protein Expression, Virion Assembly, and RNA Incorporation into Infectious Virions. *J Virol* **2017**, *91*, e02416-16.







6



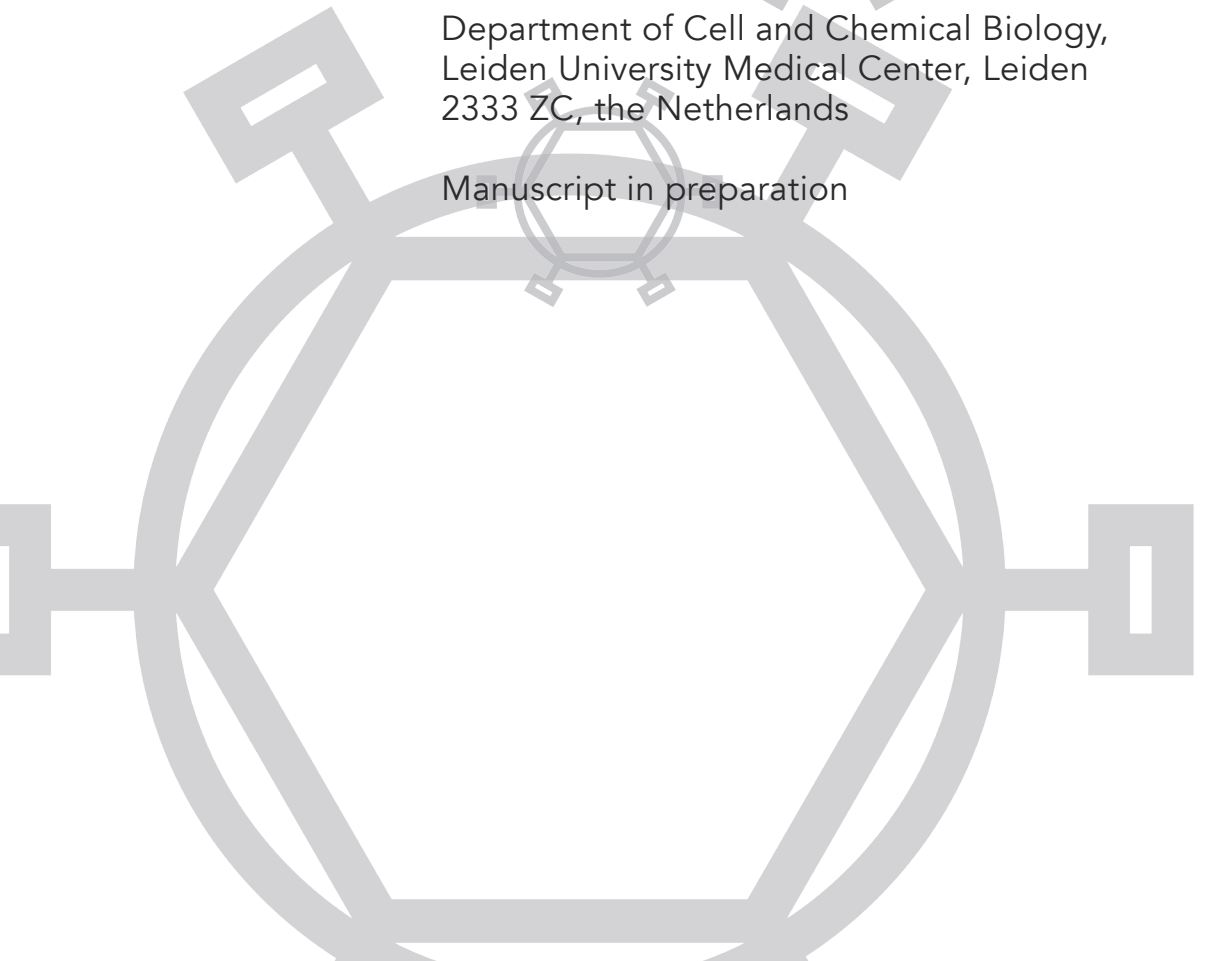
## Yields and genetic stability of replicating recombinant reoviruses



Vera Kemp, Diana J.M. van den Wollenberg,  
Ronald W.A.L. Limpens, Steve J. Cramer, Rob  
C. Hoeben

Department of Cell and Chemical Biology,  
Leiden University Medical Center, Leiden  
2333 ZC, the Netherlands

Manuscript in preparation



## **ABSTRACT**

Wild-type (wt) mammalian orthoreovirus Type 3 Dearing (T3D) has shown evidence of clinical activity as an oncolytic agent in cancer therapy, but its therapeutic efficacy remains to be augmented. Using a reverse genetics method, replication-competent reoviruses can be generated that encode a potentially therapeutic transgene. Insight into the infectivity and genetic stability of these modified reoviruses are prerequisites for their clinical use. We generated a series of transgene-containing reoviruses by replacing part of the spike protein  $\sigma$ 1-encoding segment by heterologous sequences. Although these recombinants could be propagated and stocks of recombinant reoviruses could be produced with relative ease, two phenomena currently limit their implementation in clinical translation programs. We observed a 10- to 750-fold lower infectious yield compared to wt T3D virus stocks. This was attributed to a lower infectivity of the transgene-containing reoviruses as the particle yields were similar to the wt viruses. We propose that the truncation of  $\sigma$ 1 hampers its stable insertion into the capsid and thereby negatively affects infectivity of the recombinant reoviruses. Moreover, occasionally mutants with deletions in S1 appeared from which transgene- and sometimes virus-derived sequences had been lost. The size of the deletions ranged from 47 to 519 nucleotides in length. The deletion mutants reveal the minimally required sequences for efficient packaging of modified segments into reovirus capsids. Our data suggest that the S1 RNA structure is underlying the deletions. Although medium-sized batches can be produced for preclinical research, routine monitoring of genome and particle integrity is essential when producing replication-competent reoviruses containing heterologous transgenes.

## INTRODUCTION

Mammalian orthoreovirus T3D, hereafter called reovirus, is a non-enveloped virus harboring a segmented double-stranded RNA genome with a total length of 23.5 kb [1]. The name reovirus is an acronym of *respiratory and enteric orphan virus*, to indicate the sites of infection and the notion that the virus has not been associated with severe pathology in humans. In cell culture, reovirus infection usually initiates a lytic replication cycle and preferentially infects and lyses transformed cells. The tumor cell preference can be attributed to the inhibition of innate immune sensing by an activated RAS signaling pathway, and the stimulation of virus uncoating, genome replication, virus egress and the induction of apoptosis. These factors have contributed to the adoption of this virus as a candidate anti-cancer agent for various cancer types.

While the results of the clinical trials published so far demonstrate the safety and feasibility of this approach, the anti-cancer efficacy as a stand-alone therapy remains to be improved [2]. On the one hand this may be accomplished by increasing the infection efficiency of the viruses, especially in tumors with a downregulated expression level of the canonical reovirus receptor junction adhesion molecule-A (JAM-A). Alternatively, the anti-cancer potency may be improved by inserting a therapeutic transgene in the reovirus genome.

Recently, a strategy has been developed that allows the insertion of transgenes in the reovirus genome without increasing the size of the recipient reovirus genome segment. This was achieved by exploiting a unique feature of the *jin* mutant reoviruses, which have the capacity to infect cells independent of the presence of the JAM-A receptor on the cell surface [3]. The causative mutations locate in the S1 segment which encodes the viral spike protein  $\sigma 1$ . The mutations affect the shaft region of  $\sigma 1$ , clustering in the region that interacts with sialic acids on the host cell surface. We showed that the mutations increase the affinity of  $\sigma 1$  for sialic acids, allowing the virions to undergo endosomal uptake independent of a high-affinity ligation to the JAM-A receptor. The head domain of  $\sigma 1$  mediates interactions with JAM-A but it is not essential for spike protein trimerization [4]. Since the *jin* mutants do not rely on ligation of  $\sigma 1$  to JAM-A for infection, the S1 region encoding the  $\sigma 1$  head domain can be replaced by heterologous sequences. This allows the insertion of up to 450 bp of heterologous sequences without exceeding the size of the unmodified S1 segment. In this approach the codons for the non-structural protein  $\sigma 1s$ , which overlaps the  $\sigma 1$  open reading frame but is read from another frame, is left intact. The feasibility and efficiency of this approach have been elegantly demonstrated by generating a reovirus in which the codons for the  $\sigma 1$  head domain were replaced by a sequence encoding the 13 kDa fluorescent protein iLOV [5]. To achieve simultaneous expression of the  $\sigma 1$  spike and of iLOV, a

poly-cistronic expression system exploiting the ribosomal skipping 2A sequence derived from the porcine tescho-1 virus (P2A) was used. This resulted in the separate synthesis of the truncated spike and the iLOV reporter protein.

We have expanded this approach to generate a number of replication-competent expanded-tropism reoviruses that harbor a heterologous transgene, without the need of a helper cell line expressing the modified genome segment [5-7]. A prerequisite for further clinical development of these recombinant viruses is that they can be produced to high titers and stably carry the transgene. In our routine propagation of transgene-containing reovirus batches, we observed a lower infectivity compared to wild-type reovirus and *j1n* mutants. Moreover, a number of deletion mutants occurred, in which (parts of) the transgene and occasionally reovirus-derived sequences were deleted. Here, we describe the reduced infectivity of the reoviruses in which a transgene replaces the codons for the head domain of  $\sigma 1$ . Moreover we characterized a series of spontaneous deletion mutants that were found in batches of recombinant reoviruses and we speculate on the mechanisms involved in their generation.

## **MATERIALS AND METHODS**

### *Cell lines and viruses*

The cell lines U118-MG (obtained from ATCC, Manassas, VA, USA) and 911 [8] were cultured in high glucose Dulbecco's Modified Eagle's Medium (DMEM; Invitrogen, Life Technologies, Bleiswijk, the Netherlands), supplemented with 8% fetal bovine serum (FBS; Invitrogen) and with penicillin and streptomycin (pen-strep) as described [8, 9]. The 911scFvHis cells were generated by transduction of 911 cells with the lentivirus vector pLV-scFvHis-IRES-Neo as described before [10]. The resulting polyclonal cell line was cultured in DMEM containing 8% FBS, pen-strep and 400  $\mu\text{g}/\text{mL}$  G418. The T7-RNA polymerase-expressing cell line BSR-T7 [11] was provided by K. Conzelmann and cultured in DMEM, 8% FBS, pen-strep and 400  $\mu\text{g}/\text{mL}$  G418. All cell cultures were maintained in an atmosphere of 5%  $\text{CO}_2$  at 37°C.

The wild-type Type 3 Dearing (wt T3D) reovirus strain R124 was isolated from reovirus T3D stock VR-824 from the ATCC (stock VR-824) by two rounds of plaque purification and propagated on 911 cells. Hereafter, this virus is referred to as wt T3D. The viruses were quantitated by plaque assays on 911 cells as described and virus concentrations and MOIs were defined on the basis of these titers [12]. For our experiments, we used cleared freeze-thaw lysates as reovirus stocks, unless indicated otherwise. Cesium chloride (CsCl) purified batches were generated as described before [7].

### *Generation of transgene-containing S1 segments*

The recombinant reoviruses were constructed essentially as was described before [5-7]. Synthetic S1 segments were designed *in silico* and a DNA copy was synthesized by Eurofins MWG Operon (Ebersberg, Germany). The segment sequences were designed to contain the following features: (1) nucleotides (nts) 1 to 768 from the S1 segment of reovirus mutant *jin-3*; this includes the 5'-untranslated region, entire  $\sigma$ 1s open reading frame (ORF) and the first 252 amino acids of the *jin-3*  $\sigma$ 1, including the codons for the G196R change near the sialic acid binding domain; (2) the codons for a 6 $\times$  His-tag (18 bp), which is placed in-frame with the  $\sigma$ 1-encoding part; (3) the codons for the porcine teschovirus-1 2A (P2A) sequence (66 bp +3 additional bp); followed by the (4) transgene with its stop codon; and (5) downstream of the transgene the 3' end of the S1 segment from nt 1219 to 1416 of wt T3D, which include A-, B- and C-box elements predicted to facilitate encapsidation of the reoviral positive strand ssRNA in the capsid [13, 14], as well as the 3'-untranslated region. The recombinant viruses rS1-mmGMCSF and rS1-hsGMCSF(co) contain the C-box but not the A- and B-boxes.

The fusion constructs were PCR cloned into the pBACT7 backbone of pBacT7-S1T3D as described before [5-7]. Plasmid pBacT7-S1T3D was purchased at Addgene (Cambridge, MA, USA) (plasmid 33282, <http://www.addgene.org>). The resulting plasmid was characterized by restriction analysis and a single clone was expanded and used for virus generation.

### *Generation of recombinant reoviruses*

For the generation of recombinant reoviruses, we used the procedure described by Boehme *et al.* [15] with some modifications [5]. Whereas the original system uses 10 plasmids for providing the full complement of reovirus segments [16], our approach uses five plasmids. In addition to pBT7-modified S1, we used the following plasmids, pT7-L1T1L (Addgene, plasmid #33286), pT7-L2-M3T3D (Addgene, plasmid #33300), pT7-L3-M1T3D (Addgene, plasmid #33301) and pT7-M2-S2-S3-S4T3D (Addgene, plasmid #33302). For generating recombinant reoviruses, the five plasmids were transfected into BSR-T7 cells using the TransIT-LT1 transfection reagent (Mirus; Sopachem BV, Ochten, the Netherlands), according to the manufacturer's manual.

At 72 hours post transfection, the cells were harvested and lysed by three cycles of freeze-thawing. After pelleting the cell debris, the cleared supernatant containing the recombinant reoviruses was added to 911scFvHis cells in a 6-well plate. Upon the first appearance of cytopathic effect (CPE), the cells were harvested and the recombinant reovirus was released from the cells by three cycles of freeze-thawing. The cell debris was removed from the reovirus-containing lysate by

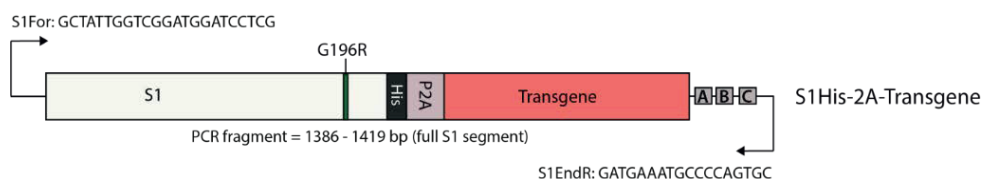
centrifugation (10 min at 3000g), and stored at  $-20^{\circ}\text{C}$  until further use. The virus was routinely passaged by exposing fresh semi-confluent cultures of 911scFvHis cells to dilutions of the cleared lysates.

Medium-sized batches of cesium chloride (CsCl) purified recombinant reoviruses were prepared as described before [7]. The CsCl-purified reoviruses were recovered in reovirus storage buffer (RSB: 10 mM Tris-HCl pH 7.5, 150 mM NaCl, 10 mM  $\text{MgCl}_2 \cdot 6\text{H}_2\text{O}$ ) supplemented with 0.1% Bovine Serum Albumin (BSA), and were aliquoted and stored at  $4^{\circ}\text{C}$  until use. The amount of particles was calculated based on the  $\text{OD}_{260}$  values. The infectious titers were determined based on  $\text{TCID}_{50}$  assays as described before [5].

For routine production, the reoviruses were amplified by infecting near-confluent cultures of 911 cells or 911scFvHis cells at an MOI of 2-5 and harvesting the cells after 48 - 64 hours depending on the progression of the cytopathic effects in the cultures. Upon harvesting the combined cells and medium, the harvest was freeze-thawed 3 times and the lysate was cleared by low-speed centrifugation.

#### *Reverse transcriptase PCR and sequence analysis*

911scFvHis cells were infected with the recombinant reoviruses. As we had no indication of the titer of the early passaged batches (P1 of the recombinant viruses) obtained upon the initial transfection experiment, 1/20th part of the isolated viruses was used for exposure of the cells. Total RNA was extracted from the infected cells with the Absolutely RNA Miniprep Kit (Stratagene, Agilent Technologies, Amstelveen, the Netherlands) according to the manual. Subsequently, cDNA was synthesized using the S1EndR primer (5'-GATGAAATGCCCCAGTGC-3') and SuperScript III reverse transcriptase (Invitrogen, Life Technologies). In the PCR, the following primers were used to detect S1: S1For – 5'-GCTATTGGTCGGATGGATCCTCG-3' – and S1EndR, with GoTaq polymerase (Promega, Leiden, the Netherlands). The positions of the primer binding sites are shown in Supplementary figure 1.



**Supplementary figure 1.** Primer locations on S1 for S1 RT-PCR analysis. Schematic representation of the PCR analysis, showing the S1 segment, the locations of the primers S1For and S1EndR, and the length of the PCR fragment.

For sequence analysis, Pfu DNA polymerase (Fermentas, FisherScientific, Landsmeer, the Netherlands) was used to amplify the genome segments and the PCR products of the S1 segments were sent to the Leiden Genome Technology Center (Leiden University Medical Center, Leiden, the Netherlands) for Sanger sequencing. Primers used in the sequence reactions were S1For and S1EndR.

#### *Electron microscopy*

For electron microscopy analyses, reovirus batches were fixed in 0.75% Glutaraldehyde in 0.1 M cacodylate buffer for 30 minutes at room temperature. Subsequently, they were adsorbed for 1 minute to freshly glow-discharged, carbon-coated pioloform grids, followed by negative staining with a 2% phosphotungstic acid (PTA) solution for 30 seconds. Analyses were performed using a Tecnai 12 electron microscope (FEI) at 120 kV, equipped with a 4K OneView CMOS Camera (Gatan).

#### *Western blot*

Purified virus particles were subjected to western blot analysis. Western sample buffer (final concentration: 10% glycerol, 2% SDS, 50 mM Tris-HCl pH 6.8, 2.5%  $\beta$ -mercaptoethanol and 0.025% bromophenol blue) was added to  $1 \times 10^9$  or  $1 \times 10^{10}$  viral particles (based on OD<sub>260</sub> measurements) in RSB. Samples were heated for 3 minutes at 97°C before loading on a 10% polyacrylamide-SDS gel. The proteins were transferred to Immobilon-PSQ (Merck-Millipore, Amsterdam, the Netherlands) for detection with the Odyssey system (LI-COR Biotechnology, Westburg, Leusden, the Netherlands). Separate blots were prepared for the detection of  $\sigma 1$  (blot 1), and  $\lambda 2$  (blot 2). Primary antibody used to detect  $\lambda 2$  (7F4) was obtained from the Developmental Studies Hybridoma Bank developed under the auspices of the NICHD and maintained by the University of Iowa, Department of Biology [17]. Primary antibody against the  $\sigma 1$  tail was described before [5]. Blot 2 was re-stained for P2A, using a rabbit anti-P2A peptide serum ABS31 (Merck-Millipore, Amsterdam, the Netherlands). For the detection of the primary antibodies, the IRDye 800CW Donkey-anti-Rabbit IgG and IRDye 680RD Donkey-anti-Mouse IgG (LI-COR Biotechnology, Westburg BV, Leusden, the Netherlands) were used.

#### *ISVP experiment*

Intermediate subviral particles (ISVPs) of rS1-mmGMCSF and wt T3D were generated as described previously [3]. In short, both viruses were diluted to  $\sim 5 \times 10^{11}$  particles/ml, and incubated with 200  $\mu\text{g}/\text{mL}$   $\alpha$ -chymotrypsin (C3142, Sigma) at 37°C for 1 hour. Subsequently, the reaction was stopped by addition of 5 mM PMSF

(78830, Sigma) at 4°C. The control rS1-mmGMCSF and wt T3D were diluted to the same extent as the ISVPs by adding the same volumes of RSB.

911 cells were seeded in 24-well plates at  $3 \times 10^5$  cells/well. Each well was mock-treated or infected with ISVP-mmGMCSF, rS1-mmGMCSF, ISVP-T3D, or wt T3D at  $2 \times 10^4$  particles/cell. After 1 hour incubation at 4°C to synchronize the infection, cells were incubated for 5 hours and 24 hours at 37°C. Then, the cells were permeabilized in Perm/Wash buffer (BD Biosciences) for 15 minutes at room temperature, spun down, and stained for reovirus  $\sigma 3$  protein. Used antibodies are Mouse-anti- $\sigma 3$  (4F2), and PE-conjugated Goat-anti-Mouse (BD Biosciences). Each condition was measured in duplicate.

## RESULTS AND DISCUSSION

### *Construction of recombinant reoviruses*

Genetic modification of reovirus has been greatly facilitated by the development of the plasmid-based reverse genetics strategy. We previously described the generation of reoviruses expressing the fluorescent reporter iLOV (rS1-iLOV) [5], the oncolytic E4orf4 (rS1-E4orf4), its inactive variant RFA (rS1-RFA) [6], human GM-CSF (rS1-hsGMCSF) and murine GM-CSF (rS1-mmGMCSF) [7]. As illustrated in Figure 1a, BSR-T7 cells were transfected with plasmids encoding the different reovirus segments. The cells were harvested after 72 hours and the lysates were added to 911scFvH cells for virus amplification. As illustrated in Figure 1b, we replaced the codons for the  $\sigma 1$  head domain, which is responsible for binding to the canonical reovirus receptor junction adhesion molecule-A (JAM-A), for generating reoviruses carrying the transgene of interest. Furthermore, the constructed S1 segments contain a G196R mutation that we previously identified in the *jin-3* reovirus mutant [3]. This mutation mediates JAM-A independent entry through enhanced sialic acid binding. To allow for the separate synthesis of the  $\sigma 1$  and the heterologous protein, a porcine teschovirus-1 2A (P2A) sequence was incorporated. Lastly, the codons for a 6x His tag were inserted to augment initial propagation in 911scFvH cells harboring a His receptor [10].

During the construction of the recombinant S1 segments, we took care not to exceed the 1416 base pairs (bp) length of the wild-type (wt) Type 3 Dearing (T3D) S1 segment. As can be seen in Figure 1b, all successfully generated recombinant viruses contain a S1 segment within this size, except for the viruses harboring S1His-2A-E4orf4 and S1His-2A-RFA which are only 3 bp longer (*i.e.* 1419 bp). Our attempts to generate batches of recombinant reoviruses harboring the codons for either DsRed [5] or Gaussia Luciferase with S1 segment sizes of 1722 bp and 1539 bp, respectively, were unsuccessful despite various attempts. We concluded that a

considerable increase in the length of the S1 segment hampers the production of these reoviruses.

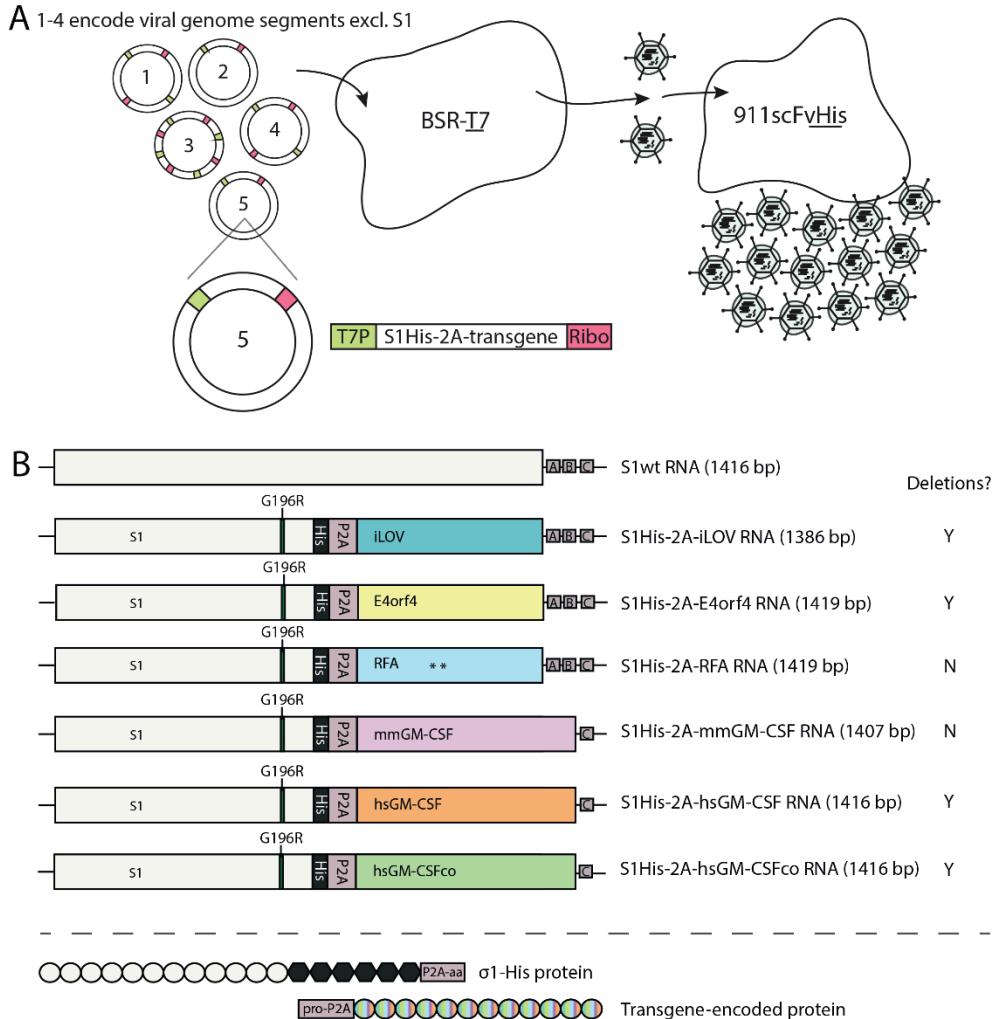


**Figure 1.** Overview of the generation of recombinant reoviruses and the constructed S1 segments. A) For the generation of recombinant reoviruses, BSR-T7 cells were transfected with 4 plasmids encoding the different reovirus segments except for S1, and the pBT7-modified S1 segment encoding the transgene of interest. The cells were harvested after 72 hours and the lysates were added to 911scFvH cells for virus amplification. B) The modified S1 segments encoding the different transgenes, adapted from Kemp *et al.* 2018 [7]. The

segment sequences were designed to contain the following features: (1) nucleotides (nts) 1 to 768 from the S1 segment of *jin-3*; harboring the 5'-UTR, entire  $\sigma 1$ s ORF and the first 252 amino acids of the *jin-3*  $\sigma 1$ , including the codons for the G196R change near the sialic acid binding domain; (2) the codons for a 6 $\times$  His-tag (18 bp); (3) the codons for the P2A sequence; followed by the (4) transgene encoding the heterologous protein – iLOV, E4orf4, RFA, mmGM-CSF, hsGM-CSF, and hsGM-CSFco – including a stop codon. Downstream of the transgene (5) the 3' end of the wt T3D S1 segment, which includes the A-, B- and C-box elements predicted to facilitate encapsidation of the reovirus positive strand ssRNA in the capsid [13, 14], as well as the 3'-UTR. The recombinant viruses rS1-mmGMCSF and rS1-hsGMCSF(co) contain the C-box but not the A- and B-boxes. The occurrence or absence of deletion mutants is indicated by Y (yes) or N (no), respectively.

### *Production and stability of virus particles*

During the routine production, we noted that the infectious titers of our purified recombinant reovirus batches were relatively low compared to batches of wt T3D reovirus or mutants such as *jin-3* (representative examples of the obtained yields per T75 flask in Table 1). Initially, we were unable to purify the recombinant viruses due to the absence of a clear virus band in the CsCl gradient. However, the freeze-thawed virus-containing cell lysates did contain infectious viruses prior to purification, as demonstrated by titrations based on TCID<sub>50</sub> assays (examples in Table 1). We had implemented benzonase treatments in our purification protocol, to remove undesired free nucleic acids. For optimal benzonase activity during our purifications, the buffer in which the viruses are harvested had a NaCl concentration of 100 mM. While this procedure yields very pure and concentrated stocks for the wt reovirus, we lost the *jin* mutant viruses and the transgene-containing viruses. We speculated that the G196R mutation responsible for enhanced sialic acid binding mediates negative charge dependent binding to cellular debris (membranes, DNA, RNA, etc.). As the cellular debris will be cleared from the cell lysate during Vertrel extractions, the *jin* and transgene-containing reoviruses would be lost prior to CsCl purification. We could remedy this by increasing the salt concentration of the harvest buffer to 250 mM NaCl. This retained benzonase activity and presumably sufficiently weakens the charge-dependent bonds between the viruses and the cellular debris. Indeed, after this amendment of the protocol we obtained clear virus bands upon CsCl purification with all reoviruses.

Importantly, despite the now similar particle yields of the transgene containing reoviruses, the infectious titers were approximately a 10-750 fold lower than those of wt T3D and *jin* reoviruses. Typically, we obtained roughly 10<sup>8</sup> infectious units (IU) of recombinant reovirus from 1 infected T75 flask of 911 or 911scFvH cells, compared to around 10<sup>10</sup> IU for wt T3D or *jin* reoviruses. However, the particle yields

as measured by the OD<sub>260</sub> values were similar, demonstrating that similar amounts of virus particles were produced. As a result, the particle-to-IU ratios of the recombinant virus batches were relatively high (usually around 10000:1 compared to 100:1 for *jin* mutants and wt T3D). Moreover, we found that the infectivity of the transgene-containing reoviruses decreased in time (approximately 1000-fold in 6 months) upon storage at 4°C. This could be fully remedied by the inclusion of 0.1% BSA in the reovirus storage buffer. This suggested that the inactivation may have been caused by aggregation of the recombinant reovirus particles.

Virus	Purified	Yield (IU/flask)
T3D	Yes	1.14x10 <sup>10</sup>
<i>jin-3</i>	Yes	1.27x10 <sup>10</sup>
rS1-iLOV	Yes	1.83x10 <sup>8</sup>
rS1-iLOV	No	1.03x10 <sup>8</sup>
rS1-mmGMCSF	Yes	9.91x10 <sup>7</sup>
rS1-mmGMCSF	No	1.74x10 <sup>8</sup>

**Table 1.** Yields obtained for wt T3D and recombinant reoviruses. Table overview of examples of yields obtained for batches of wt T3D, *jin-3*, and recombinant reoviruses rS1-iLOV and rS1-mmGMCSF. Infectious yields are displayed as infectious units (IU) per T75 flask and are representative for the various produced virus batches.

#### *Differences in morphology of rS1-mmGMCSF and wt T3D reoviruses*

To examine potential differences in the overall appearance of recombinant reovirus and wild-type reovirus particles, we used electron microscopy of purified rS1-mmGMCSF and wt T3D reovirus particles. As can be seen in Figure 2, the virus particles of rS1-mmGMCSF and wt T3D appeared similar in morphology and size. No increase in the abundance of electron-dense empty particles was seen for rS1-mmGMCSF. A closer examination of the particles revealed a potential difference in appearance, with a fuzzy outer capsid displaying ‘dark spots’ on the rS1-mmGMCSF particles but not the wt T3D particles. Possibly, these electron-dense areas represent empty locations in the reovirus outer capsid in which the dye concentrated. This suggests that a capsid protein, most likely  $\sigma 1$ , is not stably incorporated. For the structurally similar adenovirus, it has been shown that truncation of its fiber protein leads to a decreased stability and faster disassembly of the viral particle [18]. If this

also is the case for the truncated  $\sigma 1$  in our recombinant reoviruses, it could be that the viral capsid of rS1-mmGMCSF is intrinsically less stable than that of wt T3D.

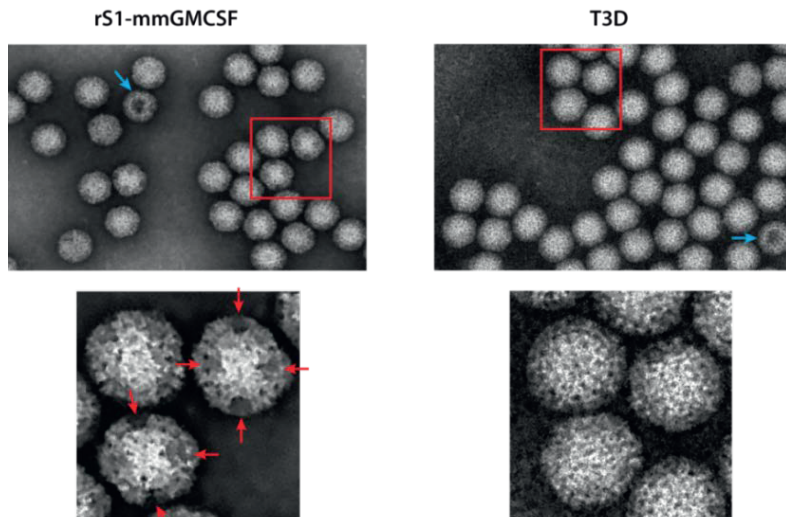


**Figure 2.** Electron microscopic pictures of rS1-mmGMCSF and wt T3D particles. Purified reovirus batches were fixed and adsorbed to carbon-coated grids, followed by negative staining. Electron microscopic photographs were taken. The lower pictures represent zoomed in parts of the upper photographs (red boxes). Electron-dense spots on the outer capsid are indicated by red arrows. Blue arrows indicate empty virus particles.

#### *Expression levels of capsid proteins in purified rS1-mmGMCSF and wt T3D particles*

We hypothesized that the truncated  $\sigma 1$  is expressed in the viral particle, and thereby should be able to mediate viral entry. However, its truncated form may interfere with capsid integrity by affecting the stability of its own trimerized form or of interacting capsid protein  $\lambda 2$ . The reovirus  $\lambda 2$  protein is implicated in  $\beta 1$ -integrin mediated internalization [19]. Destabilization of this protein in the capsid may therefore hamper infectivity. We performed a semi-quantitative western blot analysis on the expression levels of  $\sigma 1$  and  $\lambda 2$  in purified reovirus particles, comparing rS1-mmGMCSF with wt T3D. Notably, we did not see differences in the expression levels of  $\lambda 2$  (Figure 3), suggesting that the truncated  $\sigma 1$  does not influence the stability and abundance of this neighboring capsid protein.

It has been shown that the N-terminal fibrous proportion of  $\sigma 1$  is able to form trimers [4]. Although there are contradictory reports [20], truncations of  $\sigma 1$  can sometimes result in reduced levels of  $\sigma 1$  in the capsid [21]. We speculated that encapsidation of the truncated  $\sigma 1$  protein in our recombinant reoviruses may be

reduced, resulting in a lower  $\sigma 1$  abundance in the capsid. Possibly, not all vertices are occupied by  $\sigma 1$  trimers. To see whether the amount of  $\sigma 1$  in the capsid is reduced by the truncation, we compared the  $\sigma 1$  levels in the purified rS1-mmGMCSF and wt T3D particles. Indeed, purified rS1-mmGMCSF particles seem to harbor a lower level of truncated  $\sigma 1$  ( $\sigma 1$ -trunc) compared to the level of full-length  $\sigma 1$  ( $\sigma 1$ -FL) in wt T3D particles (Figure 3). As  $\sigma 1$ -trunc expression in rS1-mmGMCSF particles was almost undetectable, we checked the P2A expression level to confirm the presence of  $\sigma 1$ -trunc. We usually obtain stronger stained bands with the anti-P2A antibody compared to anti- $\sigma 1$  [5]. The detected P2A is attached to the  $\sigma 1$ -trunc protein, so can be used as a different measure of  $\sigma 1$ -trunc expression. Indeed, P2A bands were clearly identified in the rS1-mmGMCSF particles, confirming that  $\sigma 1$ -trunc is present, albeit possibly at a low level. Taken together, we propose that the truncation of  $\sigma 1$  does not influence the stability of neighboring capsid proteins, but instead seems to inhibit its own stable insertion into the capsid. Interestingly, it has been demonstrated that three  $\sigma 1$  trimers per virion are the minimum to retain full infectivity [22]. It remains to be determined whether the truncated  $\sigma 1$  proteins in our recombinant reoviruses are able to trimerize, and if so, how many  $\sigma 1$  trimers are stably present in the viral capsid. The semi-quantitative western blot analysis does not give a decisive answer to this. Instable spike trimers could lead to the leakage of RNA from the viral particles. As we did not observe an increase in the amount of empty particles in rS1-mmGMCSF batches compared to wt T3D batches, there seems to be no dramatic increase in RNA leakage from the rS1-mmGMCSF particles. Future research is warranted to elucidate this phenomenon.

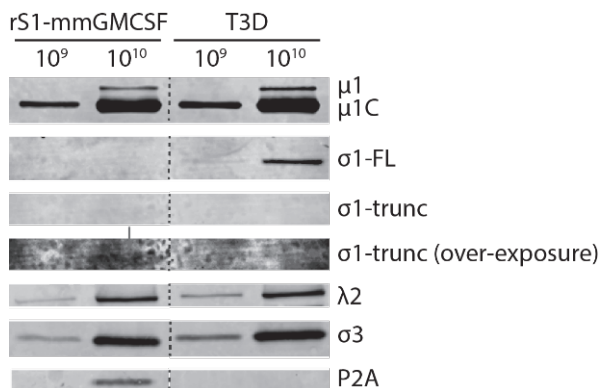


**Figure 3.** Expression of full-length  $\sigma 1$ , truncated  $\sigma 1$ ,  $\lambda 2$ , and P2A in purified rS1-mmGMCSF and wt T3D particles. Purified virus ( $10^9$  and  $10^{10}$  particles) was subjected to a semi-quantitative western blot analysis of  $\sigma 1$ ,  $\lambda 2$ , and P2A expression. Detection was performed using the Odyssey system. The red arrow indicates a faint  $\sigma 1$  band.

6

### *Infectivity or rS1-mmGMCSF is not enhanced by ISVP generation*

For adenovirus, it has been described that truncation of its fiber protein leads to a decreased adsorption onto, and entry into, cells [23]. We speculated that the truncation of the reovirus  $\sigma 1$  protein reduces infectivity by hampering the cell entry capacity of the virions, either due to reduced levels of  $\sigma 1$  in the capsid or through a direct effect of the truncation on the cell binding ability of  $\sigma 1$ . To test this hypothesis, we made intermediate subviral particles (ISVPs) of rS1-mmGMCSF (ISVP-mmGMCSF) and wt T3D (ISVP-T3D) reoviruses. ISVPs may enter cells independent from  $\sigma 1$  binding to JAM-A and/or sialic acids [9]. Therefore, if truncation of the  $\sigma 1$  spike interferes with entry, it is expected that ISVP-mmGMCSF would enter cells more efficiently than rS1-mmGMCSF. For wt T3D, this positive effect of ISVP generation on cell entry is expected to be lower, because wt T3D can already efficiently enter cells. To study the degree to which the reoviruses can enter cells, we checked the  $\sigma 3$  expression in 911 cells at 5 and 24 hours upon infection with rS1-mmGMCSF, ISVP-mmGMCSF, wt T3D, or ISVP-T3D. As a control, U118-MG cells were taken along. U118-MG cells lack JAM-A expression and therefore resist wt T3D but not ISVP-T3D infection. Because of their S1 G196R mutation, both rS1-mmGMCSF and ISVP-mmGMCSF can infect U118-MG cells through enhanced sialic acid binding. Therefore, U118-MG cells can be used to check for successful ISVP generation. Indeed, ISVP generation of wt T3D increased the  $\sigma 3$  expression in U118-MG cells. Surprisingly, we found no increase in  $\sigma 3$  expression in infected 911 cells for both rS1-mmGMCSF and wt T3D upon ISVP generation (Figure 4). If anything, the original rS1-mmGMCSF and wt T3D reoviruses seem to enter more efficient than the ISVPs. These results indicate that the relatively low infectivity of rS1-mmGMCSF compared to wt T3D is not caused by a reduced cell penetration capacity, suggesting that a post-entry step is inhibited during infection with these recombinant reoviruses.

### *S1 deletion mutants*

As indicated in Figure 1, several of the produced recombinant reoviruses acquired deletions during passaging. As described before, the deletion mutants overgrow the virus populations upon prolonged propagation, suggesting that they have a selective growth advantage over the intact recombinant reoviruses [7]. The overview in Figure 5 summarizes the sequences that were found deleted. The S1 sequences that were deleted provide insight into the elements that are dispensable for incorporation of the segment into the viral capsid. We previously reported the deletion of the A- and B-boxes in an rS1-iLOV deletion mutant, suggesting that these sequences are not essential for the formation of infectious reovirus [5]. This notion was strengthened by the successful generation of rS1-hsGMCSF and rS1-mmGMCSF in which the A- and

B-boxes were omitted from the recombinant segments [7]. Furthermore, rS1-hsGMCSF del3 reveals that a small proportion of the S1 segment upstream of the His-tag insertion, and including the trypsin cleavage site implicated in the trypsin-mediated conversion of reovirus virions to ISVPs, is non-essential [24]. As only 7 amino acids would be released protein upon trypsin digestion, this observation may not come unexpected.

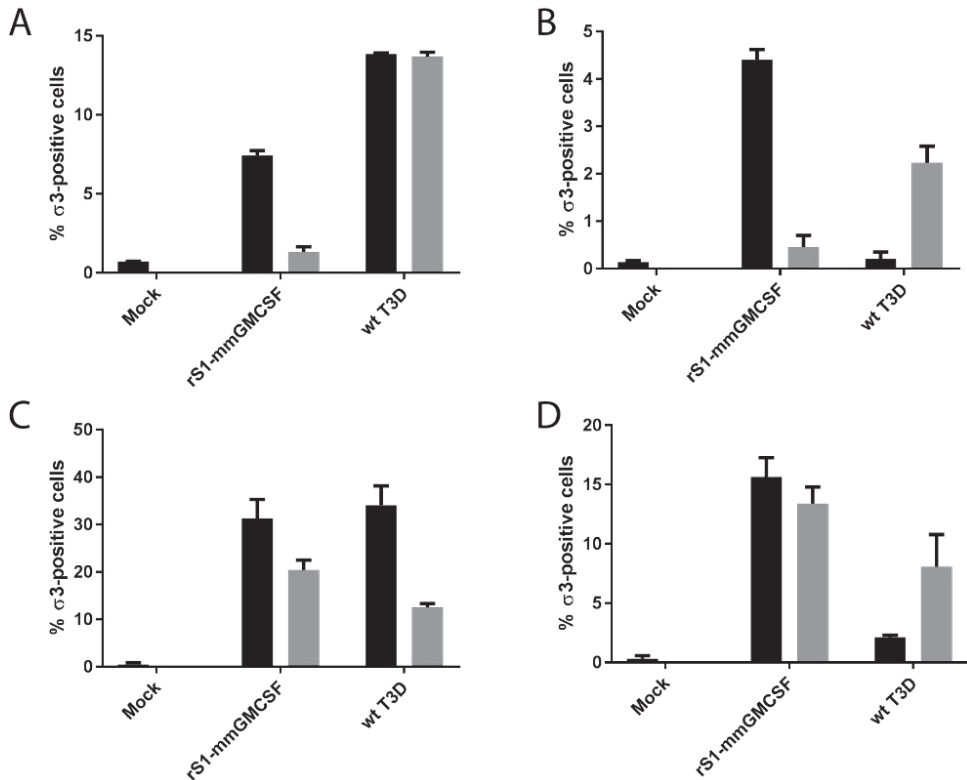


**Figure 4.** Percentage of  $\sigma 3$ -positive 911 and U118-MG cells upon infection with ISVPs or normal rS1-mmGMCSF/wt T3D. ISVPs of rS1-mmGMCSF and wt T3D were generated by exposing  $\sim 5 \times 10^{11}$  particles/ml to 200  $\mu\text{g}/\text{mL}$   $\alpha$ -chymotrypsin. The reaction was stopped by addition of 5 mM PMSF. Cultures of 911 (A, C) and U118-MG (B, D) cells were mock-treated or infected with ISVP-mmGMCSF, rS1-mmGMCSF, ISVP-T3D, or wt T3D at  $2 \times 10^4$  particles/cell. After synchronization of the infection, cells were left for 5 hours (A-B) and 24 (C-D) hours. Then, the cells were stained for intracellular  $\sigma 3$  protein. Each condition was measured in duplicate. Light grey bars represent ISVP treatments; black bars represent non-ISVP treatments.

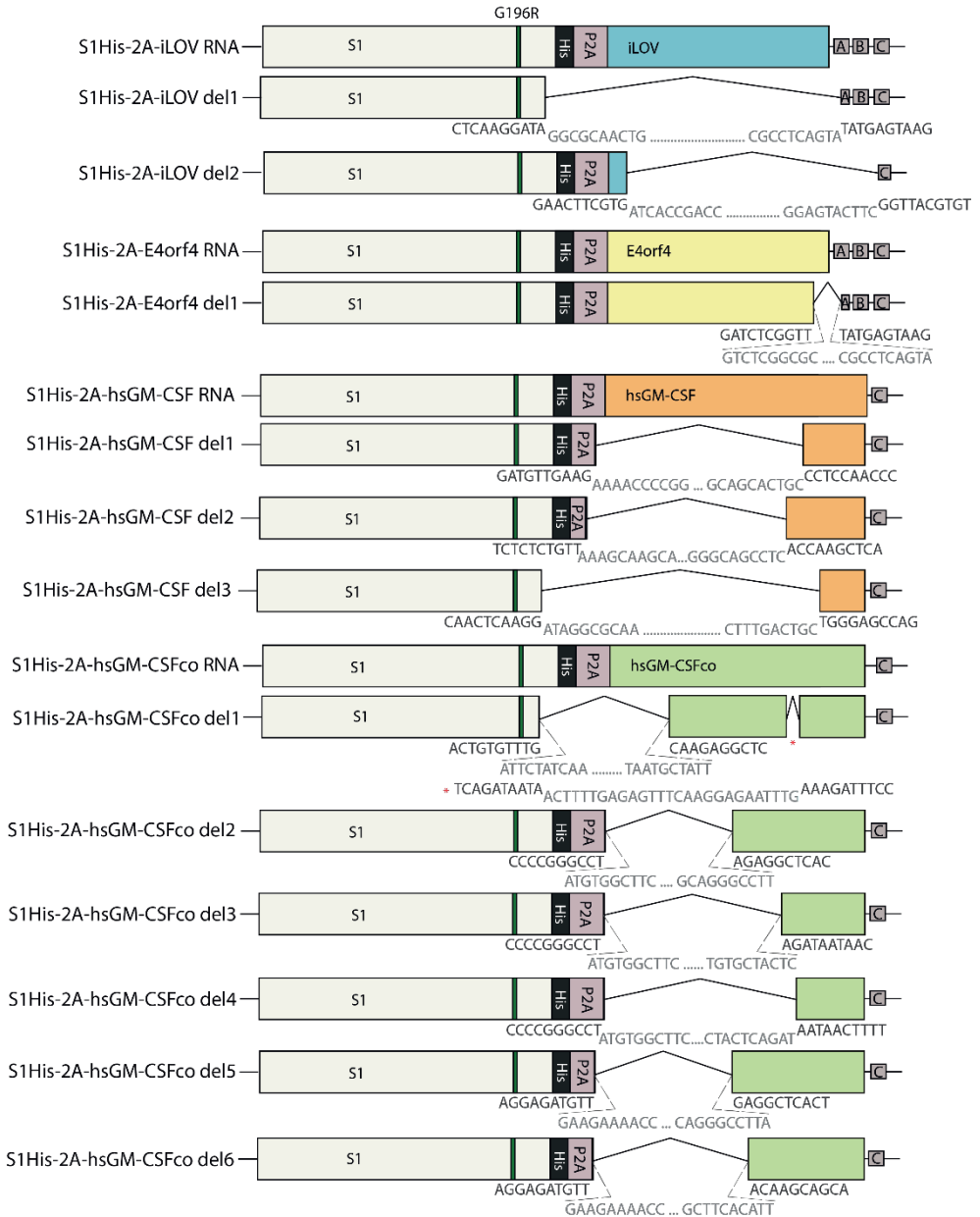


**Figure 5.** Overview of deletion mutants including sequences at the deletion junctions. Schematic overview showing the different deletions occurring in the recombinant reovirus batches. Indicated are the sequences at the junctions (retained sequence in black, deleted

sequence in grey). Various lengths of transgene-derived and occasionally reovirus-derived sequences were deleted.

*S1 deletions are unlikely caused by replacing the S1 head domain or removing the A- and B-boxes*

To gain more insight into the requirements for generating batches of genetically stable recombinant reoviruses, we need more insight into the mechanism(s) underlying the deletions. The fact that we find deletions for various recombinant reoviruses and their appearance in separate propagation experiments implies that the different deletions are caused by a pervasive mechanism. It seems unlikely that the deletions are merely an intrinsic consequence of replacing the S1 head domain by a transgene, as we only observed deletions in 3 of the 5 recombinant reoviruses. It can also be ruled out that it is an inevitable result of removal of the A- and B-boxes for the construction of the rS1-mmGMCSF and rS1-hsGMCSF(co) viruses, as deletions also occur in batches of rS1-iLOV and rS1-E4orf4, in which the A- and B-boxes have been retained.

*S1 deletions are unlikely caused by adverse effects of the transgene-encoded protein*

The deletion mutants overgrow the virus population within a few passages, suggesting that the removal of the transgene positively affects the viral replication cycle. We hypothesized that the deletion mutants could be the result of a negative effect of the transgene-encoded protein on the virus replication cycle. However, this seems unlikely because the deletions are found for a variety of transgenes. There is no evidence that would suggest that the iLOV fluorescent protein negatively influences viral replication and that therefore a deletion mutant has a growth advantage. For GM-CSF, it could be speculated that it influences cells expressing the GM-CSF receptor, and thereby affects viral replication in the cell culture. Although hsGM-CSF and mmGM-CSF proteins share 54% identity of their amino acid sequences, their biological activities are species-specific [25]. As we grow our reoviruses on a human cell line, and deletions were only observed for rS1-hsGMCSF and not rS1-mmGMCSF, a deleterious effect of hsGM-CSF could be underlying the sequence deletions. The GM-CSF receptor is generally expressed on a subset of immune cells specifically, but its expression on our propagation cell line 911 has never been tested and can therefore not be ruled out. To circumvent any effect of hsGM-CSF production on our production cell line, we attempted to generate the rS1-hsGMCSF virus on a non-human cell line. However, several attempts to stably propagate this virus on L929 cells failed, suggesting that the deletions are unrelated

to adverse effects of the transgene-encoded protein on the producer cell line (data not shown).

#### *The mechanism responsible for generating the S1 deletions*

There are two distinct mechanisms that could give rise to deletion mutants. In a first mechanism, sequences are removed from an existing RNA molecule. Such a mechanism would require the break of an internal phosphodiester bond, by a nuclease or in a non-enzymatic reaction, and subsequently the re-establishment of a new bond at another position. This reaction would require an RNA ligase, or a splicing type of reaction. Alternatively, the deletion may be resulting from a template switch or jump by the reoviral RNA-dependent RNA polymerase. The polymerase could stall and reinitiate the RNA synthesis at another part of the template. This would skip a part of the template and result in the loss of genetic information.

#### *S1 deletions are unlikely caused by splicing-related events*

A potential mechanism underlying the deletions could be splicing-mediated events. This process is typically thought to exclusively take place in the cell nucleus, but a growing number of transcripts has been found to undergo cytoplasmic splicing [26]. To see whether this could explain the S1 deletions in our recombinant reoviruses, we inspected the sequences flanking the deletions for the presence of splice sites (Figure 5). We have not found common sequences at the junctions and no similarity with any nuclear consensus splice site donor and acceptor sequences (5' GU and 3' AG) at the deletion junctions. In some cases, an AG sequence was apparent in the minus strand of the deletion (S1His-2A-iLOV del2 and S1His-2A-hsGM-CSFco del 3). The recognition of this site by the cytoplasmic splicing machinery seems doubtful, as the minus strand RNA of the reovirus genome is synthesized within the new viral cores and therefore should not reside free in the cytoplasm of the cell [1]. In conclusion, we have no evidence that cytoplasmic splicing causes the deletions.

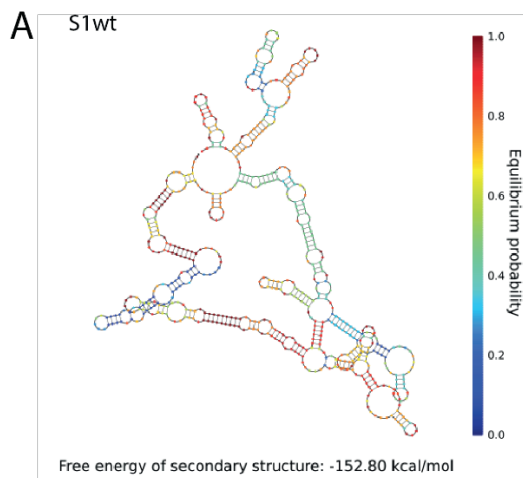
#### *S1 deletions are unlikely caused by homology-related events*

In one of the deletion mutants, rS1-hsGMCSF del2, we found some degree of homology between the six nucleotides flanking the 5' of the deletion (5' – GGGCCT – 3') and the final 3' seven nucleotides (5' – GGGCCTT – 3') of the deletion (Figure 5). Therefore, we hypothesized that homology-related events are causing the S1 segment deletion. However, for none of the other deletion mutants we have observed a substantial degree of homology in the sequences flanking the deletion or elsewhere in the S1 segment.

*S1 deletions may be caused by complexities in RNA structure*

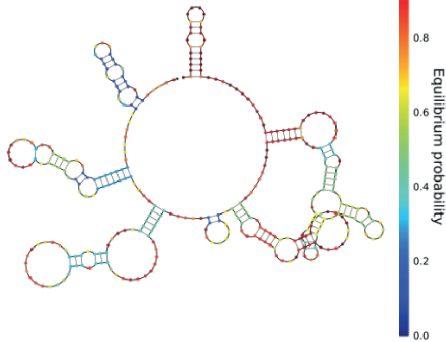
We proposed that the underlying cause for the deletions may reside in complexities in the secondary or tertiary RNA structure of the transgene sequences in the S1 segment. As a result, deleting the sequences would increase the simplicity and stability of the S1 segment structure. Experimental validation and *in silico* prediction of the RNA structure is complex for relatively long sequence stretches (> 1000 nt) and the results are often unreliable. Also, we should realize that the transcription of the reovirus RNAs takes place on dsRNA templates.

Instead, one could analyze the smaller-sized deletions only. We compared the secondary RNA structures (<http://www.nupack.org>) and specifically their free energy values of the plus strand wild-type S1 sequence encoding the  $\sigma$ 1 head domain (Figure 6a) and the different transgenes (Figure 6b). As expected, it can be seen that codon-optimizing the hsGM-CSF sequence resulted in a lower negative free energy value, indicating that the codon-optimized version may have an advantage over the original sequence in terms of stability. Interestingly, the RNA structures of the successfully expressed transgenes had higher negative free energy values than the ones that have yielded deletions. The wild-type S1 sequence had a free energy value of -151.80 kcal/mol, the highest negative value of all structures analyzed. This suggests that the deletion mutants do not appear and overgrow the virus population due to harboring a more stable S1 RNA structure with a reduced negative free energy value. However, it should be noted that the structure analyses of only the transgenes could give a biased interpretation because it does not take into account the context of the rest of the S1 segment it is embedded in. Based on the variety and apparent randomness of the deletions, we propose that complexities in RNA structure still represent the most likely underlying cause of the deletions.



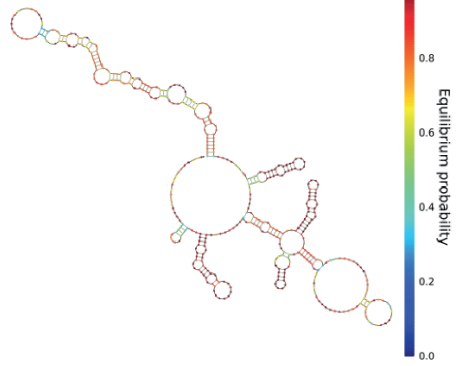
**B**

iLOV



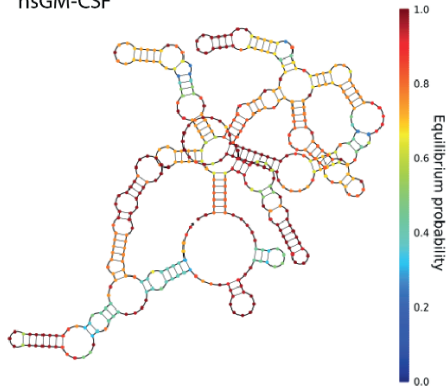
Free energy of secondary structure: -82.40 kcal/mol

mmGM-CSF



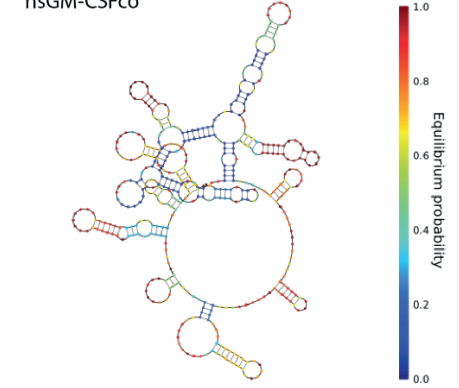
Free energy of secondary structure: -97.77 kcal/mol

hsGM-CSF



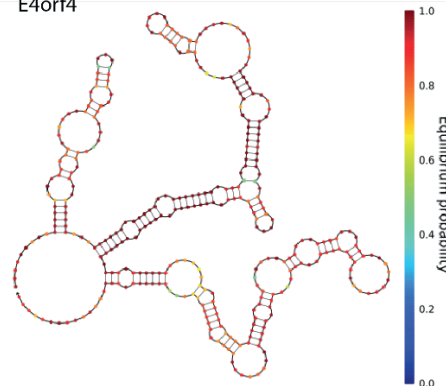
Free energy of secondary structure: -137.50 kcal/mol

hsGM-CSFco



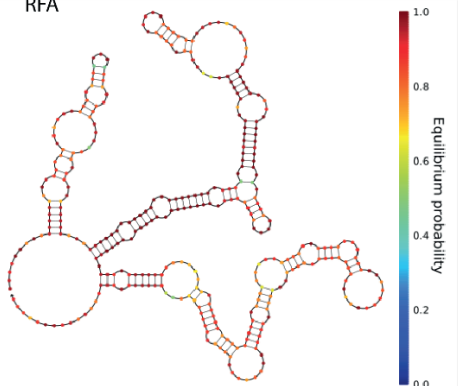
Free energy of secondary structure: -107.70 kcal/mol

E4orf4



Free energy of secondary structure: -95.30 kcal/mol

RFA



Free energy of secondary structure: -97.30 kcal/mol

**Figure 6.** RNA structures of the wt S1 head domain region, and the different transgenes. Analysis of the RNA structure and free energy values of A) the wt S1 head domain region, and B) the different transgenes encoding iLOV, mmGM-CSF, hsGM-CSF, hsGM-CSFco, E4orf4, and RFA. Analysis was performed on <http://www.nupack.org>.

Alternatively, the modified genomes may exhibit stable secondary structures that cannot be efficiently resolved by the reovirus RNA-dependent RNA polymerase. This may result in template jumping or template switching, which could yield deletion transcripts. In the newly formed cores, these deletion transcripts may serve as templates for negative strand formation, and thereby result in deletion segments.

## CONCLUDING REMARKS

We demonstrated that during the routine production of virus batches, recombinant reoviruses show a lower infectivity compared to wild-type Type 3 Dearing (wt T3D) and *jln* reoviruses. We showed that the overall morphologies of recombinant reovirus and wild-type reovirus are similar, but that there may be empty spots on the recombinant virus capsid. We proposed that the  $\sigma 1$  protein is not stably built into the capsid. This may interfere with virus infection, possibly at a post-entry level.

Next to the reduced infectivity, we noticed the occasional occurrence of deletion mutants, in which (parts of) the transgene and sometimes reovirus-derived sequences were deleted. An overview of the observed S1 deletions can be found in Table 2. The deletion mutant reoviruses overgrew the transgene-containing reovirus population within a few passages, demonstrating that they have a growth advantage over the intact recombinant reoviruses. The deletions occurred despite the transgene-containing segments having a size similar to the wild-type S1 segment. The deletions ranged from 47 to 519 nucleotides in size, showing that S1 segments with a smaller size than usual (as small as 897 base pairs) can be successfully packaged into virions. We speculated about the mechanisms underlying the deletions. We found no evidence for the involvement of splicing or homology-directed mechanisms. Furthermore, the deletions are unlikely caused by replacing the  $\sigma 1$  head domain, removing the A- and B-boxes, or by adverse effects of the transgene-encoded protein. Although speculative, we propose that the most likely mechanism underlying the deletions is that complexities in the RNA structure may provoke template jumping of the RNA-dependent RNA polymerase and loss of S1 sequences. Interestingly, a similar mechanism was proposed before to underlie M1 deletions arising during the passaging of T1L/T3D reovirus reassortants [27]. Like for the deletion mutants we describe, these reassortants overgrew the virus populations upon propagation and the authors speculated too on the involvement

of secondary RNA structures. Moreover, difficulties in obtaining reoviruses expressing relatively long heterologous sequence stretches have also been attributed to complexities in the RNA structure [28]. These issues could be tackled by wobble-mutagenizing the constructs in order to reduce complexities in RNA secondary structure. Possibly, this could be attempted for our recombinant S1 constructs as well.

Virus clone	Deletion	Length	1st observ.	# observ.	Selective advantage
rS1-iLOV del1	GGCGCAACTG ... ... CGCCTCAGTA	464bp	Passage #10	1	Yes
rS1-iLOV del2	ATCACCGACC ... ... GGAGTACTTC	385bp	Passage #3	1	Yes
rS1-E4orf4 del1	GTCTCGGGCGC ... ... CGCCTCAGTA	47bp	Passage #3	Several	Yes
rS1-RFA	<i>No deletions found in any of the batches, up to 10 passages</i>				
rS1-hsGMCSF del1	AAAACCCCGG ... ... GCAGCACTGC	329bp	Passage #2	1	Yes
rS1-hsGMCSF del2	AAAGCAAGCA ... ... GGGCAGCCTC	298bp	Passage #2	2	Yes
rS1-hsGMCSF del3	ATAGGCGCAA ... ... CTTTGACTGC	519bp	Passage #2	1	Yes
rS1-hsGMCSFco del1	ATTCTATCAA ... ... TAATGTATT	230bp	Passage #2	1	Yes
rS1-hsGMCSFco del2	ATGTGGCTTC ... ... GCAGGGCCTT	249bp	Passage #2	2	Yes
rS1-hsGMCSFco del3	ATGTGGCTTC ... ... TGTGCTACTC	346bp	Passage #2	1	Yes
rS1-hsGMCSFco del4	ATGTGGCTTC ... ... CTA CTACAGAT	350bp	Passage #2	2	Yes
rS1-hsGMCSFco del5	GAAGAAAACC ... ... CAGGGCCTTA	268bp	Passage #2	1	Yes
rS1-hsGMCSFco del6	GAAGAAAACC ... ... GCTTCACATT	319bp	Passage #2	1	Yes
rS1-mmGMCSF	<i>No deletions found in any of the batches, up to 10 passages</i>				
rS1-dsRed	<i>No virus obtained despite several attempts</i>				
rS1-GaussiaLuc	<i>No virus obtained despite several attempts</i>				

**Table 2.** Overview of deletion mutant characteristics. Table showing the different recombinant reoviruses, the obtained deletion mutants, the deleted sequences, the length of the deletions, the passage number at which the deletion was first observed, the number of independent observations of this specific deletion, and whether the deletion mutant had a growth advantage over the reovirus harboring the intact S1 segment.

We did not examine whether the transgene-encoding S1 segments (and the other segments) are efficiently packaged into the recombinant reovirus particles. However, the  $\sigma 1$  expression levels were similar in cell cultures infected with recombinant reoviruses compared to wt T3D or *jin* reoviruses (data not shown). This indicates that the S1 segments are expressed in infected cells, and therefore must have been present in the incoming reovirus particles. Therefore, we concluded that packaging of S1 is not hampered by encoding a transgene. Nevertheless, it remains to be determined whether the transgene-encoding S1 segments are efficiently packaged in every virus particle.

To our best knowledge, we are the first to discuss S1 deletions occurring in recombinant reoviruses through reverse genetics. Our findings highlight that routine monitoring of the integrity of the transgene-containing reoviruses is essential when generating batches of replication-competent reoviruses containing heterologous transgenes. We demonstrate that small- and medium-scale batches of recombinant reoviruses can be generated with relative ease. Moreover, the deletion mutants reveal the minimally required sequences for efficient packaging of modified segments into reovirus capsids.



## REFERENCES

1. Schiff, L.A.; Nibert, M.L.; Tyler, K.L. Orthoreoviruses and their replication. *Fields Virology* **2007**, 5th edition, 1853–1915.
2. Gong, J.; Sachdev, E.; Mita, A.C.; Mita, M.M. Clinical development of reovirus for cancer therapy: An oncolytic virus with immune-mediated antitumor activity. *World J Methodol* **2016**, *6*, 25-42.
3. van den Wollenberg, D.J.; Dautzenberg, I.J.; van den Hengel, S.K.; Cramer, S.J.; de Groot, R.J.; Hoeben, R.C. Isolation of reovirus T3D mutants capable of infecting human tumor cells independent of junction adhesion molecule-A. *PLoS One* **2012**, *7*, e48064.
4. Leone, G.; Duncan, R.; Mah, D.C.W.; Price, A.; Cashdollar, L.W.; Lee, P.W.K. The N-terminal heptad repeat region of reovirus cell attachment protein  $\sigma 1$  is responsible for  $\sigma 1$  oligomer stability and possesses intrinsic oligomerization function. *Virology* **1991**, *182*, 336-345.
5. van den Wollenberg, D.J.; Dautzenberg, I.J.; Ros, W.; Lipinska, A.D.; van den Hengel, S.K.; Hoeben, R.C. Replicating reoviruses with a transgene replacing the codons for the head domain of the viral spike. *Gene Ther* **2015**, *22*, 267-79.
6. Kemp, V.; Dautzenberg, I.J.C.; Cramer, S.J.; Hoeben, R.C.; van den Wollenberg, D.J.M. Characterization of a replicating expanded tropism oncolytic reovirus carrying the adenovirus E4orf4 gene. *Gene Therapy* **2018**, *25*, 331–34.
7. Kemp, V.; van den Wollenberg, D.J.M.; Camps, M.G.M.; van Hall, T.; Kinderman, P.; Pronk-van Montfoort, N.; Hoeben, R.C., Arming oncolytic reovirus with GM-CSF gene to enhance immunity. *Cancer Gene Ther* **2019**, doi: 10.1038/s41417-018-0063-9.
8. Fallaux, F.J.; Kranenburg, O.; Cramer, S.J.; Houweling, A.; Van Ormondt, H.; Hoeben, R.C.; Van Der Eb, A.J. Characterization of 911: a new helper cell line for the titration and propagation of early region 1-deleted adenoviral vectors. *Hum Gene Ther* **1996**, *7*, 215-22.
9. Dautzenberg, I.J.; van den Wollenberg, D.J.; van den Hengel, S.K.; Limpens, R.W.; Barcena, M.; Koster, A.J.; Hoeben, R.C. Mammalian orthoreovirus T3D infects U-118 MG cell spheroids independent of junction adhesion molecule-A. *Gene Ther* **2014**, *21*, 609-17.
10. van den Wollenberg, D.J.; van den Hengel, S.K.; Dautzenberg, I.J.; Cramer, S.J.; Kranenburg, O.; Hoeben, R.C. A strategy for genetic modification of the spike-encoding segment of human reovirus T3D for reovirus targeting. *Gene Ther* **2008**, *15*, 1567-78.
11. Buchholz, U.J.; Finke, S.; Conzelmann, K.K. Generation of bovine respiratory syncytial virus (BRSV) from cDNA: BRSV NS2 is not essential for virus

- replication in tissue culture, and the human RSV leader region acts as a functional BRSV genome promoter. *J Virol* **1999**, *73*, 251-9.
12. Ni, Y.W.; Kemp, M.C. Subgenomic S1 Segments Are Packaged by Avian Reovirus Defective Interfering Particles Having an S1 Segment Deletion. *Virus Res* **1994**, *32*, 329-342.
  13. Roner, M.R.; Roehr, J. The 3' sequences required for incorporation of an engineered ssRNA into the Reovirus genome. *Virology* **2006**, *3*, 1.
  14. Roner, M.R.; Steele, B.G. Features of the mammalian orthoreovirus 3' Dearing I1 single-stranded RNA that direct packaging and serotype restriction. *J Gen Virol* **2007**, *88*, 3401-12.
  15. Boehme, K.W.; Ikizler, M.; Kobayashi, T.; Dermody, T.S. Reverse genetics for mammalian reovirus. *Methods* **2011**, *55*, 109-13.
  16. Kobayashi, T.; Antar, A.A.; Boehme, K.W.; Danthi, P.; Eby, E.A.; Guglielmi, K.M.; Holm, G.H.; Johnson, E.M.; Maginnis, M.S.; Naik, S. *et al.* A plasmid-based reverse genetics system for animal double-stranded RNA viruses. *Cell Host Microbe* **2007**, *1*, 147-57.
  17. Virgin, H.W.; Mann, M.A.; Fields, B.N.; Tyler, K.L. Monoclonal-Antibodies to Reovirus Reveal Structure-Function-Relationships between Capsid Proteins and Genetics of Susceptibility to Antibody Action. *Journal of Virology* **1991**, *65*, 6772-6781.
  18. Kupgan, G.; Hentges, D.C.; Muschinske, N.J.; Picking, W.D.; Picking, W.L.; Ramsey, J.D. The effect of fiber truncations on the stability of adenovirus type 5. *Mol Biotechnol* **2014**, *56*, 979-91.
  19. Maginnis, M.S.; Forrest, J.C.; Kopecky-Bromberg, S.A.; Dickeson, S.K.; Santoro, S.A.; Zutter, M.M.; Nemerow, G.R.; Bergelson, J.M.; Dermody, T.S. Beta1 integrin mediates internalization of mammalian reovirus. *J Virol* **2006**, *80*, 2760-70.
  20. Kim, M.; Garant, K.A.; zur Nieden, N.I.; Alain, T.; Loken, S.D.; Urbanski, S.J.; Forsyth, P.A.; Rancourt, D.E.; Lee, P.W.; Johnston, R.N. Attenuated reovirus displays oncolysis with reduced host toxicity. *Br J Cancer* **2011**, *104*, 290-9.
  21. Bokiej, M.; Ogden, K.M.; Ikizler, M.; Reiter, D.M.; Stehle, T.; Dermody, T.S. Optimum length and flexibility of reovirus attachment protein sigma1 are required for efficient viral infection. *J Virol* **2012**, *86*, 10270-80.
  22. Larson, S.M.; Antczak, J.B.; Joklik, W.K. Reovirus Exists in the Form of 13 Particle Species That Differ in Their Content of Protein Sigma-1. *Virology* **1994**, *201*, 303-311.
  23. Shayakhmetov, D.M.; Lieber, A. Dependence of adenovirus infectivity on length of the fiber shaft domain. *J Virol* **2000**, *74*, 10274-86.

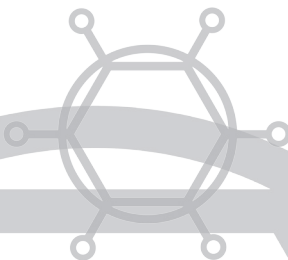
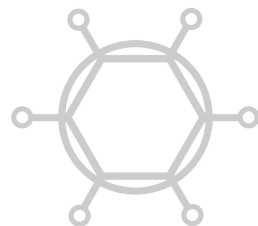
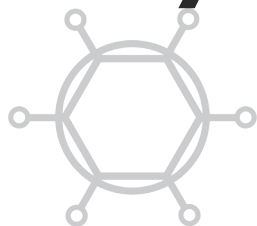
24. Chappell, J.D.; Barton, E.S.; Smith, T.H.; Baer, G.S.; Duong, D.T.; Nibert, M.L.; Dermody, T.S. Cleavage susceptibility of reovirus attachment protein sigma 1 during proteolytic disassembly of virions is determined by a sequence polymorphism in the sigma 1 neck. *Journal of Virology* **1998**, *72*, 8205-8213.
25. Metcalf, D. The molecular biology and functions of the granulocyte-macrophage colony-stimulating factors. *Blood* **1986**, *67*, 257-67.
26. Buckley, P.T.; Khaladkar, M.; Kim, J.; Eberwine, J. Cytoplasmic intron retention, function, splicing, and the sentinel RNA hypothesis. *Wiley Interdiscip Rev RNA* **2014**, *5*, 223-30.
27. Zou, S.; Brown, E.G. Identification of sequence elements containing signals for replication and encapsidation of the reovirus M1 genome segment. *Virology* **1992**, *186*, 377-88.
28. Demidenko, A.A.; Blattman, J.N.; Blattman, N.N.; Greenberg, P.D.; Nibert, M.L. Engineering recombinant reoviruses with tandem repeats and a tetravirus 2A-like element for exogenous polypeptide expression. *Proc Natl Acad Sci U S A* **2013**, *110*, E1867-76.





General discussion

**7**



## **EXPLORING REOVIRUS AS AN ONCOLYTIC VIRUS**

Oncolytic viruses represent promising tools in anti-cancer therapy. The recent FDA approval of T-VEC, a herpes simplex virus expressing copies of the GM-CSF gene, gives an encouraging outlook on approval of other oncolytic virotherapies by the regulatory bodies [1]. Oncolytic reovirus has been studied in a variety of clinical trials, but its efficacy in stand-alone treatments remains moderate at best [2]. Therefore, we sought to explore ways in which we can improve the therapeutic potency of reovirus. Before effective application, we need to have a good understanding of the prerequisites for efficient viral replication, cell death stimulation, and induction of a potent long-lasting anti-tumor immune response.

## **ROLE OF AUTOPHAGY DURING REOVIRUS REPLICATION**

We discovered that specific members of the autophagy machinery are important for reovirus replication, as shown by reduced titers upon knock-out of the corresponding Atg genes [3]. Interestingly, not all autophagy-related proteins influenced reovirus replication, indicating that there may be a non-canonical use of the proteins, independent of their role in autophagy. We proposed several explanations, including a function in endosome maturation, mitochondrial function or inhibition of type I interferon (IFN) production, which are important for viral entry and replication, respectively. Importantly, the effects on viral replication could only be detected at relatively late time points during infection (48-72 hours post infection), suggesting that a late event during viral replication is influenced. Therefore, it seems unlikely that an effect of Atg knock-out on viral replication is caused by an effect on viral entry. Furthermore, we observed only minor effects of Atg knock-outs on the induction of cell death by reovirus [4]. An effect on mitochondrial homeostasis or an anti-viral type I IFN response seem more plausible explanations for the changes in viral replication. Interestingly, the expression of autophagy-related proteins in cancer is very diverse, with several cases of cancers that lack the expression of some autophagy-related protein [5]. It would be interesting to see if there is a correlation between expression of autophagy-related proteins such as Atg3 or Atg5 and cancer susceptibility to oncolytic viruses.

## **GENETIC MODIFICATION OF REOVIRUS TO ENCODE TRANSGENES**

### *E4orf4*

In order to enhance oncolytic reovirus as a monotherapy, we sought ways to genetically modify the virus to encode a potentially therapeutic transgene. We did so by exploiting a plasmid-based reverse genetics system, in which plasmids are used that encode the 10 different reovirus genome segments, driven by a T7 polymerase promoter. Conceptually, upon transfection of cells expressing the T7 polymerase,

these plasmids are transcribed and viral proteins are generated. These will assemble in viral particles which can be propagated on a producer cell line. We replaced the S1-encoding plasmid for a plasmid encoding S1 and a heterologous transgene. In order to not increase the genome size of reovirus, we replaced the S1 region encoding the  $\sigma 1$  head domain by the transgene. The  $\sigma 1$  head domain is responsible for binding to the canonical reovirus receptor JAM-A. Based on the previously isolated *jin-3* mutant reovirus, that is able to infect JAM-A negative cells, we incorporated a G196R mutation in the S1 segment that allows for enhanced sialic acid binding dependent entry. We used the reverse genetics system to encode a cell death inducing protein called E4orf4 in the reovirus S1 segment [6]. This adenovirus-derived protein is known to induce a non-classical form of apoptosis. Interestingly, we found no additional effect of encoding E4orf4 on cell death induction by reovirus. Rather, the truncation of  $\sigma 1$  seems to result in potent cell death induction, presumably making the expression of an additional cell death inducer redundant.

### *GM-CSF*

The mechanism of action by oncolytic viruses has been extended beyond the simple induction of cancer cell death. It is now widely accepted that the efficacy of oncolytic viruses not only depends on replicating capacity but also on the induction of potent and long-lasting anti-cancer immune responses. Therefore, we hypothesized that it may be of more value to genetically modify reovirus to encode an immunostimulatory transgene that can trigger anti-tumor immune responses. We generated recombinant reoviruses expressing GM-CSF [7]. GM-CSF is known to stimulate the generation and activation of dendritic cells (DCs) [8, 9]. The GM-CSF expressing reoviruses triggered the secretion of GM-CSF from infected cells [7]. Furthermore, the secreted murine GM-CSF was further tested and found to be functional in generating and activating dendritic cells *in vitro*. Importantly, we also found systemic effects on the immune composition in mice bearing pancreatic tumors. Therefore, we proposed that this virus may be of value to further test for clinical application. Future studies are needed to determine to what extent the GM-CSF expressing reoviruses improve tumor reduction and/or survival.

### **PRODUCTION AND STABILITY OF RECOMBINANT REOVIRUSES**

To make clinical application feasible, large batches of (genetically) stable reoviruses must be generated with ease. During the generation of our recombinant viruses, we noticed that the infectious titers of these reoviruses were relatively low compared to wild-type reovirus or bioselected mutants such as *jin-3*. Further experiments revealed that  $\sigma 1$  may be incorporated to a lower level into the viral particles, and we propose that this affects viral stability and infectivity. Furthermore, we

occasionally detected deletion mutants in which (parts of) the transgene and sometimes reovirus-derived sequences were removed. Further examination of the deletions revealed that the most plausible explanation for this lies in complexities of the RNA structure. Altogether, we demonstrated that medium-scale batches of recombinant reoviruses can be generated with relative ease. However, before large-scale batches can be generated that are suitable for clinical application, the production to high titers and the (genetic) stability of batches have to be optimized. Therefore, it may be easier to move wild-type reovirus or bioselected mutants into the clinic, as these do not give the infectivity and stability issues that the recombinant reoviruses do. In addition, it may be less complex and more effective to let the virus come up with a solution for eliminating cancer cells than to develop a tumor-specific cell death trigger ourselves. The mutation rate of reovirus makes it possible to generate pools of mutants during virus propagation. Perhaps in this way viruses can be generated that potentially combat cancers that resist current therapies.

## **FUTURE DIRECTIONS**

For moving forward, and for getting the right treatment for cancer patients, we need to focus on markers that predict the susceptibility of a cancer to the oncolytic virus treatment. With each cancer having different susceptibility profiles to different oncolytic viruses, it would be of great value to consider therapeutic approaches that combine different oncolytic viruses. Alternatively, many promising combinations of oncolytic viruses with other anti-cancer agents are studied and often work synergistically [10, 11]. The heterogeneity in tumor composition within patients and also between patients continue to form a hurdle. However, with the viruses' intrinsic tumor tropism as a starting point and with the aid of directed virus evolution methodology we have the means to overcome this hurdle and to improve the therapeutic efficacy of oncolytic virus treatment. With new and improved viruses, and in combination with new immunomodulatory approaches and potentially synergizing cytostatic drugs, we may one day reach the point where each patient receives treatment involving the personalized administration of dedicated, efficient, and safe oncolytic viruses.

## REFERENCES

1. Pol, J.; Kroemer, G.; Galluzzi, L. First oncolytic virus approved for melanoma immunotherapy. *Oncoimmunology* **2016**, *5*, e1115641.
2. Zhao, X.; Chester, C.; Rajasekaran, N.; He, Z.; Kohrt, H.E. Strategic Combinations: The Future of Oncolytic Virotherapy with Reovirus. *Mol Cancer Ther* **2016**, *15*, 767-73.
3. Kemp, V.; Dautzenberg, I.J.C.; Limpens, R.W.; van den Wollenberg, D.J.M.; Hoeben, R.C. Oncolytic Reovirus Infection Is Facilitated by the Autophagic Machinery. *Viruses* **2017**, *9*, 266.
4. Kemp, V.; Dautzenberg, I.J.; van den Wollenberg, D.J.; Hoeben, R.C. Autophagy has minor effects on reovirus-induced cytolysis. *Unpublished data*. **2017**.
5. Uhlen, M.; Zhang, C.; Lee, S.; Sjostedt, E.; Fagerberg, L.; Bidkhori, G.; Benfeitas, R.; Arif, M.; Liu, Z.; Edfors, F. *et al.* A pathology atlas of the human cancer transcriptome. *Science* **2017**, 357.
6. Kemp, V.; Dautzenberg, I.J.C.; Cramer, S.J.; Hoeben, R.C.; van den Wollenberg, D.J.M. Characterization of a replicating expanded tropism oncolytic reovirus carrying the adenovirus E4orf4 gene. *Gene Therapy* **2018**, *25*, 331–34.
7. Kemp, V.; van den Wollenberg, D.J.M.; Camps, M.G.M.; van Hall, T.; Kinderman, P.; Pronk-van Montfoort, N.; Hoeben, R.C. Arming oncolytic reovirus with GM-CSF gene to enhance immunity. *Cancer Gene Ther* **2019**, doi: 10.1038/s41417-018-0063-9.
8. Xu, Y.; Zhan, Y.; Lew, A.M.; Naik, S.H.; Kershaw, M.H. Differential Development of Murine Dendritic Cells by GM-CSF versus Flt3 Ligand Has Implications for Inflammation and Trafficking. *The Journal of Immunology* **2007**, *179*, 7577-7584.
9. Zhan, Y.; Carrington, E.M.; van Nieuwenhuijze, A.; Bedoui, S.; Seah, S.; Xu, Y.; Wang, N.; Mintern, J.D.; Villadangos, J.A.; Wicks, I.P.; Lew, A.M. GM-CSF increases cross-presentation and CD103 expression by mouse CD8(+) spleen dendritic cells. *Eur J Immunol* **2011**, *41*, 2585-95.
10. Bommareddy, P.K.; Shettigar, M.; Kaufman, H.L. Integrating oncolytic viruses in combination cancer immunotherapy. *Nat Rev Immunol* **2018**, *18*, 498-513.
11. Lal, G.; Rajala, M.S. Recombinant viruses with other anti-cancer therapeutics: a step towards advancement of oncolytic virotherapy. *Cancer Gene Ther* **2018**.



# ADDENDUM

Nederlandse samenvatting  
Curriculum Vitae  
List of publications  
Acknowledgements (Dankwoord)



## NEDERLANDSE SAMENVATTING

Oncolytische virussen zijn bijzonder. Ze onderscheiden kankercellen van normale, gezonde cellen. Alleen kankercellen kunnen worden geïnfecteerd en gedood. De factoren die bepalen of cellen kwaadaardig worden en uitgroeien tot een kanker zorgen er vaak ook voor dat de cellen vatbaarder worden voor virusinfecties. Als gevolg daarvan faciliteren de kankercellen de virusrelicatie, dat is de vermenigvuldiging, van virussen die zich normaal gesproken niet heel effectief vermenigvuldigen in onze cellen en daarmee relatief onschadelijk zijn voor onze gezondheid. Positieve resultaten in het onderzoek naar het gebruik van virussen in anti-kankertherapieën hebben recent geleid tot het toelaten van T-VEC, Talimogene laherparepvec, voor de behandeling van een specifieke groep huidkankerpatiënten. Het middel wordt nu onder de naam Imlygic gebruikt. Wellicht maakt de goedkeuring van Imlygic het makkelijker voor andere oncolytische virussen om te worden toegelaten voor de behandeling van kankerpatiënten.

Reovirus is een virus met een dubbelstrengs RNA genoom bestaande uit tien verschillende segmenten van zo'n 23.500 baseparen in lengte. Dit virus heeft van zichzelf ook de eigenschap om zich bij voorkeur in kankercellen te vermenigvuldigen en deze cellen hierbij te doden. Daarom wordt het reovirus ook bestudeerd als anti-kankermiddel. Het lijkt niet specifiek te werken in één kanker type, maar bij een breed scala aan kankertypes. Het gebruik van reovirus in patiënten lijkt veilig, maar de effecten op tumorgrootte en overleving van de patiënten lijkt gelimiteerd. Er zijn verschillende manieren waarop geprobeerd wordt de klinische effectiviteit te verhogen.

In dit proefschrift beschrijf ik het onderzoek dat ik heb uitgevoerd naar deze reovirussen. In **hoofdstuk 2** geef ik een uitgebreid overzicht van de belangrijke aspecten waarmee rekening moet worden gehouden bij het ontwikkelen van reovirus als een effectief anti-kankermiddel. Er wordt ingegaan op de factoren die betrokken zijn bij het effectief binnengaan van het virus in de cellen, bij de replicatie, het doden van de kankercel, en het aanzetten van immuunreacties. Daarnaast beschrijft het verschillende manieren om de effectiviteit van reovirus te verhogen. In dit proefschrift wordt daarna verder ingegaan op twee van deze manieren.

Allereerst hebben wij geprobeerd verder bloot te leggen welke eigenschappen en factoren in de cel belangrijk zijn om een efficiënte replicatie van reovirus te bewerkstelligen. In **hoofdstuk 3** wordt omschreven dat verschillende Atg-eiwitten de replicatie van reovirus beïnvloeden. Dit zijn eiwitten die hoofdzakelijk bekend zijn om hun functie in de autofagie-pathway van de cel. De autofagie-pathway is een signaleringsroute in de cel die aangezet wordt wanneer er weinig voedingsstoffen voorhanden zijn. De cel kan dan zijn eigen inhoud als het ware recyclen en de bruikbare stoffen hergebruiken om te overleven. Wij hebben



gevonden dat specifieke eiwitten die betrokken zijn bij het uitvoeren van de autofagie-signaleringsroute ook belangrijk zijn voor de replicatie van reovirus. Dit doet vermoeden dat de autofagie-route belangrijk is voor de replicatie van het reovirus. Echter, een interessante bevinding was dat niet álle Atg-eiwitten uit de autofagie-pathway de replicatie van reovirus beïnvloeden. Daarom concluderen wij dat niet noodzakelijk de autofagie-route zelf belangrijk is voor reovirus replicatie. Vermoedelijk doen de Atg-eiwitten die reovirus replicatie beïnvloeden dit eerder op een manier die onafhankelijk is van hun functie in de autofagie-pathway.

Een andere manier om de effectiviteit van reovirus te verhogen is door het gebruiken van krachtigere varianten van het virus. In **hoofdstuk 4 en 5** beschrijven we verschillende genetisch-gemodificeerde varianten van reovirus. In deze virussen hebben we een deel van één van de genoom-segmenten, het S1 segment, vervangen door een zogenaamd transgen. Dit transgen is een stukje genetisch materiaal dat voor een eiwit codeert en dat niet afkomstig is van het virus. Op deze manier kan bereikt worden dat het virus een eiwit tot expressie brengt dat het normaal niet tot expressie brengt. Het S1 segment codeert voor het 'spike' eiwit van het reovirus genaamd  $\sigma 1$ . Als gevolg van het vervangen van een deel van S1 brengt het virus een verkort  $\sigma 1$  eiwit tot expressie op zijn oppervlak. **Hoofdstuk 4** gaat verder in op een reovirus variant die E4orf4 tot expressie brengt. Dit is een eiwit waarvan bekend is dat het kanker-specifieke celdood stimuleert. Door het inbouwen van E4orf4 in reovirus probeerden wij een virusvariant te maken die de kankercellen efficiënter kan doden. Echter vonden wij geen toegevoegd effect van E4orf4 op het stimuleren van celdood door reovirus. Onze bevindingen duiden erop dat reovirussen met een verkort  $\sigma 1$  maar zónder E4orf4 al erg effectief zijn in het doden van kankercellen en dat verdere toevoeging van een celdood-stimulerend eiwit overbodig is.

**Hoofdstuk 5** beschrijft de productie van reovirussen die GM-CSF tot expressie brengen. GM-CSF is een immuun-stimulerend eiwit waarvan bekend is dat het waardevol kan zijn voor toepassing in kankerpatiënten. Het stimuleert de ontwikkeling van zogenaamde dendritische cellen. Deze cellen kunnen helpen bij het aanwakkeren van een sterke anti-kanker immuunrespons. In gekweekte cellen laten wij zien dat de reovirussen die GM-CSF tot expressie brengen ook daadwerkelijk zorgen voor de productie van functioneel GM-CSF, dat de aanmaak en activatie van dendritische cellen stimuleert. Daarnaast tonen we in een muismodel van alvleesklierkanker aan dat het reovirus de systemische activatie van T-cellen stimuleert. T-cellen zijn immuun-cellen die erg belangrijk zijn bij het bewerkstelligen van een sterke, langdurige anti-kanker immuunrespons.

In **hoofdstuk 6** gaan we in op twee belemmeringen bij het klinisch inzetten van onze genetisch-gemodificeerde reovirussen: een relatief lage infectiviteit, en deletie-mutanten. De genetisch-gemodificeerde reovirussen hebben een 10- tot

750-voudige lagere infectiviteit ten opzichte van de ongemodificeerde reovirussen. Vermoedelijk komt dit doordat de gemodificeerde reovirussen een verkort  $\sigma 1$  eiwit tot expressie brengen op hun oppervlak. Het  $\sigma 1$  eiwit is betrokken bij het binnengaan van de cel en is korter in de genetisch-gemodificeerde reovirussen om plaats te maken voor de expressie van het extra potentieel therapeutische eiwit (E4orf4 of GM-CSF). Waarschijnlijk wordt de verkorte versie van  $\sigma 1$  minder stabiel ingebouwd op het virale oppervlak, waardoor de infectiviteit verlaagd is. De tweede belemmering is dat er tijdens het opgroeien van de gemodificeerde reovirussen soms deleties optreden binnen het gemodificeerde S1 segment. In de deletie-mutanten zijn verschillende delen van het ingebouwde transgen en soms ook virus-afkomstige delen verwijderd uit het S1 segment. De verschillende deleties geven inzicht in de eventuele virus-afkomstige genoom-onderdelen die schijnbaar overbodig zijn. De meest waarschijnlijke achterliggende oorzaak van de deleties ligt in de 3D structuur van het S1 RNA segment. Onze bevindingen laten zien dat het mogelijk is om genetisch-gemodificeerde reovirussen te maken, maar dat het monitoren van de infectiviteit en genetische stabiliteit hierbij belangrijk zijn.

In **hoofdstuk 7** worden alle bevindingen samengevat en wordt verder bediscussieerd wat de beste manier is om verder te gaan met reovirussen voor toekomstige anti-kankertherapie ontwikkeling. Het is belangrijk om de gevoeligheid van verschillende kankers voor reovirus in kaart te brengen, zodat het mogelijk is om de behandeling daarop af te stemmen. Reovirus blijft een waardevol middel door zijn intrinsieke kanker-specificiteit en vermogen om zowel kankercellen te doden als een anti-kanker immuunrespons op te wekken. Er liggen veel mogelijkheden in het ontwikkelen van potentere virussen en het combineren van reovirus met andere oncolytische virussen of andere anti-kankermiddelen, met als ultieme doel dat elke kankerpatiënt uiteindelijk behandeld zal worden met een effectieve gepersonaliseerde therapie.





**CURRICULUM VITAE**

Vera Kemp was born on January 8, 1990 in Hazerswoude-Rijndijk, the Netherlands. After she received her diploma in 2008 from the Stedelijk Gymnasium in Leiden, she began studying Biomedical Sciences at Utrecht University. She received her bachelor degree in 2011 and continued with a master focusing on Infection and Immunity. As a part of this education, she performed an internship in the group of Niels Bovenschen at the department of Pathology of the University Medical Center Utrecht. Supervised by Annette Wensink, she studied the role of extracellular granzyme K during inflammation. Later, she wrote her master thesis at the department of Infectious Diseases and Immunology of Utrecht University. Under the supervision of Martijn Langereis and Frank van Kuppeveld, she explored the properties of the viral RNA ligand that activates RIG-I during Influenza A virus infection. At the end of her master study, she went to the group of Rob Hoeben at the Leiden University Medical Center for her second and final internship. Here, she investigated the role of autophagy during oncolytic reovirus infection, under the supervision of Iris Dautzenberg and Diana van den Wollenberg. In 2014, Vera started her PhD studies in the group of Rob Hoeben, resulting in the research that is presented in this thesis.





## LIST OF PUBLICATIONS

- Kemp, V.; van den Wollenberg, D.J.M.; Camps, M.G.M.; van Hall, T.; Kinderman, P.; Pronk-van Montfoort, N.; Hoeben, R.C., Arming oncolytic reovirus with GM-CSF gene to enhance immunity. *Cancer Gene Therapy* **2019**, doi: 10.1038/s41417-018-0063-9
- Kemp, V.; Dautzenberg, I.J.C.; Cramer, S.J.; Hoeben, R.C.; van den Wollenberg, D.J.M., Characterization of a replicating expanded tropism oncolytic reovirus carrying the adenovirus E4orf4 gene. *Gene Therapy* **2018**, 25 (5): 331-344.
- Kemp, V.; Dautzenberg, I.J.C.; Limpens, R.W.; van den Wollenberg, D.J.M.; Hoeben, R.C., Oncolytic Reovirus Infection Is Facilitated by the Autophagic Machinery. *Viruses* **2017**, 9 (10), pii: E266.
- Kemp, V.; Hoeben, R.C.; van den Wollenberg, D.J., Exploring Reovirus Plasticity for Improving Its Use as Oncolytic Virus. *Viruses* **2015**, 8 (1), pii: E4.
- Wensink, A.C.; Kemp, V.; Fermie, J.; Garcia Laorden, M.I.; van der Poll, T.; Hack, C.E.; Bovenschen, N., Granzyme K synergistically potentiates LPS-induced cytokine responses in human monocytes. *Proc Natl Acad Sci U S A* **2014**, 111 (16), 5974-9.





## ACKNOWLEDGEMENTS (DANKWOORD)

Het zit erop. Mijn tijd als onderzoeker bij het LUMC is bijzonder leerzaam, uitdagend, en ontzettend leuk geweest. Uiteraard heb ik dit niet allemaal aan mijzelf te danken. Ik kan onmogelijk iedereen persoonlijk bedanken die bijgedragen heeft bij het realiseren van dit proefschrift, maar wil toch graag mijn waardering voor een aantal mensen uitspreken.

Allereerst Rob, mijn promotor, dat hij mij de kans heeft geboden om mijn onderzoek in zijn groep uit te voeren. Mijn interesse was gewekt toen jij een college gaf in Utrecht, en dit is niet meer weggegaan. Je hebt me geleerd om kritisch, zelfstandig, gedreven, en met plezier onderzoek te doen en daar ben ik je zeer dankbaar voor.

Diana, mijn co-promotor en lab-mama, naast een dagelijkse begeleider ben jij ook een heel fijn kantoormaatje geweest. Bij jou kon ik altijd terecht voor vragen, zowel wetenschappelijke als niet-wetenschappelijke.

Iris, dankjewel voor de fijne begeleiding toen ik als student stage kwam lopen op de (toen nog) MCB. Ik heb het ontzettend leuk gevonden dat we later als collega's hebben mogen samenwerken.

Mijn (oud-)collega's Amiet, Arnaud, Chen, Erik, Francesca, Harald, Henrique, Hidde, Igno, Jan, Jin, Kim, Lonneke, Maaïke, Malisa, Manuel, Marcella, Marjolein, Martijn, Merve, Michaela, Nanda, Pete, Qian, Sanne, Selas, Sofia, Thilo, Timo, Tobias en Willemijn: dank jullie voor alle wetenschappelijke input en gezelligheid. Steve, jij weet echt alles over kloneringen, bedankt voor alle hulp (en de occasionele etentjes).

Talitha en Vincent, dank voor jullie inzet als stage-studenten, ik hoop dat jullie beiden een leuke baan vinden in de toekomst. Alle (ex-)studenten van de afdeling, in het bijzonder Effie, Eline en Willemijn, dank voor jullie verfrissende ideeën en het mede creëren van een gezellige sfeer.

Gelilla en Ben, dank voor de praktische ondersteuning. Gelilla, ik zal onze gesprekken en roddels op de gang en bij de koffiemachine missen. Willem, mijn waardering dat jij computer-ellende altijd weer snel wist op te lossen. Julia, Marianne en Pauline, bedankt dat jullie altijd klaarstonden voor vragen en voor alles dat jullie in goede banen geleid hebben.



Montse, Ronald, Carolina (EM), Mark, Eveline (MDLZ), Marcel (IHB), Nadine, Priscilla (ONCO), en alle OVIT partners, dank voor de fijne samenwerkingen! Sanne, ver weg op de Reuma en toch hield je de boel hier in de gaten. Als trouwe vriendin was jij altijd te vinden wanneer nodig. Aleks, Edwin, Frauke, Renier, Sabine, bedankt voor allerhande uitjes en borrels, dit heeft voor de nodige ontspanning gezorgd.

Marjolein, wij zijn vrijwel tegelijk aan het PhD avontuur begonnen en hebben daarin veel lief en leed gedeeld. Van collega's zijn we tot vrienden gegroeid, en ik vind het niet meer dan logisch en ontzettend fijn dat jij één van mijn paranimfen bent.

Marco, broertje, waar we elkaar vroeger de tent uit konden vechten, hebben we nu een bijzonder hechte band. Ik waardeer je betrokkenheid enorm en ben trots dat jij als mijn andere paranimf naast mij staat.

Vrienden (in het bijzonder 'de bankers' en 'de lebbers') en (schoon)familie, jullie hebben mij met beide benen op de grond gehouden, mijn frustraties aangehoord en ontspanning geboden. Mam, Bru, jullie extra bedankt dat ik altijd bij jullie terecht heb gekund.

En traditiegetrouw als laatste natuurlijk Luuk, mijn partner, mijn maatje! Jij begrijpt mij als geen ander. Dankjewel voor jouw onvoorwaardelijke liefde en steun.

Any way the wind blows –  
Queen (1975)



